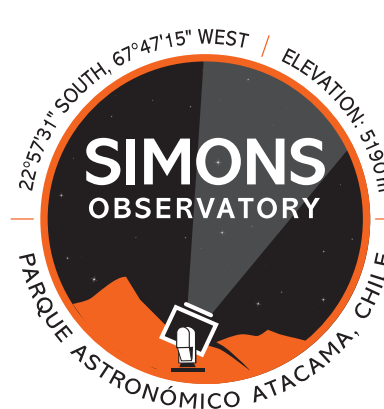


CMB LENSING & DELENSING FOR FUNDAMENTAL PHYSICS

Anton Baleato Lizancos



BERKELEY CENTER *for*
COSMOLOGICAL PHYSICS

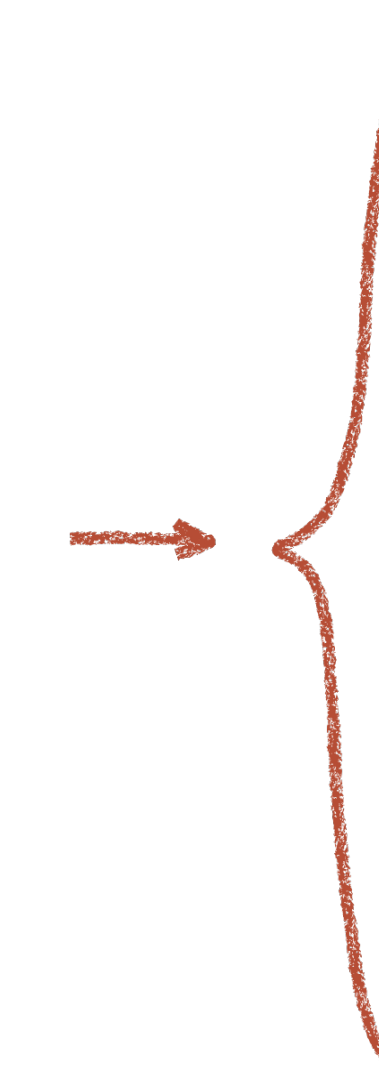


Institute of Physics of the Czech Academy of Sciences

30/9/2021

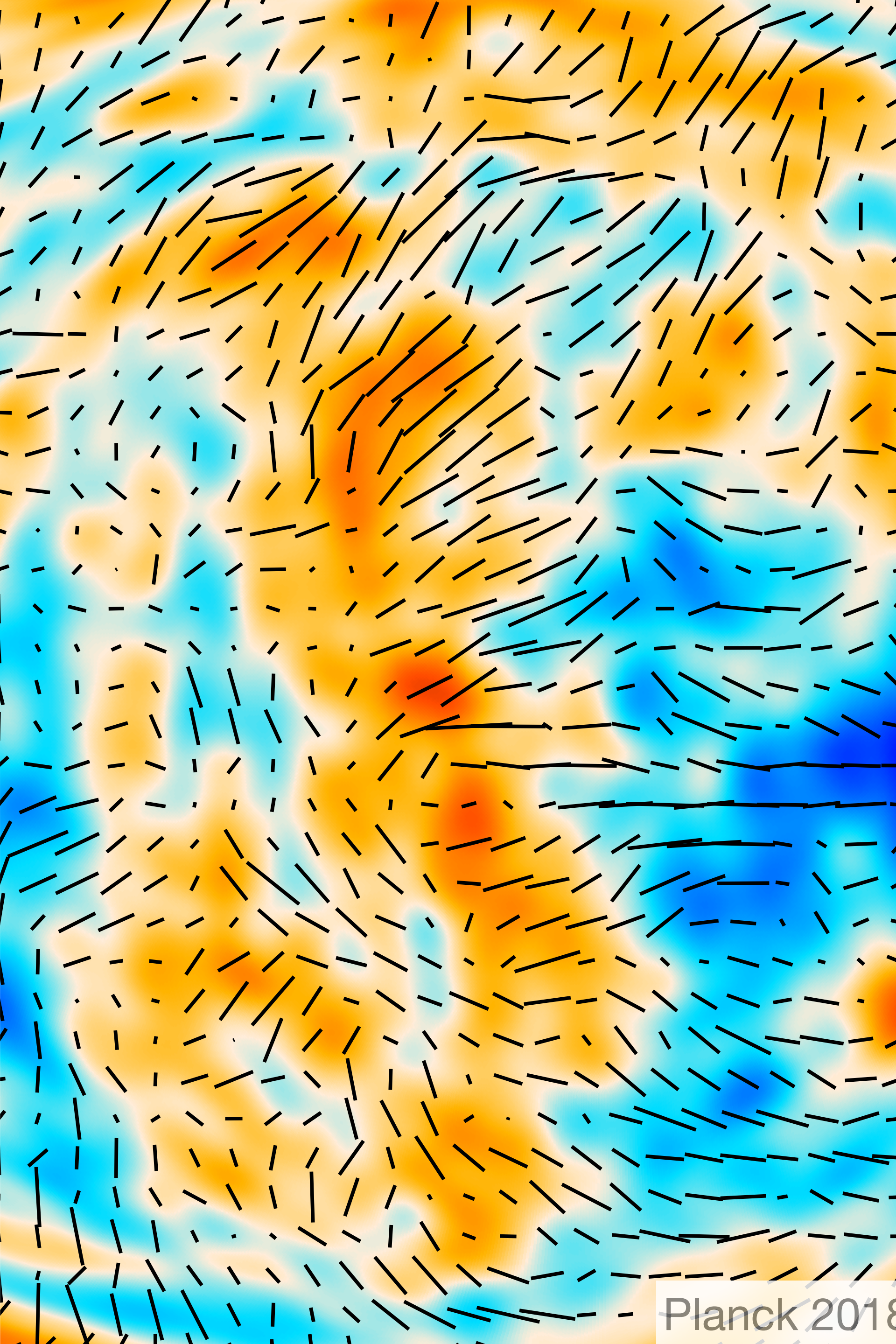
OUTLINE

1. THE PRIMORDIAL CMB
AND THE LENSING EFFECT



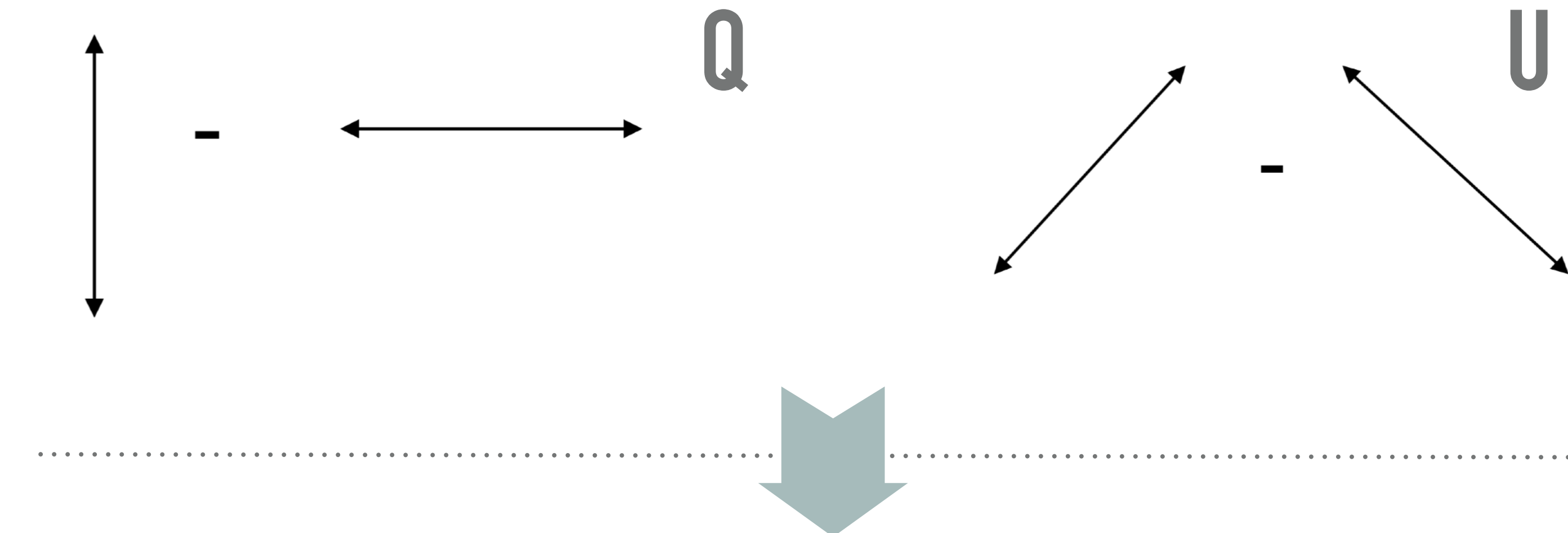
2. CMB LENSING RECONSTRUCTIONS

3. DELENSING CMB B-MODES

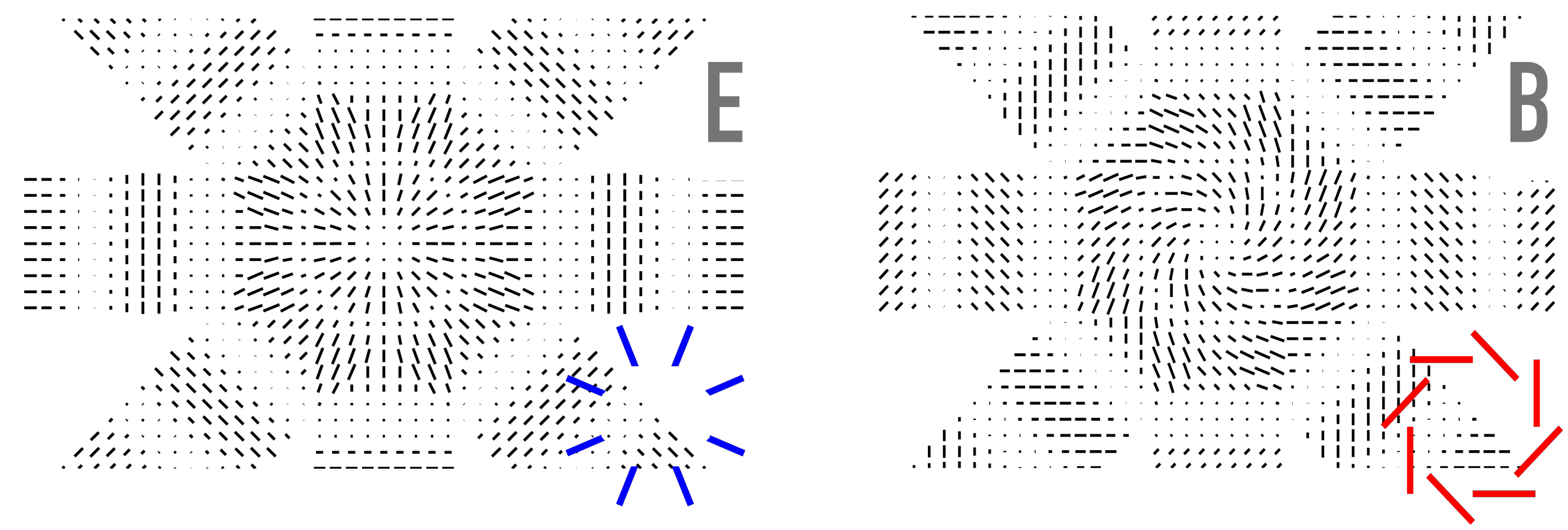


CMB OBSERVABLES — INTENSITY AND POLARISATION

Observe:

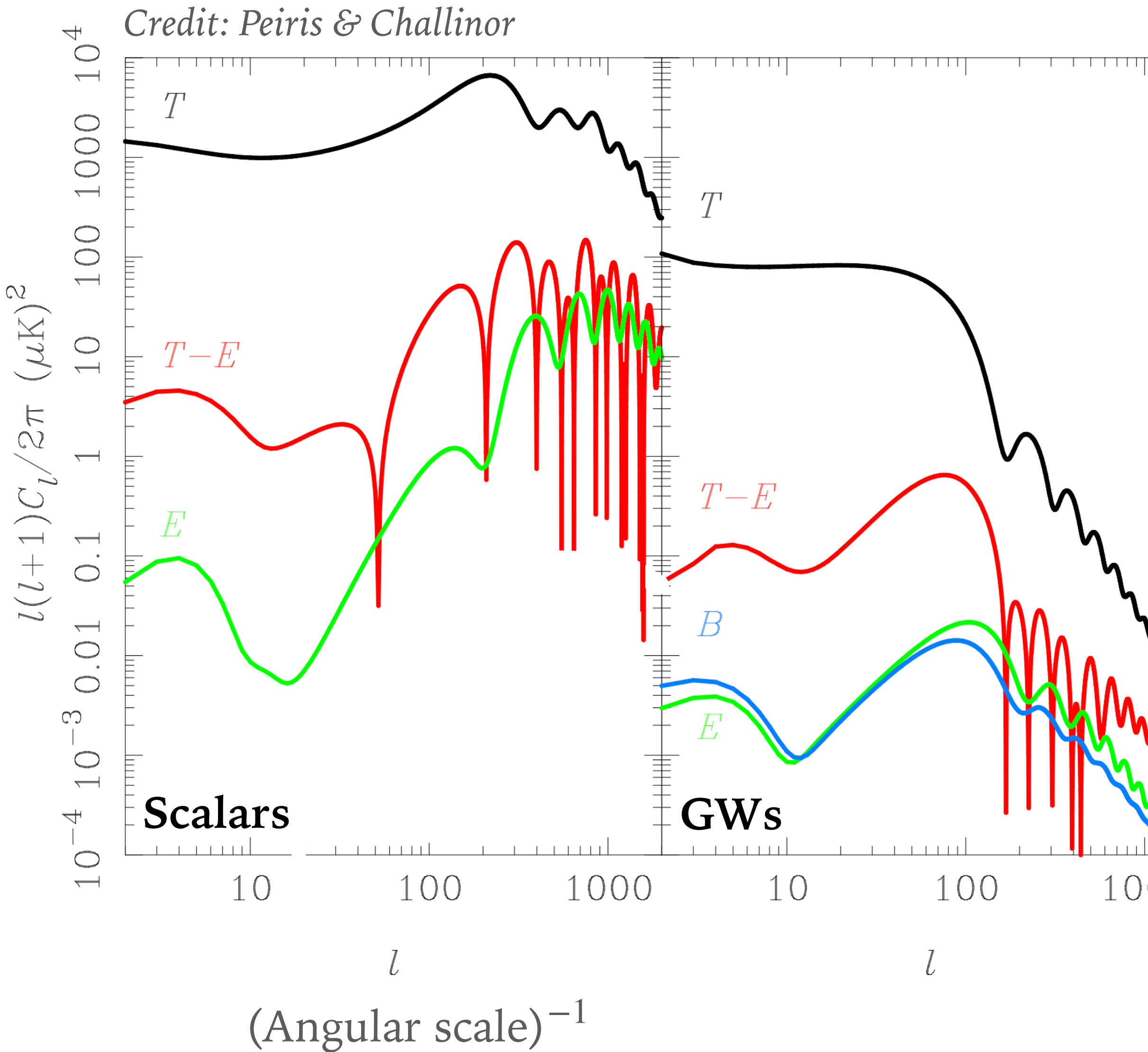


Connect with theory:



THE PRIMORDIAL CMB

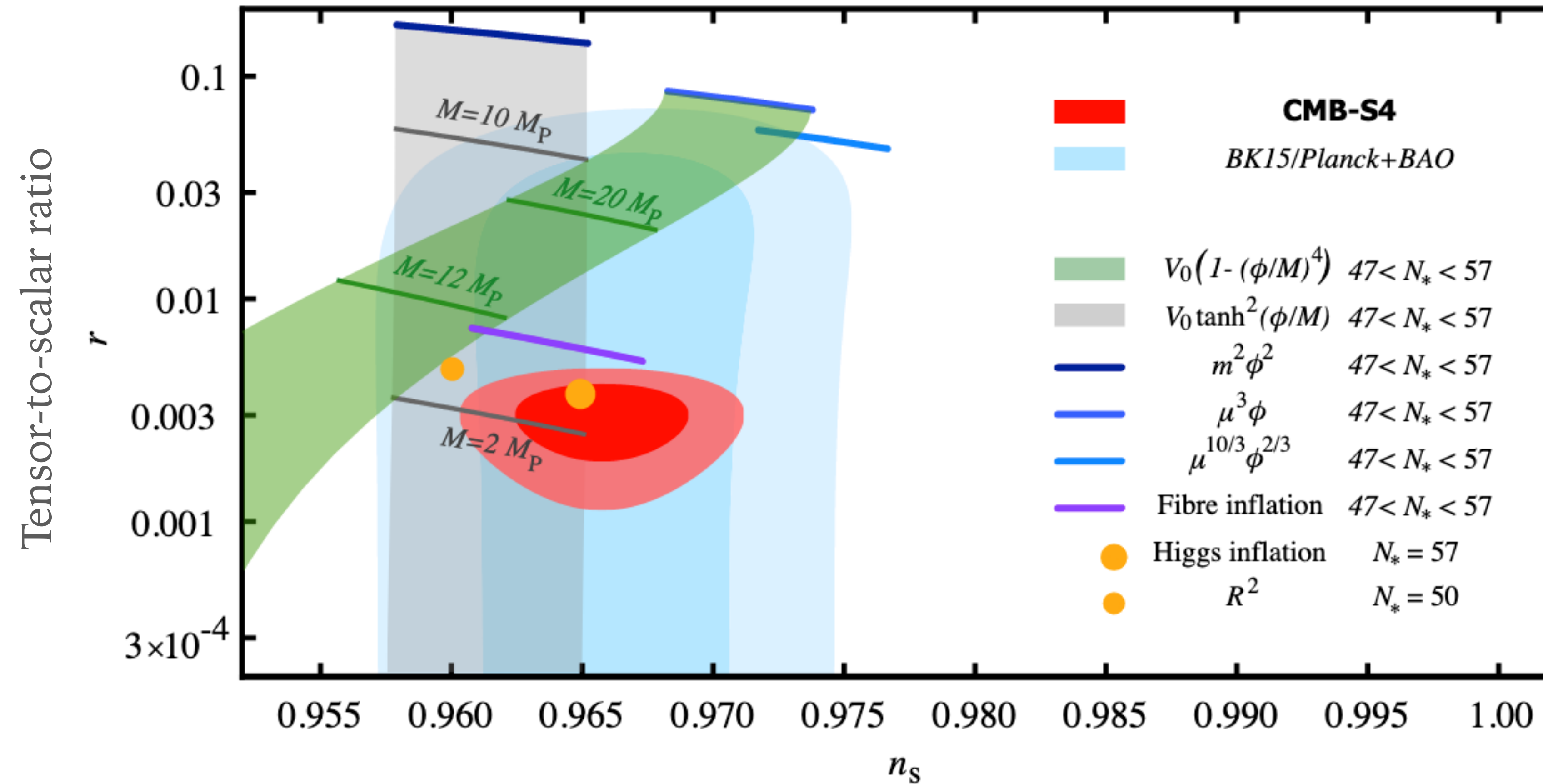
Fluctuation power



- To leading order, B-modes sourced only by primordial gravitational waves
Kamionkowski + 97 , Seljak & Zaldarriaga 97
- Statistically isotropic, Gaussian random field
 $r < 0.044$ *Planck + BICEP/Keck*

CONSTRAINING INFLATION THROUGH THE CMB

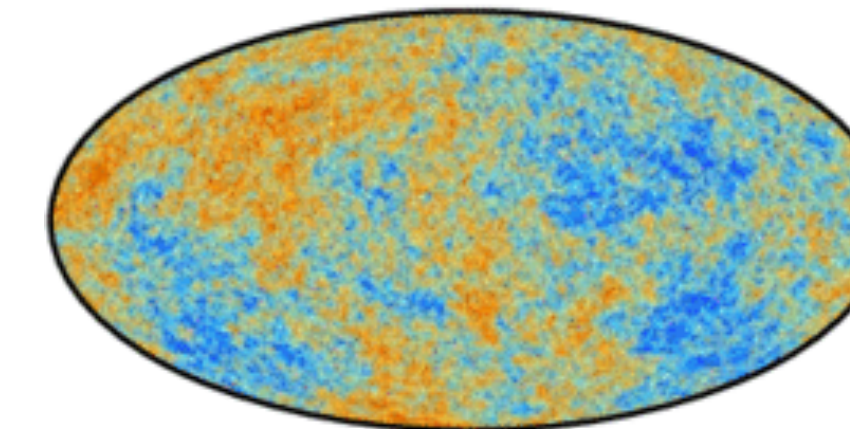
CMB-S4, arXiv:1907.04473



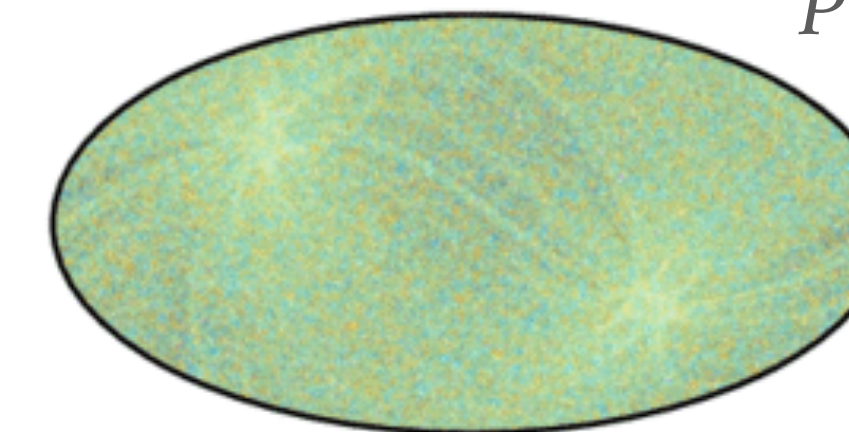
Spectral index of primordial (scalar) perturbations

BUT...

We don't observe the primordial CMB:

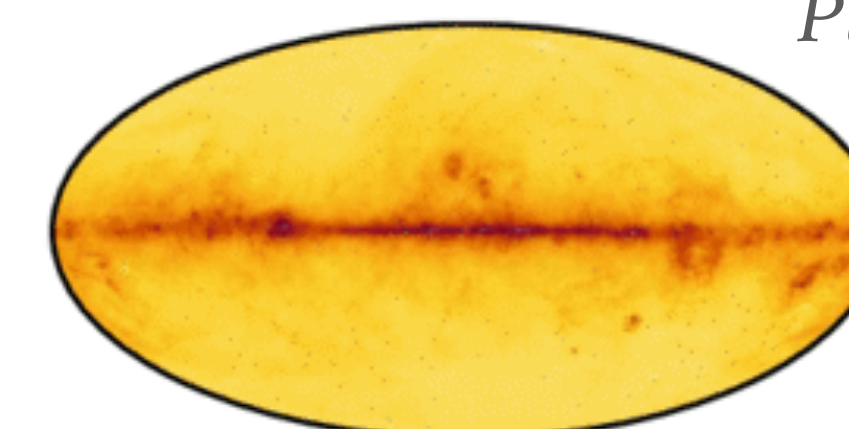


We must deal with:



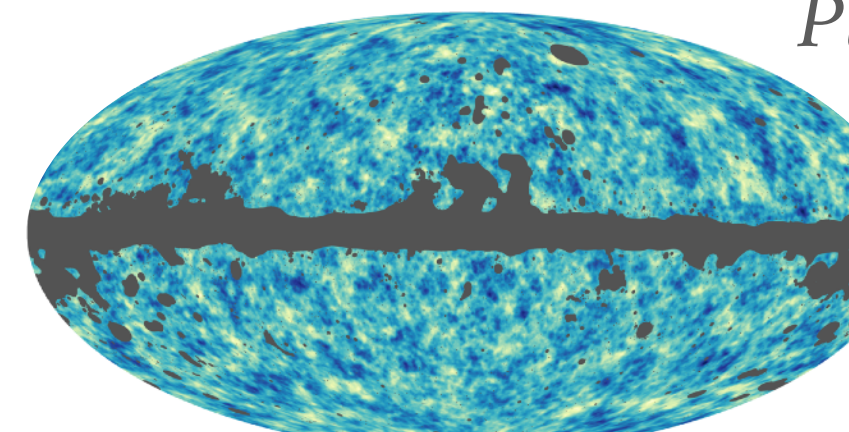
Planck FFP8 sims

- Experiment noise



Planck FFP8 sims

- Foreground emission (Atmospheric, Galactic and extra-Galactic)



Planck 20

- Lensing — Most of this talk. A nuisance, but also a blessing!

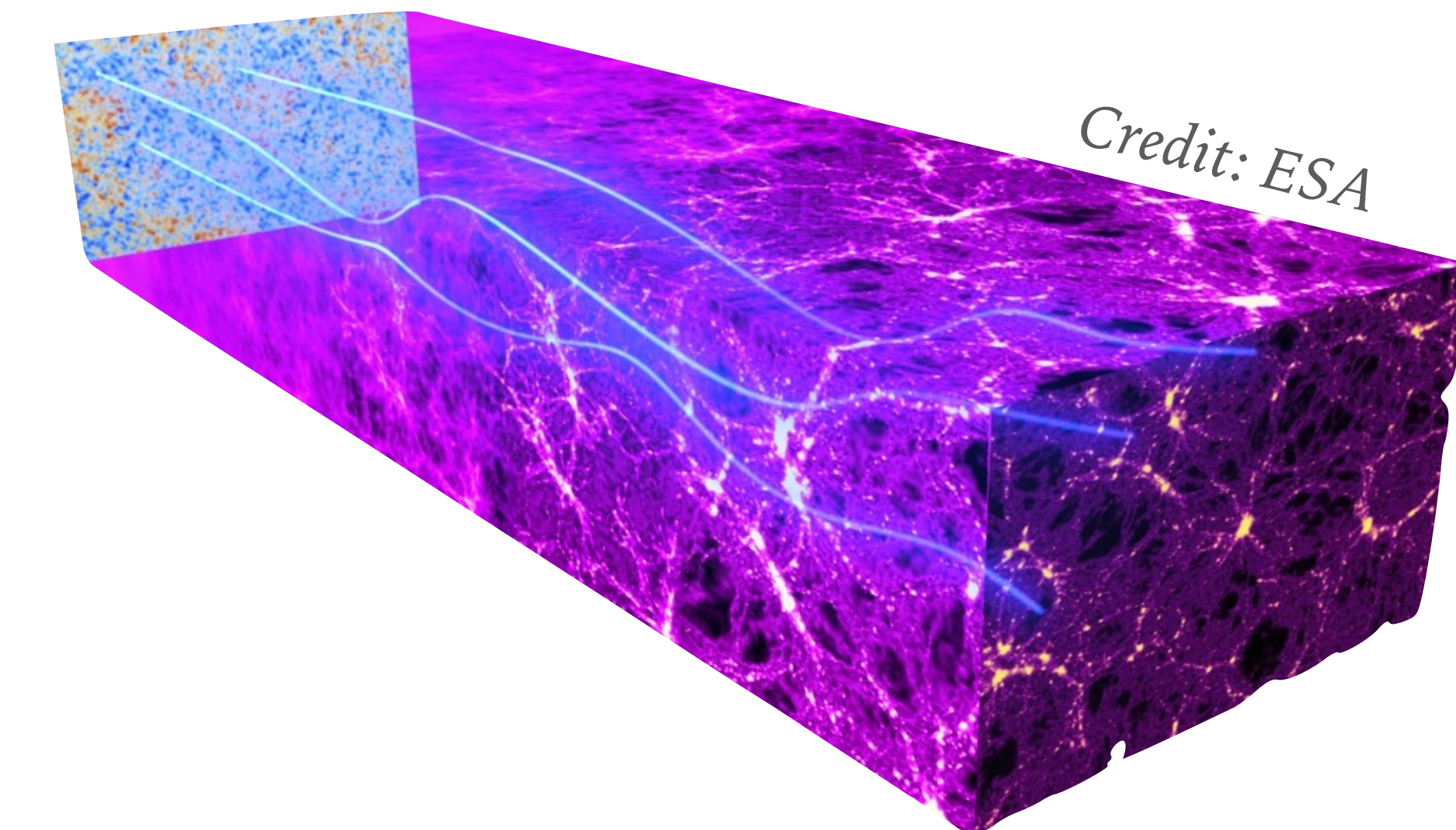
CMB LENSING

Very accurately described as:

$$\tilde{T}(\mathbf{x}) = T(\mathbf{x} + \alpha(\mathbf{x}))$$

$$\tilde{Q}(\mathbf{x}) = Q(\mathbf{x} + \alpha(\mathbf{x}))$$

$$\tilde{U}(\mathbf{x}) = U(\mathbf{x} + \alpha(\mathbf{x}))$$

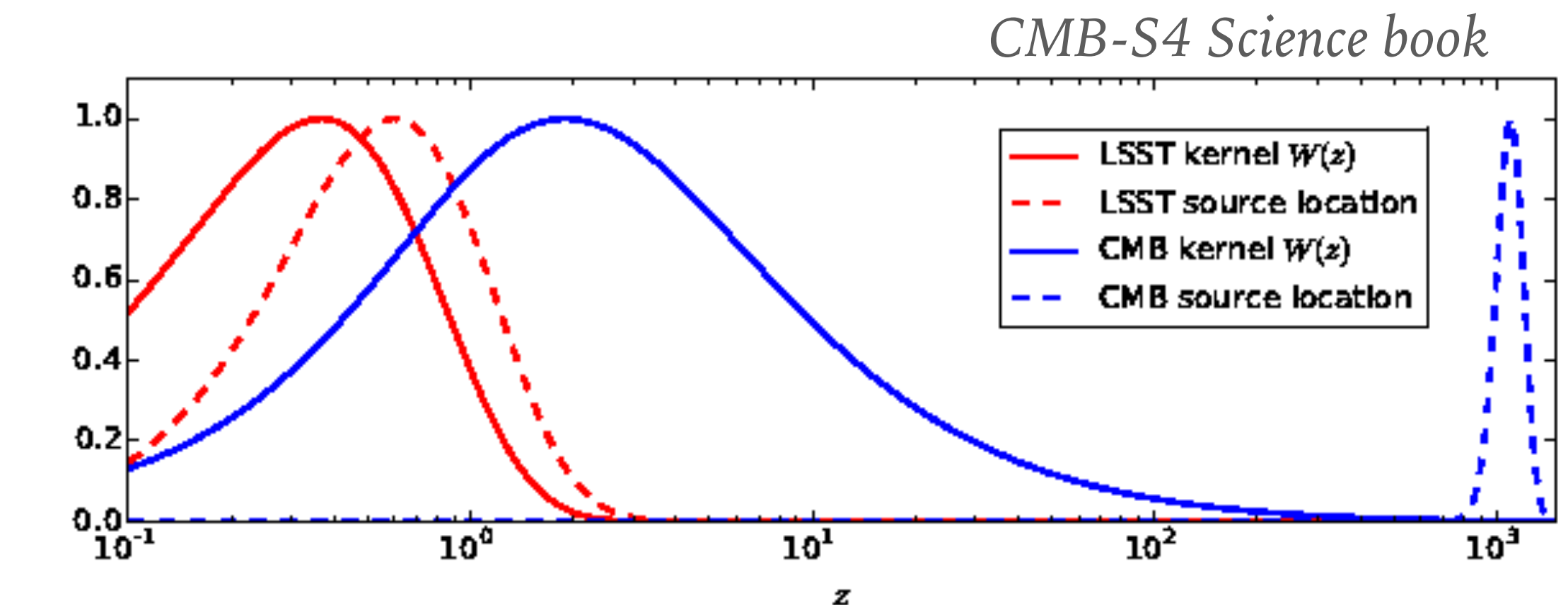


Under the Born approximation, $\alpha(\mathbf{x}) = \nabla \phi(\mathbf{x})$, where

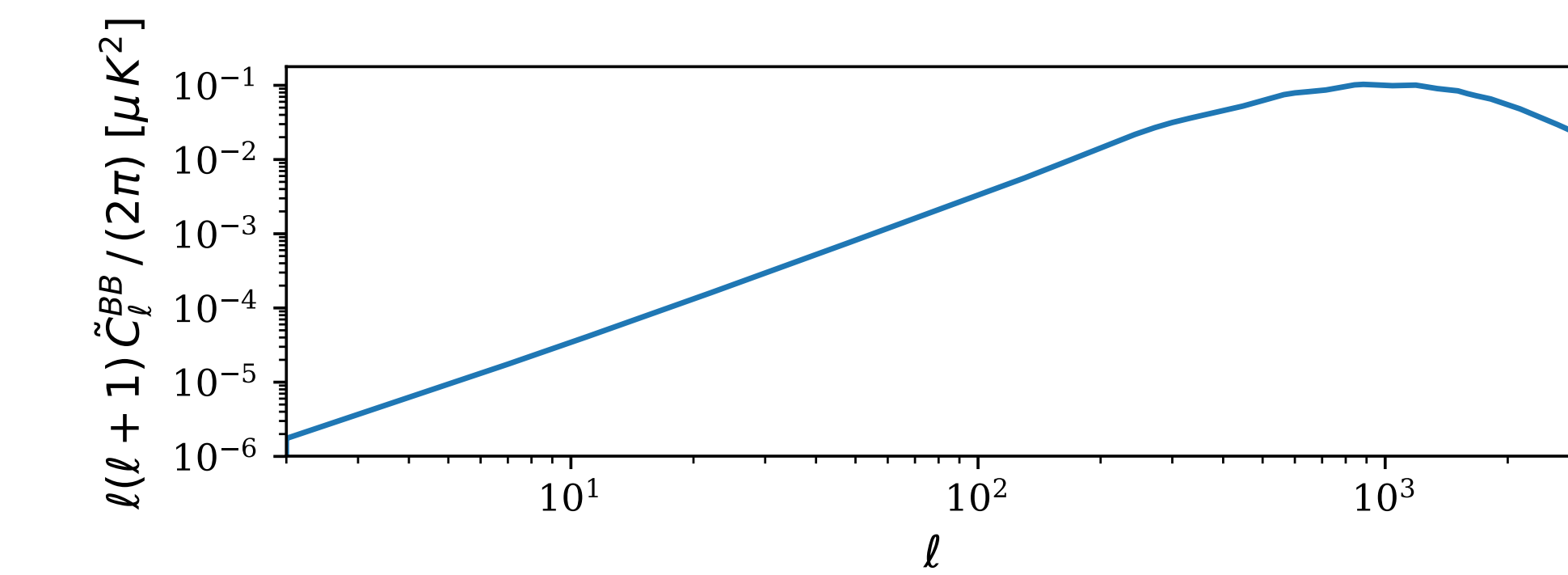
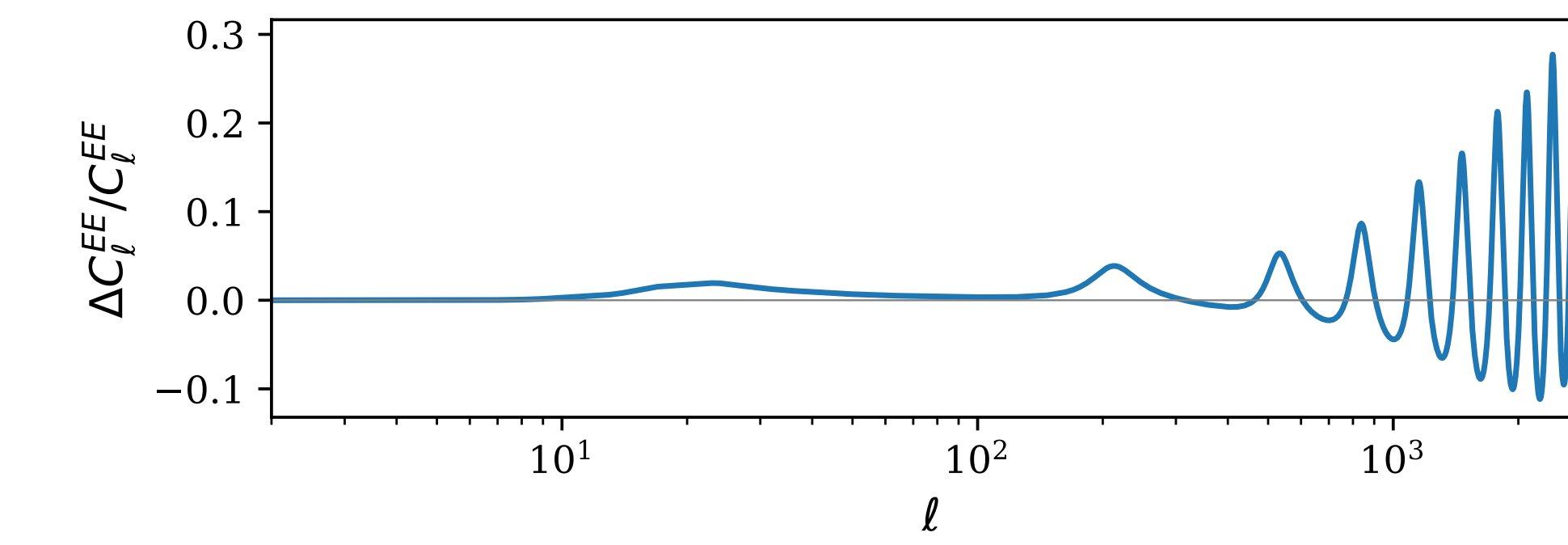
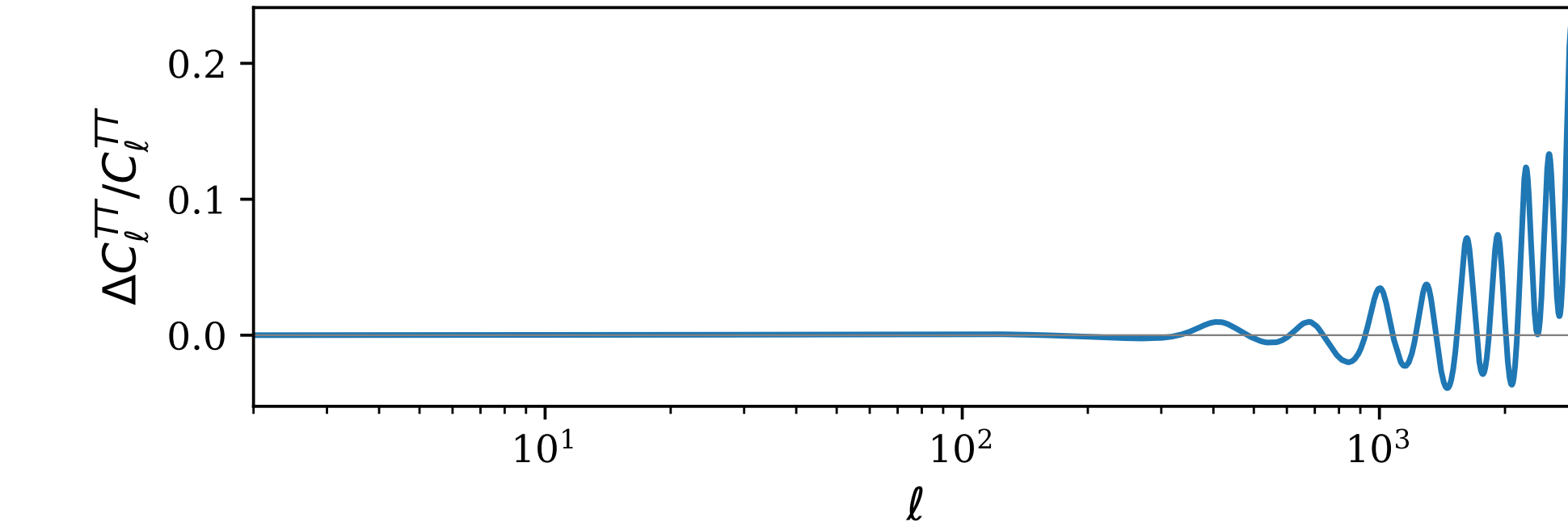
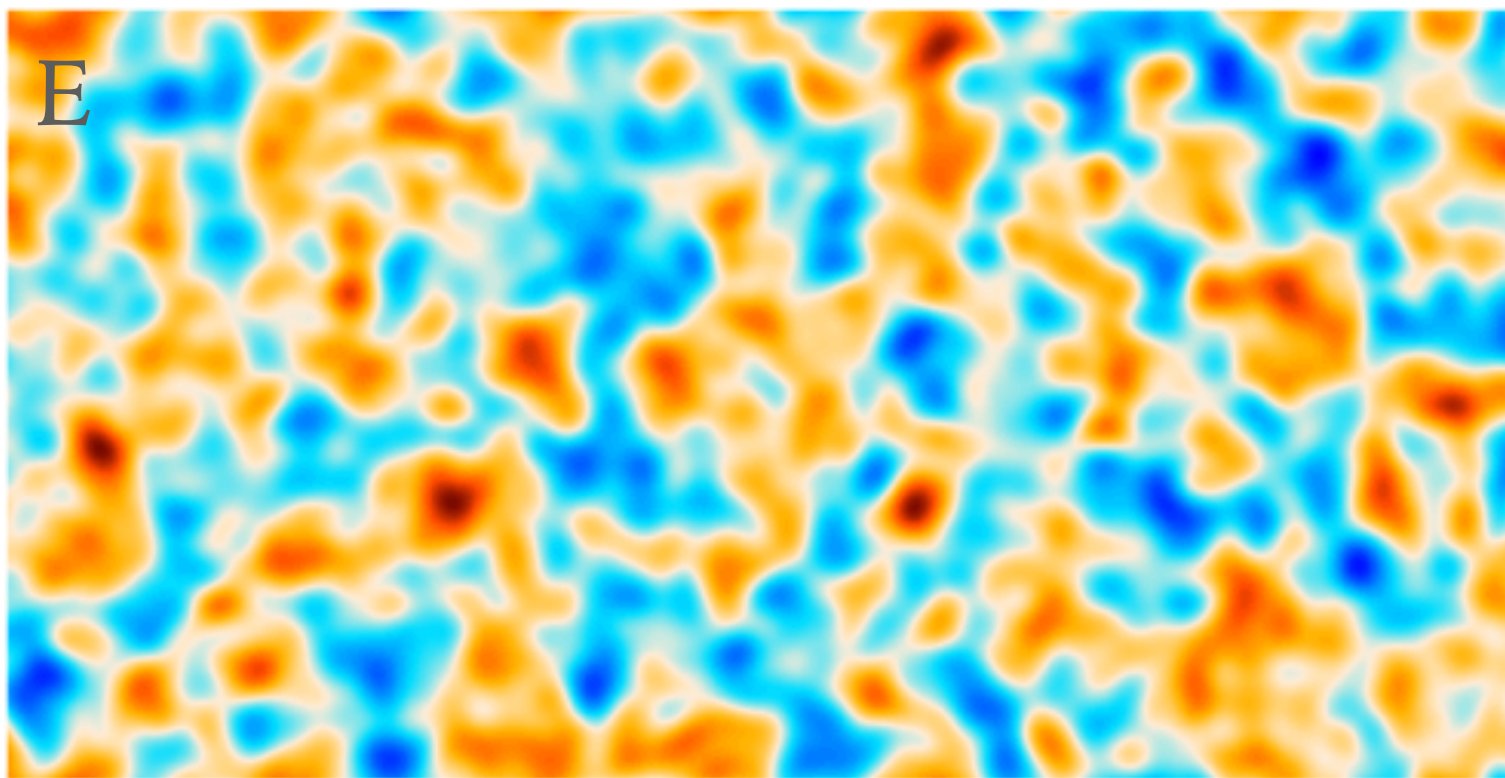
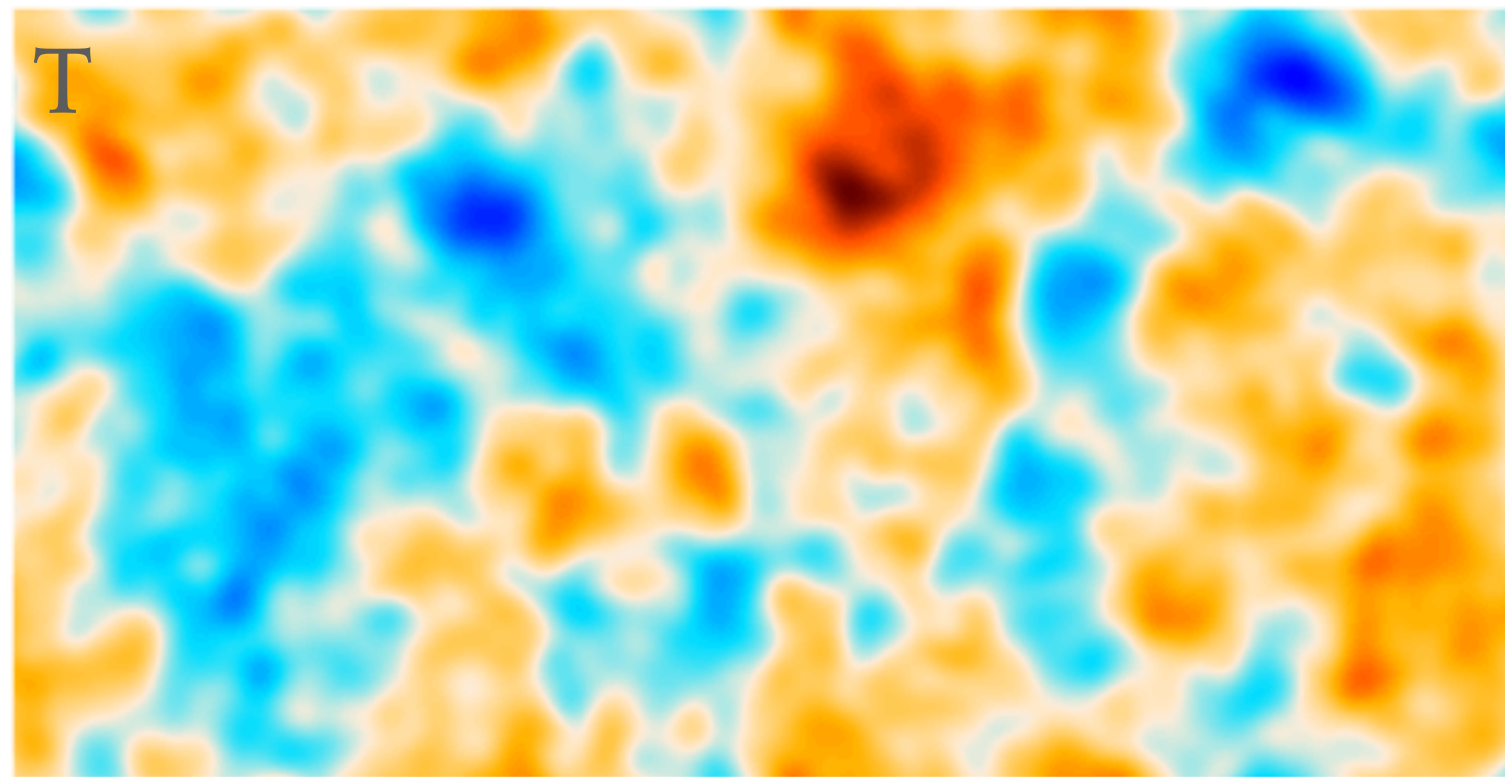
$$\phi(\mathbf{x}) = -2 \int_0^\chi d\chi g(\chi, \chi_*) \Psi(\chi \mathbf{x}, \eta_0 - \chi)$$

is related to $\kappa = -\frac{1}{2} \nabla^2 \phi$.

$\alpha \sim \text{arcmin}$, coherent on degree scales (typical lens $O(100\text{Mpc})$)



CMB LENSING



INTERNAL RECONSTRUCTIONS OF CMB LENSING

Unlensed CMB is statistically isotropic:

$$\langle T(\mathbf{l})T(\mathbf{l}') \rangle_{CMB} = (2\pi)^2 \delta^2(\mathbf{l} + \mathbf{l}') \tilde{C}_l^{TT}$$

Lensing induces statistical anisotropy:

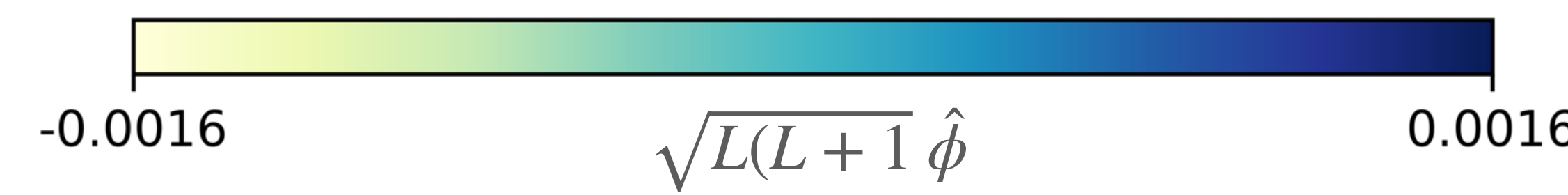
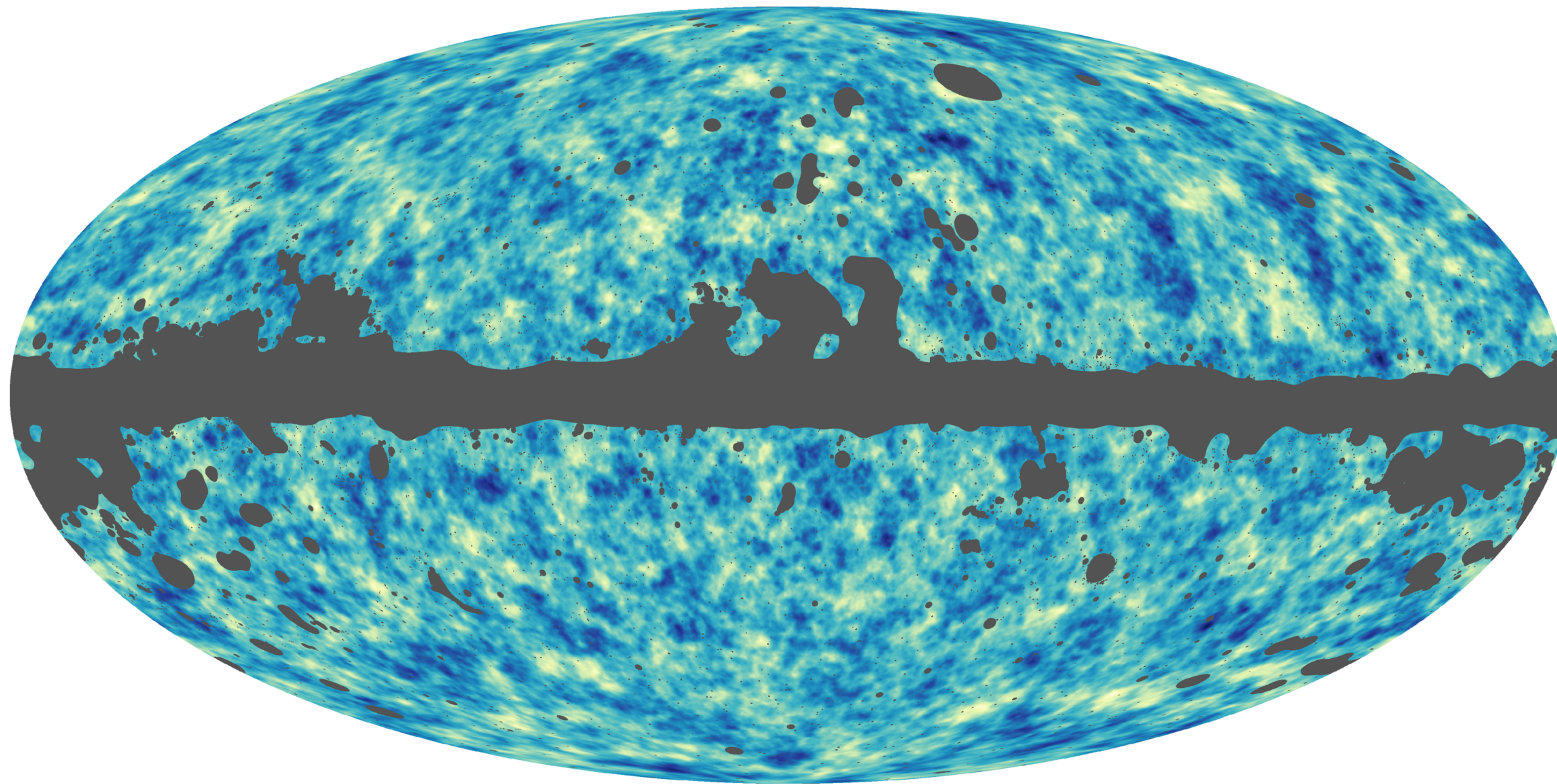
$$\langle \tilde{T}(\mathbf{l})\tilde{T}(\mathbf{l}') \rangle_{CMB} = f^{TT}(\mathbf{l}, \mathbf{l}') \phi(\mathbf{l} + \mathbf{l}')$$

In practice, off-diagonal correlations probe the lensing potential. The **quadratic estimator**:

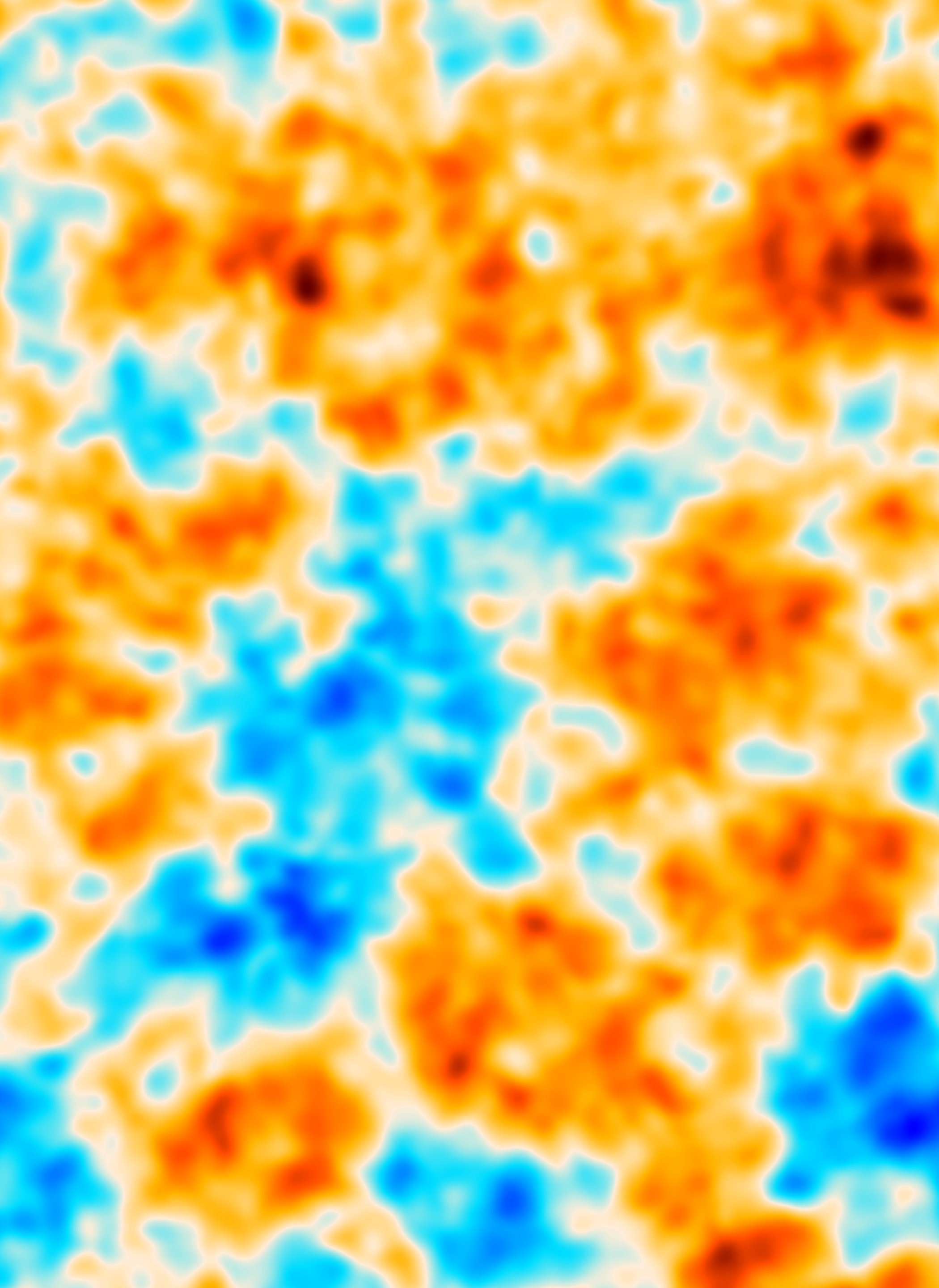
$$\hat{\phi}^{TT}(\mathbf{L}) \equiv N(\mathbf{L}) \int \frac{d^2\mathbf{l}}{2\pi} \tilde{T}(\mathbf{l}) \tilde{T}^*(\mathbf{l} - \mathbf{L}) g(\mathbf{l}, \mathbf{L}) \quad Hu \& Okamoto 01$$

Much more information in the polarization (particularly in small-scale *B*-modes).

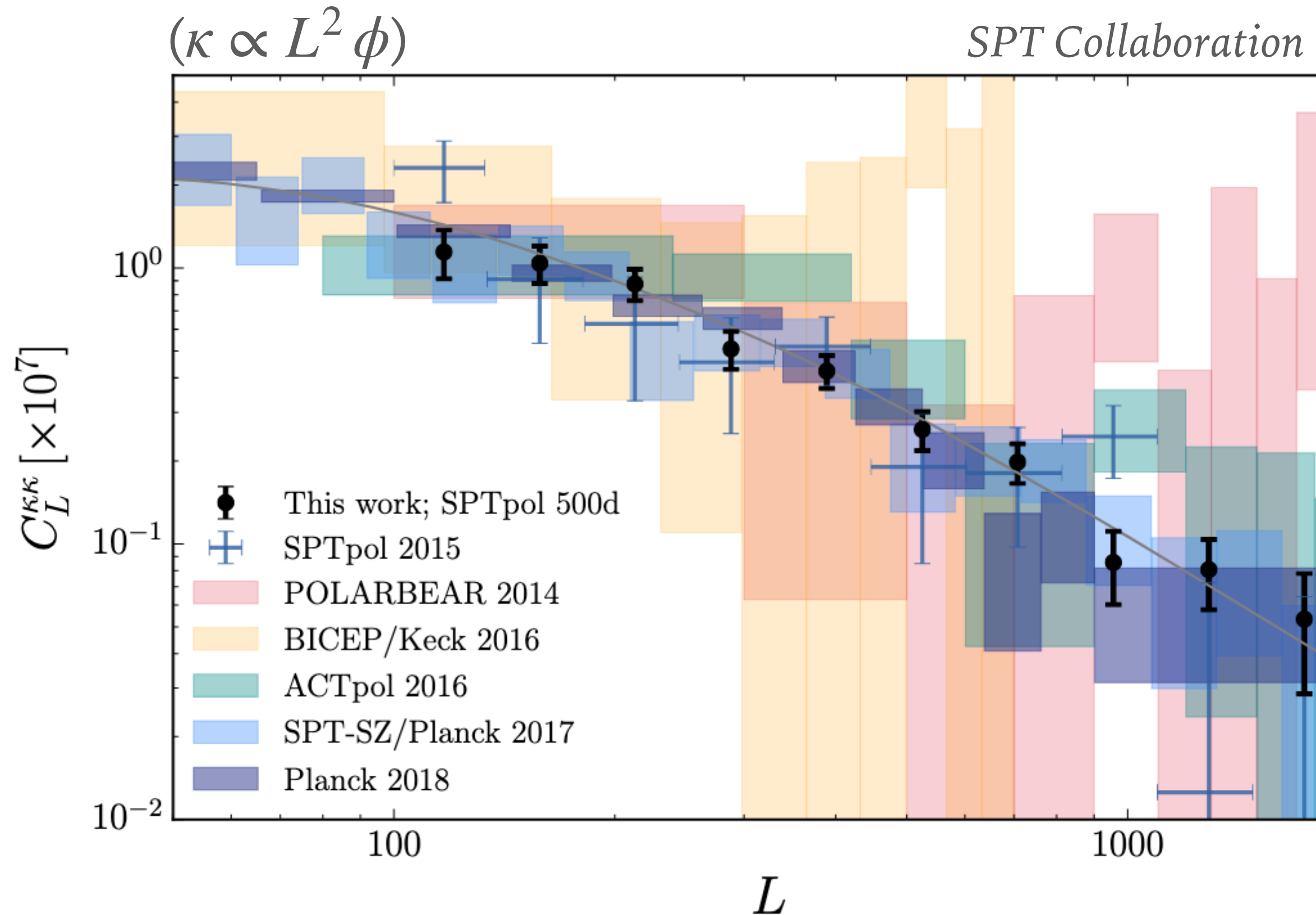
PLANCK'S LENSING RECONSTRUCTION



CMB LENSING SPECTRA



CMB LENSING SPECTRA



Breaks degeneracy among late-time Physics in primary CMB

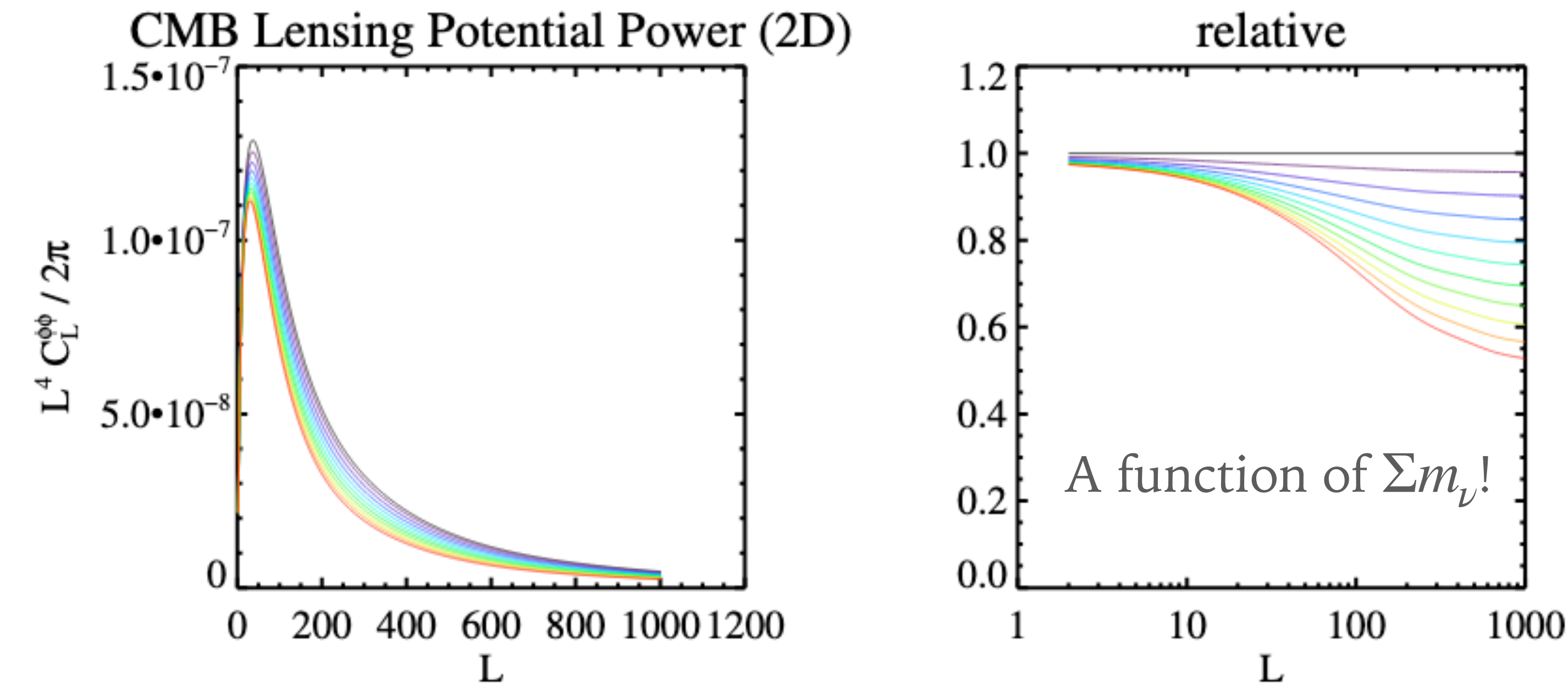
Auto- and cross-correlations probe geometry, neutrino masses, dark energy + +

Cross-correlations useful to calibrate photo-z's and weak lensing shear estimators

Vallinoto 11, Das+14, Schaan+ 17, ...

CMB LENSING CONSTRAINTS OF NEUTRINO MASSES

Massive ν 's cause suppression of power on small scales relative to large scales



SO + DESI
SO forecasts 19

$$\left. \begin{array}{l} \sigma(\Sigma m_\nu) \approx 31 - 33 \text{ meV} \text{ (with current } \tau \text{ prior)} \\ \sigma(\Sigma m_\nu) \approx 17 - 22 \text{ meV (with CLASS/LiteBird } \tau \text{ prior)} \end{array} \right\} \xrightarrow{\quad} \text{Guaranteed detection!} \quad (\Sigma m_\nu > 60 \text{ meV})$$

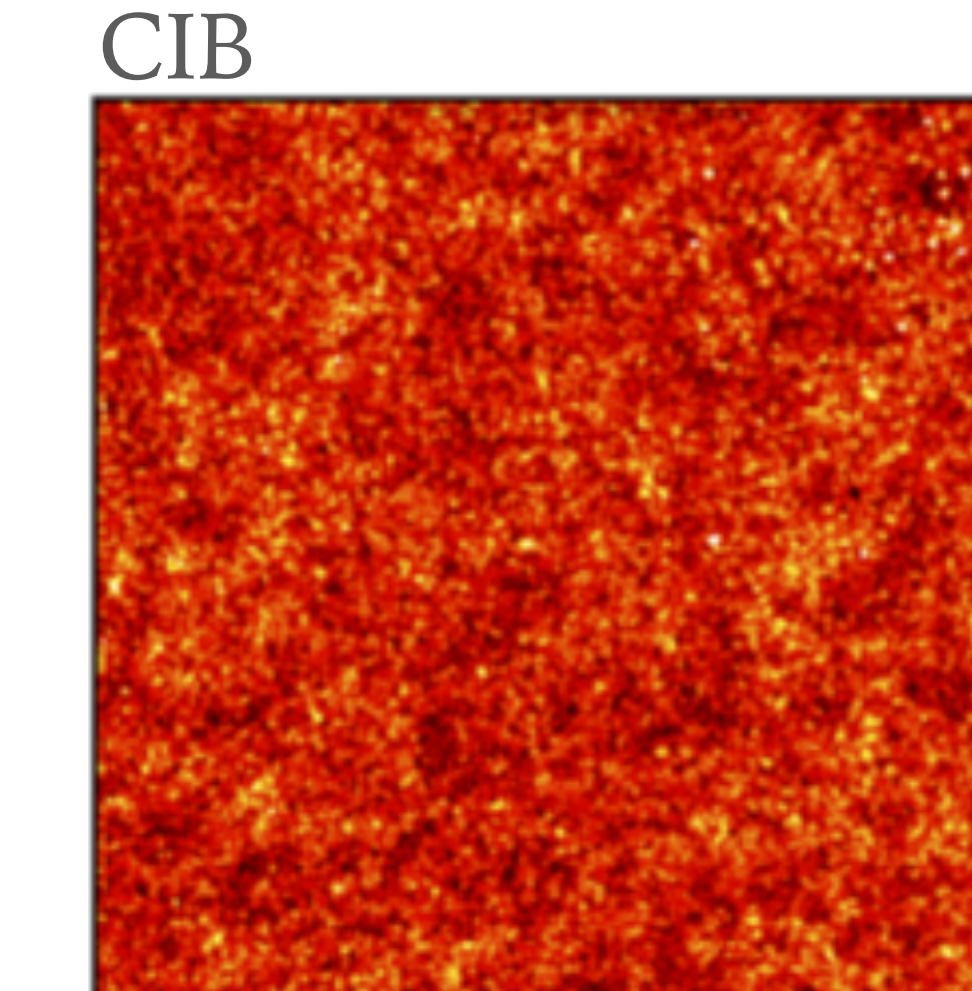
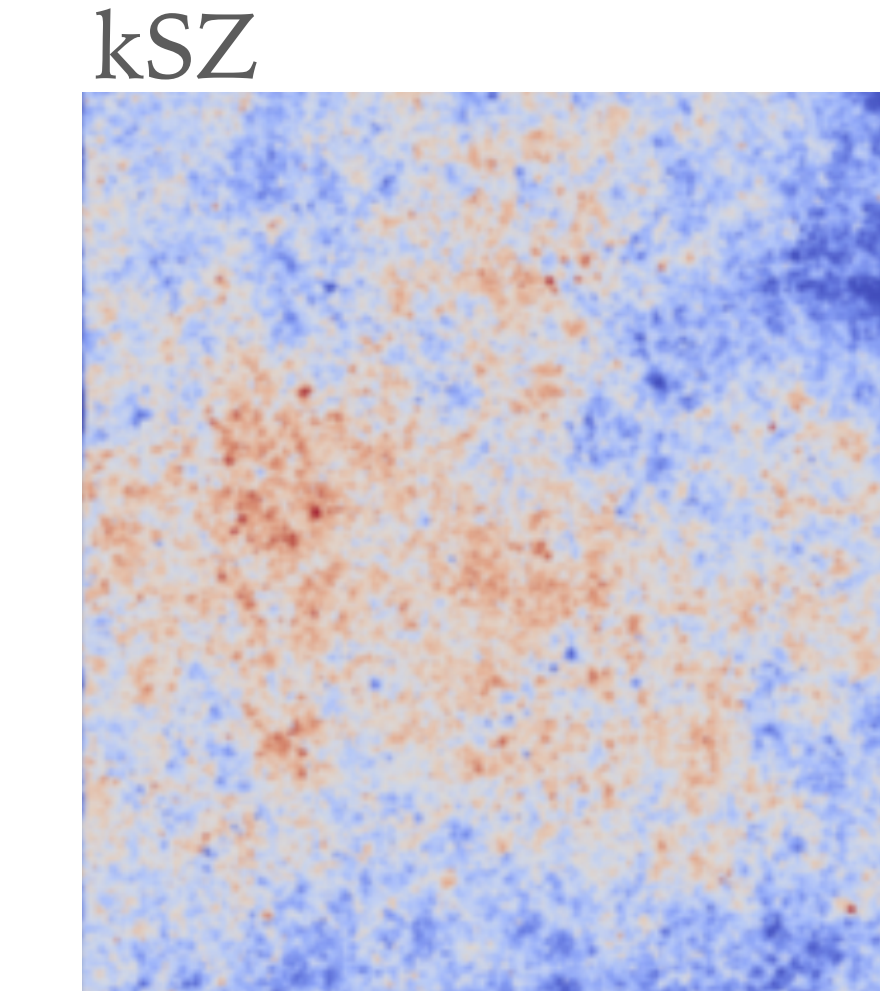
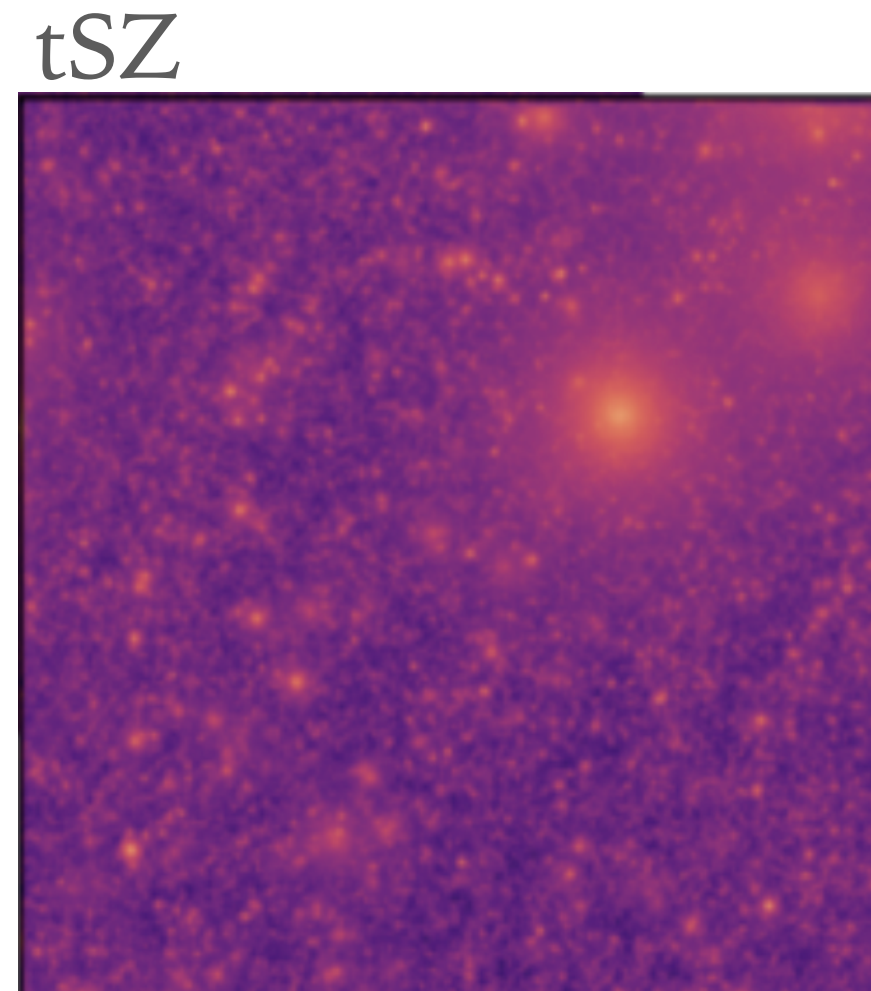
Cross-correlations show great promise (also for $\sigma_8, f_{\text{nl}}, +$) — can partially get around τ prior

LENSING POWER SPECTRUM MEASUREMENTS

- ✓ Modeling: very easy — little non-linearities, negligible baryonic effects, no galaxy bias
- ✓ Foregrounds: polarization-based reconstructions very robust

- ⚠ Temperature reconstructions still important for Stage-2 & 3 CMB (AdvACT, Simons Array, SO...)
- ⚠ In intensity, microwave sky contaminated by non-Gaussian extragalactic sources: tSZ, kSZ, CIB

Van Engelen+14, Osborne+14, Ferraro & Hill 18



Adapted from WebSky

BIASES TO LENSING SPECTRA FROM EXTRAGALACTIC FOREGROUNDS

$$\hat{\phi} = \hat{\phi}[\tilde{T} + s, \tilde{T} + s]$$

Lensing Foreground (correlated with ϕ)


Can bias lensing reconstruction power spectrum

$$\langle \hat{\phi} \hat{\phi} \rangle = \langle \hat{\phi}[\tilde{T}, \tilde{T}] \hat{\phi}[\tilde{T}, \tilde{T}] \rangle + 2 \langle \hat{\phi}[\tilde{T}, \tilde{T}] \hat{\phi}[s, s] \rangle + 4 \langle \hat{\phi}[\tilde{T}, s] \hat{\phi}[\tilde{T}, s] \rangle + \langle \hat{\phi}[s, s] \hat{\phi}[s, s] \rangle$$

“Primary bispectrum bias”


“Secondary bispectrum bias”

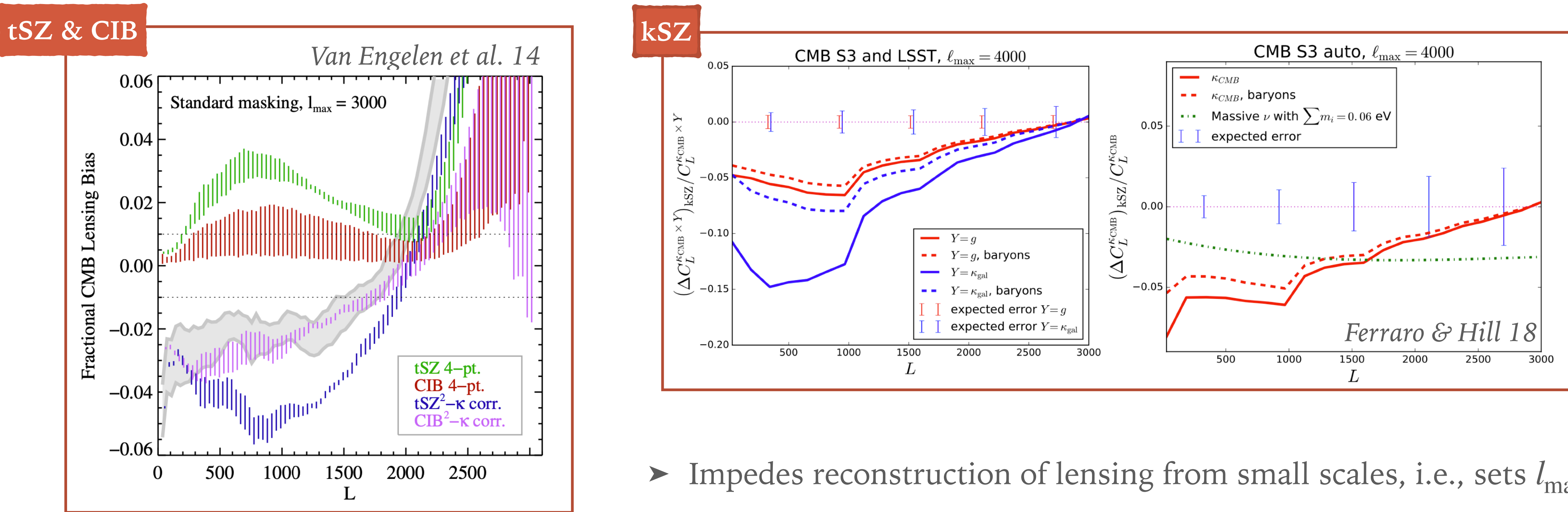

“Trispectrum bias”


and cross-correlations with low-z matter tracers

$$\langle g[\phi] \hat{\phi} \rangle = \langle g[\phi] \hat{\phi}[\tilde{T}, \tilde{T}] \rangle + \langle g[\phi] \hat{\phi}[s, s] \rangle$$

“Bispectrum bias”


BIASES TO LENSING SPECTRA FROM EXTRAGALACTIC FOREGROUNDS



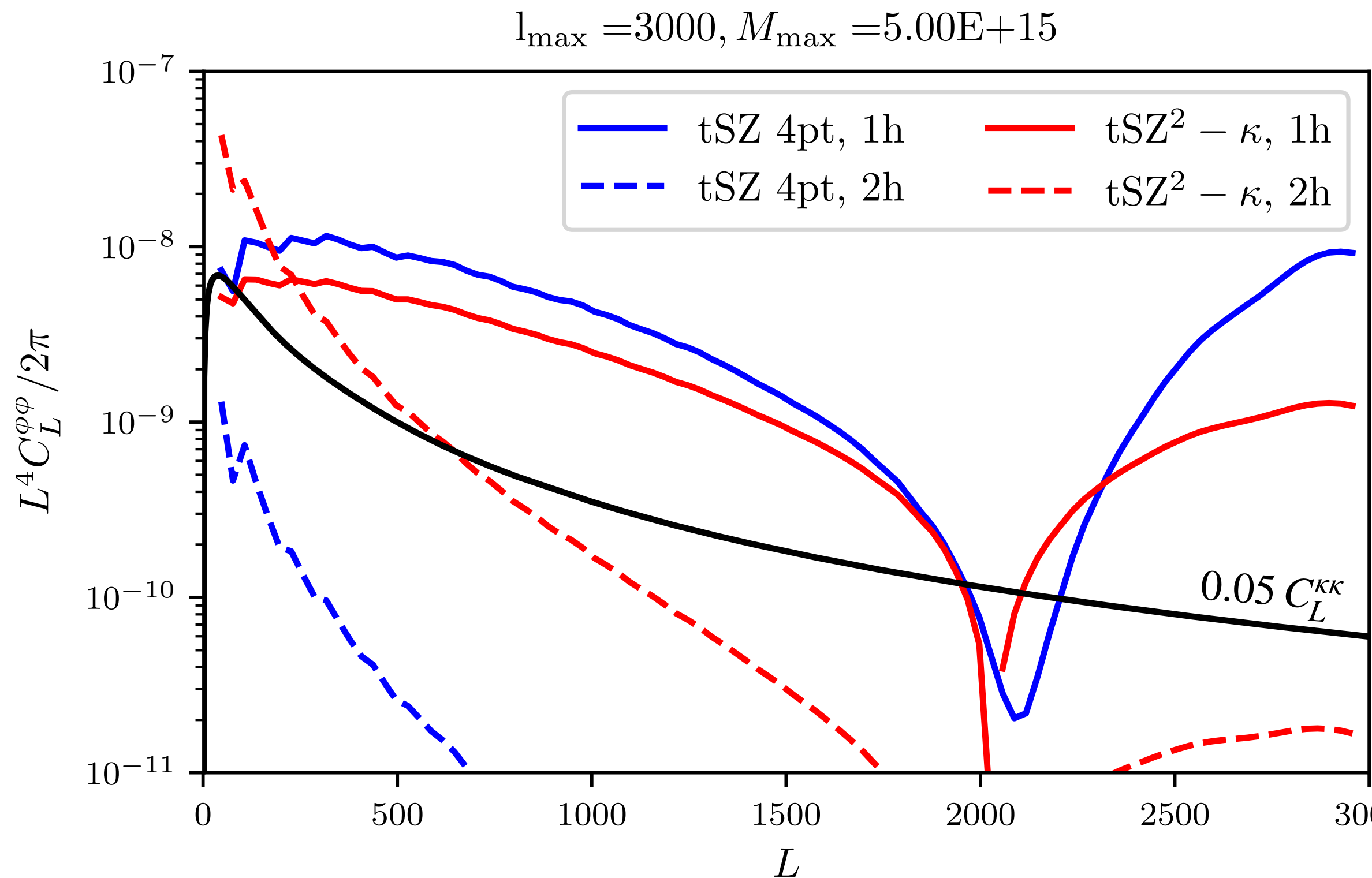
- Impedes reconstruction of lensing from small scales, i.e., sets l_{\max}

- Multi-frequency cleaning helps to some extent
- Mitigation techniques:
 - Simulations *Van Engelen+ 14*
 - Bias hardening *Namikawa+13, Osborne+14, Sailer+ 20*

- Cleaning of gradient leg in QE *Madhavacheril & Hill 18*
- Shear-only estimators *Schaan & Ferraro 18*

MODELING LENSING BIASES FROM EXTRAGALACTIC SOURCES

We calculate these biases analytically as a function of experimental sensitivity, resolution, point-source masking, etc, using a halo model prescription

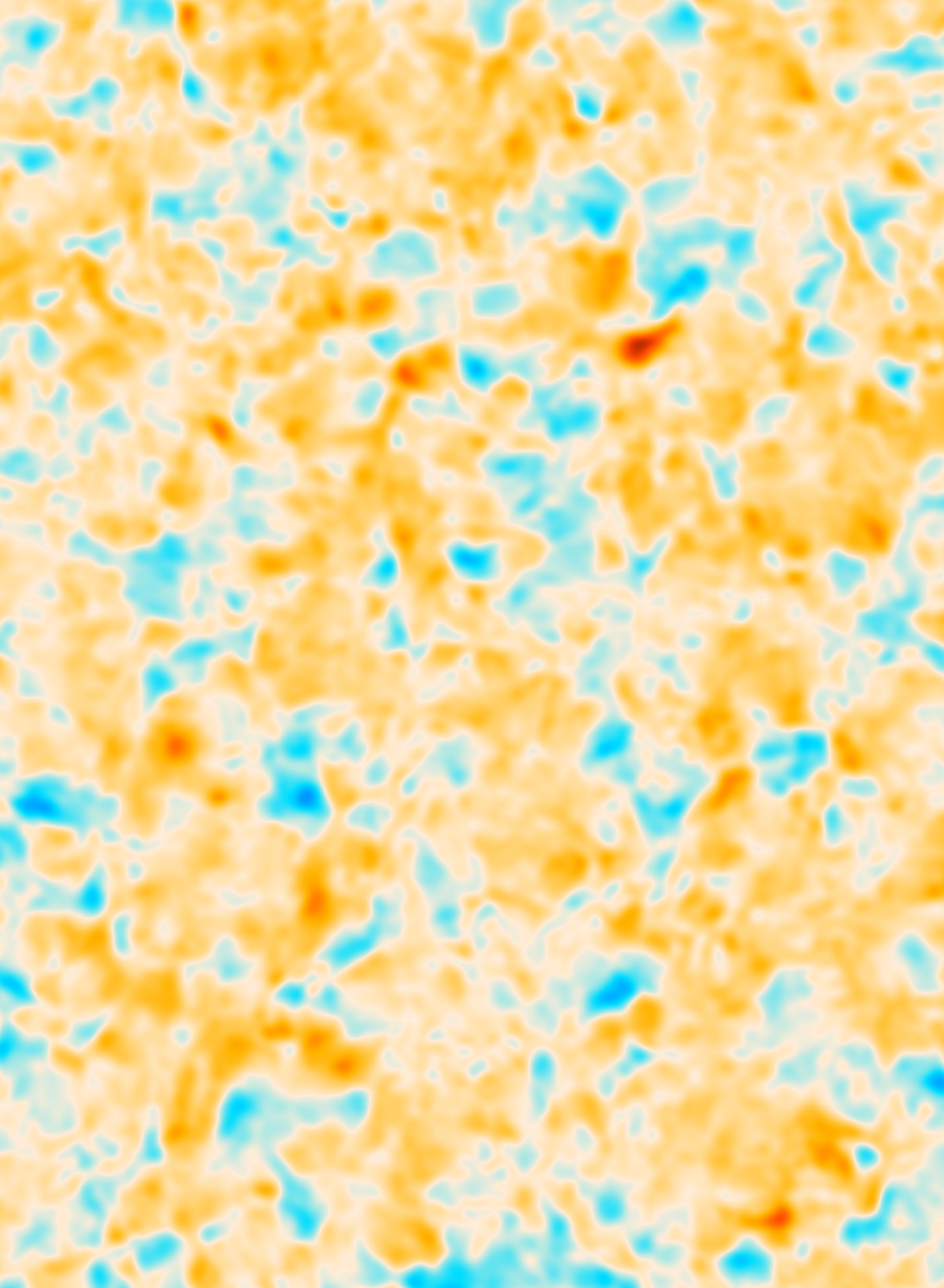


(Example: subset of tSZ biases for an SPT-like experiment)

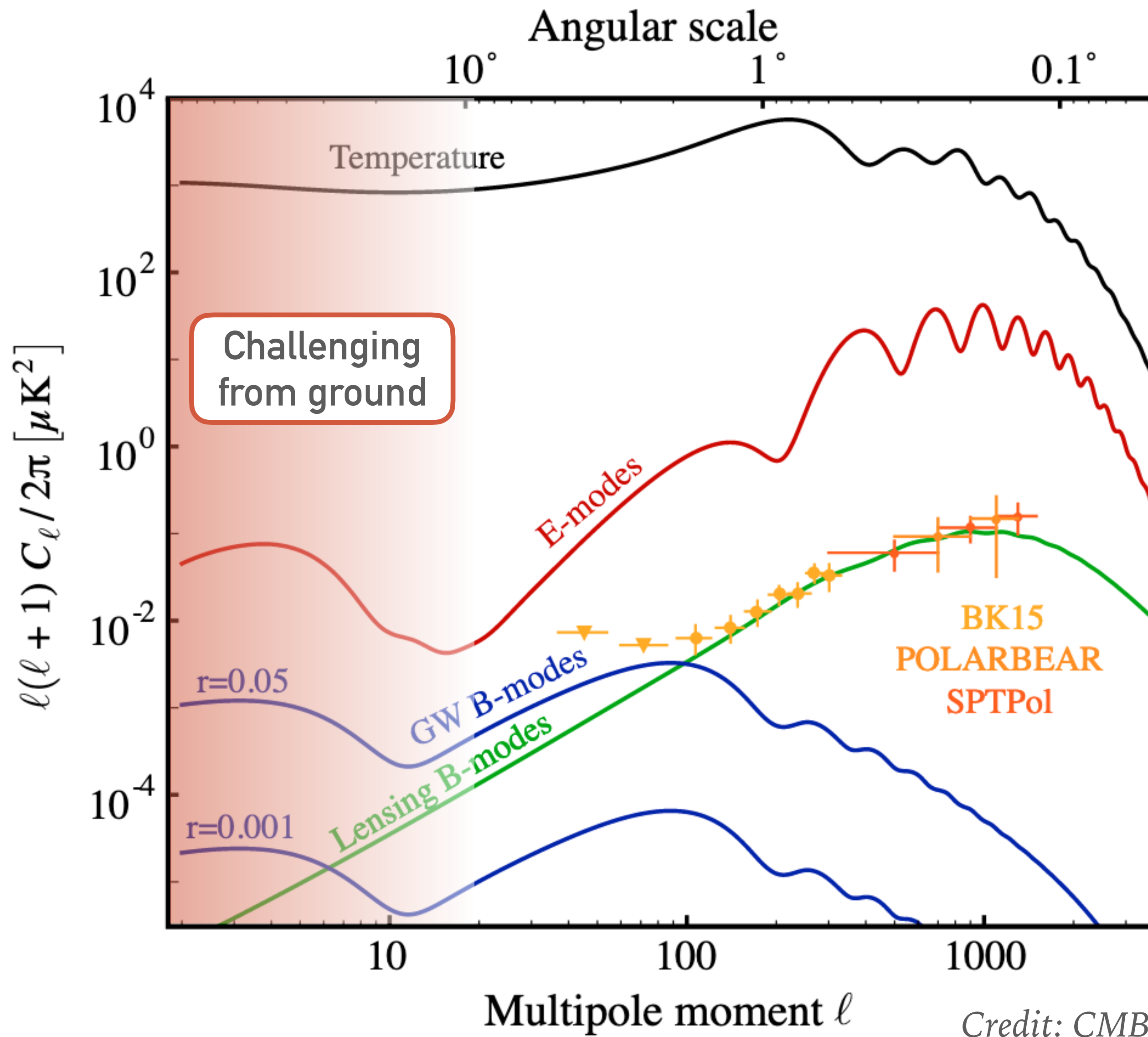
Preliminary

- Very fast, 1D method. Lensing reconstructions done using FFTlog (for fast, discrete Hankel transforms), taking $O(10\text{ms})$ per lensing reconstruction on a single laptop core.
- Can calculate biases and associated uncertainties
- Perhaps we could use QE down to smaller scales and correct bias at PS level?

DELENSING B-MODES



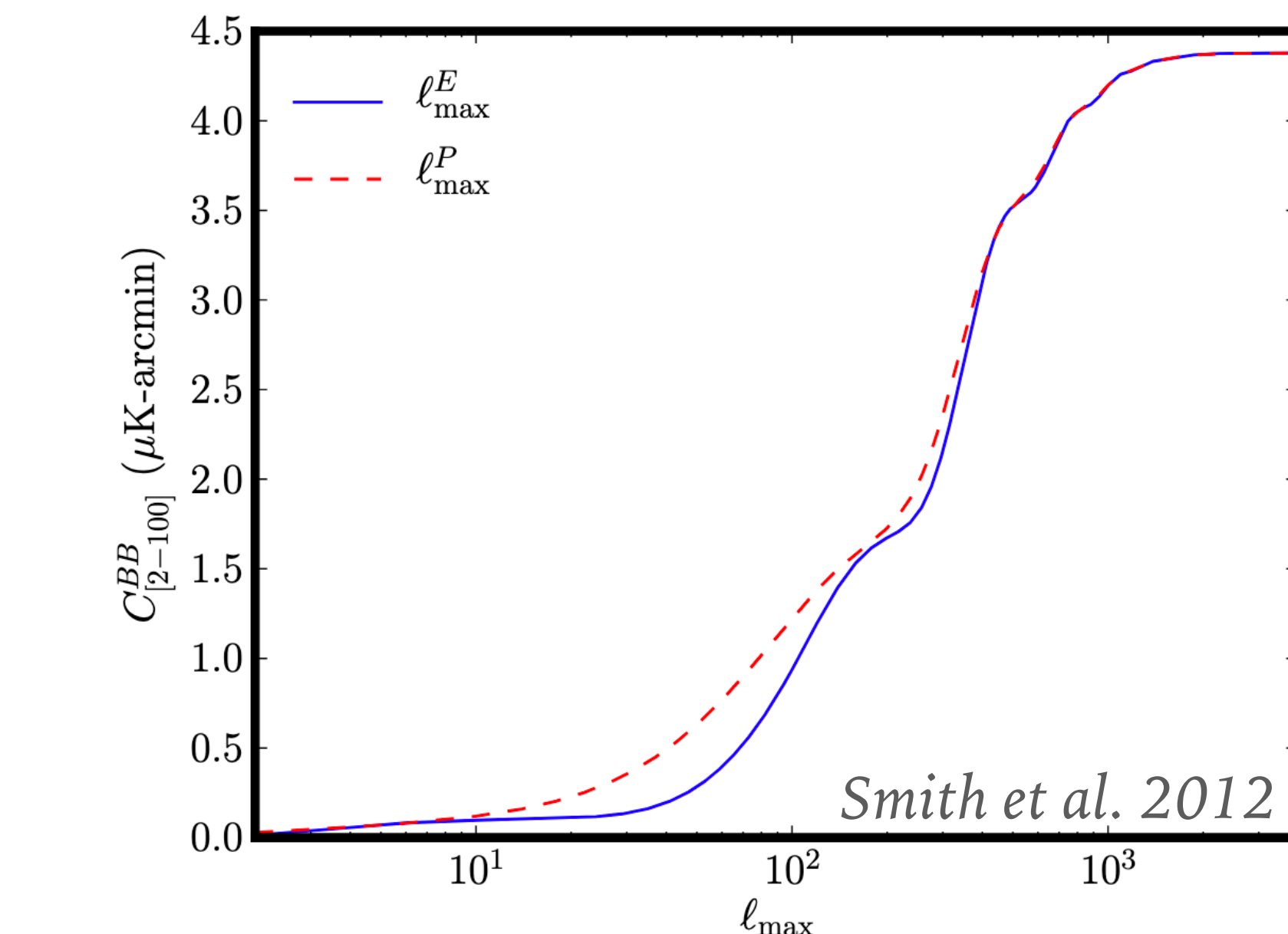
THE LENSING B-MODE



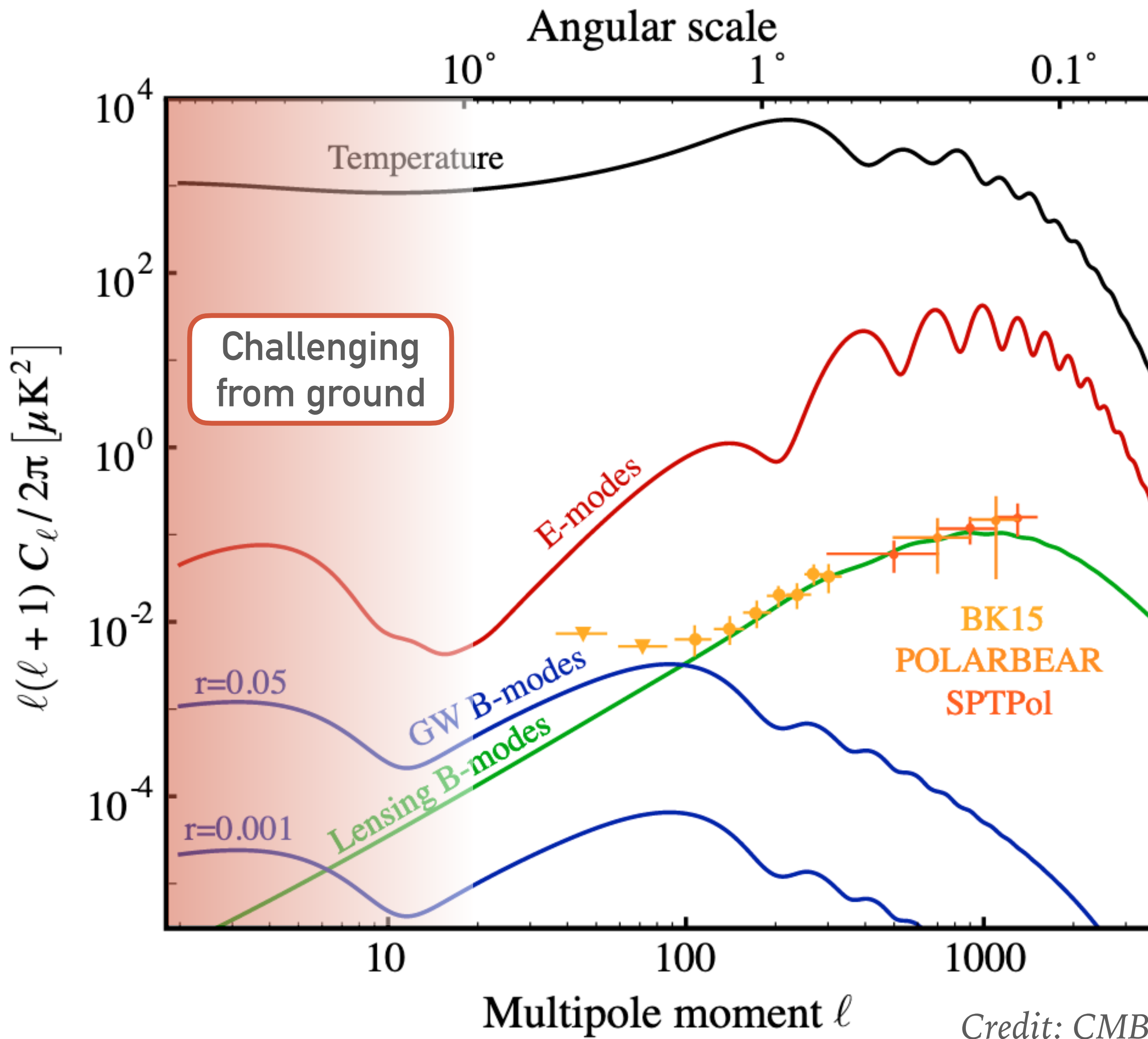
Lensing converts E- into B-modes, inducing noise with $\Delta_P \approx 5\mu\text{K arcmin}$

Zaldarriaga & Seljak 98

Why does it look like white noise?



THE LENSING B-MODE



Lensing converts E- into B-modes, inducing noise with $\Delta_P \approx 5\mu\text{K}\text{arcmin}$

Zaldarriaga & Seljak 98

$$\sigma(r) \propto C_l^{BB} + N_l^{BB}$$

- Primordial
- Foregrounds
- Lensing

For CMB-S4, delensing improves $\sigma(r)$ by $\times 5$ or more

B-MODE DELENSING

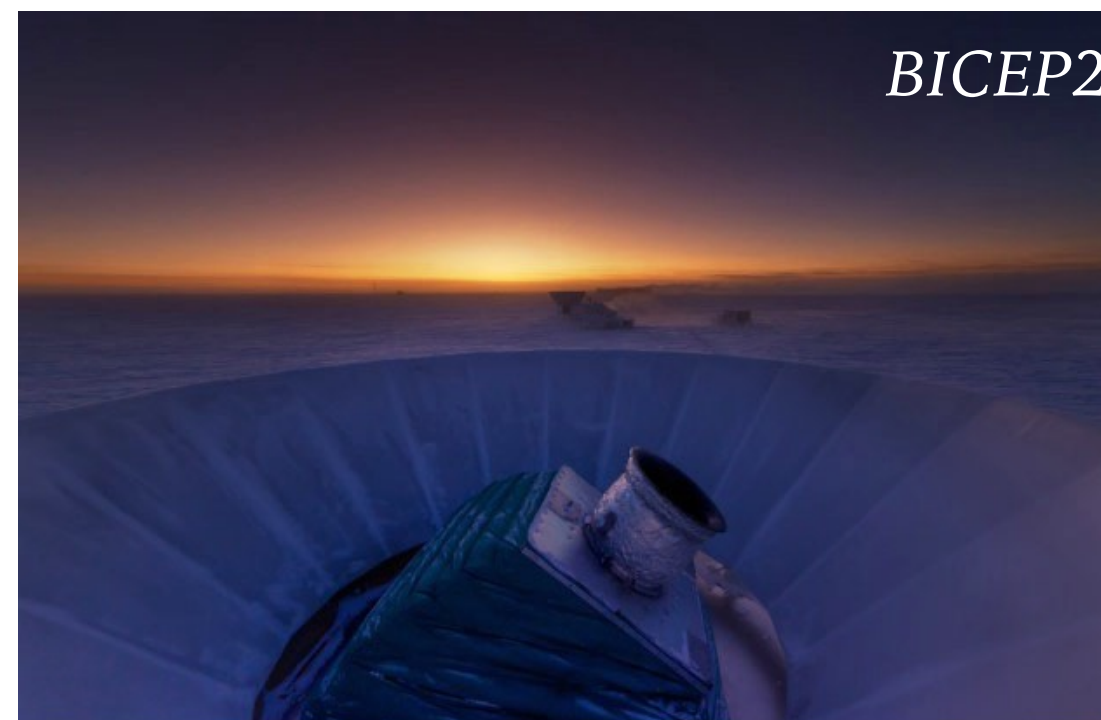
$$\text{Lensing: } \tilde{P}(\mathbf{x}) = P(\mathbf{x} + \alpha(\mathbf{x}))$$

$$\implies \text{Delensing: } P^{\text{del}}(\mathbf{x}) = \tilde{P}(\mathbf{x} + \alpha^{-1}(\mathbf{x})) \quad (\text{often } \alpha^{-1} \approx -\alpha)$$

Challenge: r goals require measuring both

- large (degree) angular scale B -modes, where primordial signal peaks
- intermediate & small scale lenses and E -modes, to delens those B -modes

Small
Aperture
Telescope
(SAT)



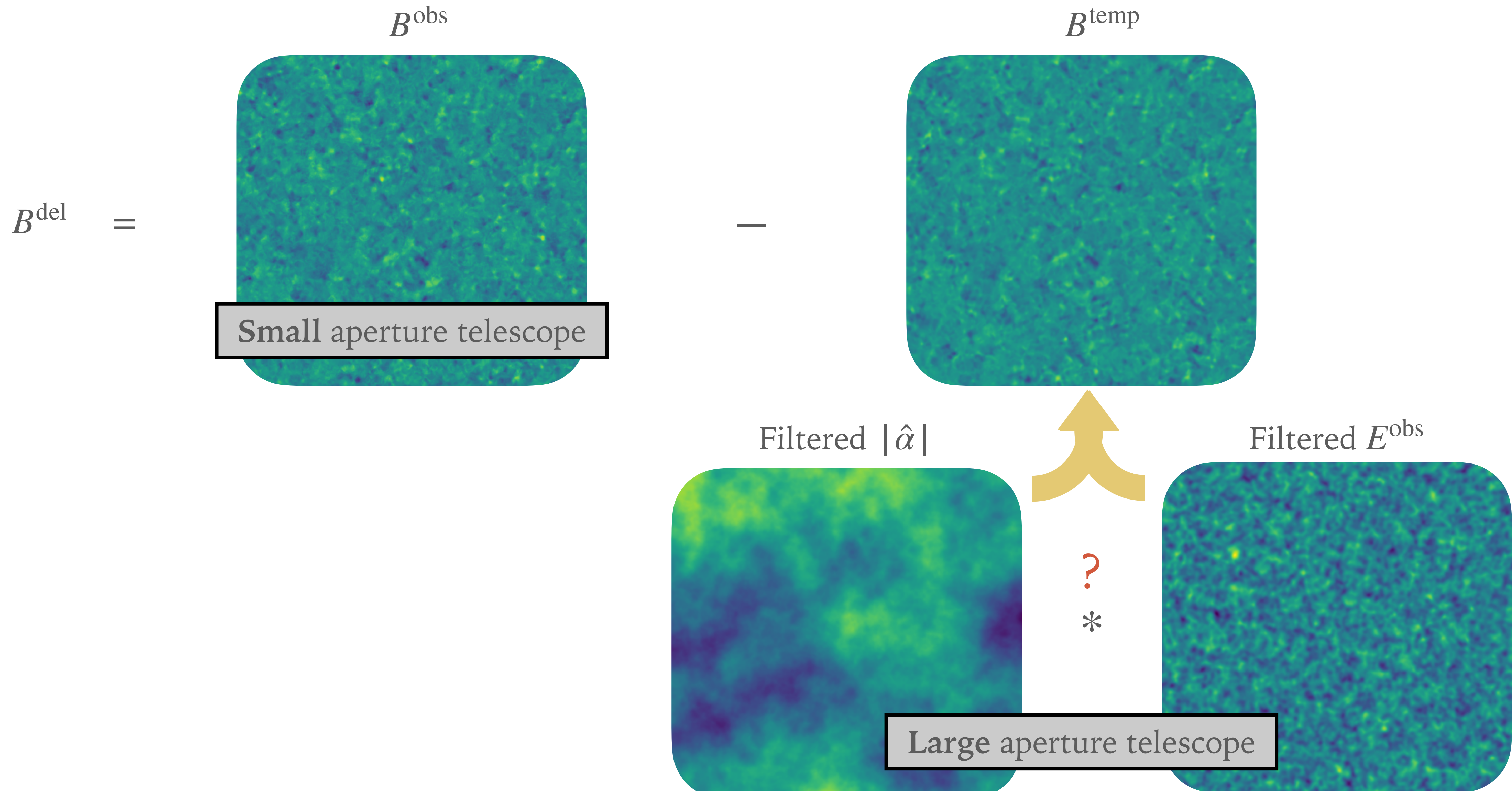
e.g., BICEP/Keck, SO SATs, CLASS, ABS, QUBIC...

Large
Aperture
Telescope
(LAT)



e.g., SPT, ACT, SO LAT, POLARBEAR/SA

B-MODE TEMPLATE DELENSING



HOW EXACTLY IS THE TEMPLATE BUILT?

The lensing B-mode is

$$\tilde{B} = E \circledast \phi + O(\phi^2) + \dots$$

So the template is often built to leading (“gradient”) order

$$B^{\text{temp}} = \bar{E}^{\text{obs}} \circledast \hat{\phi}. \quad \text{e.g., SPT 17}$$

Why?

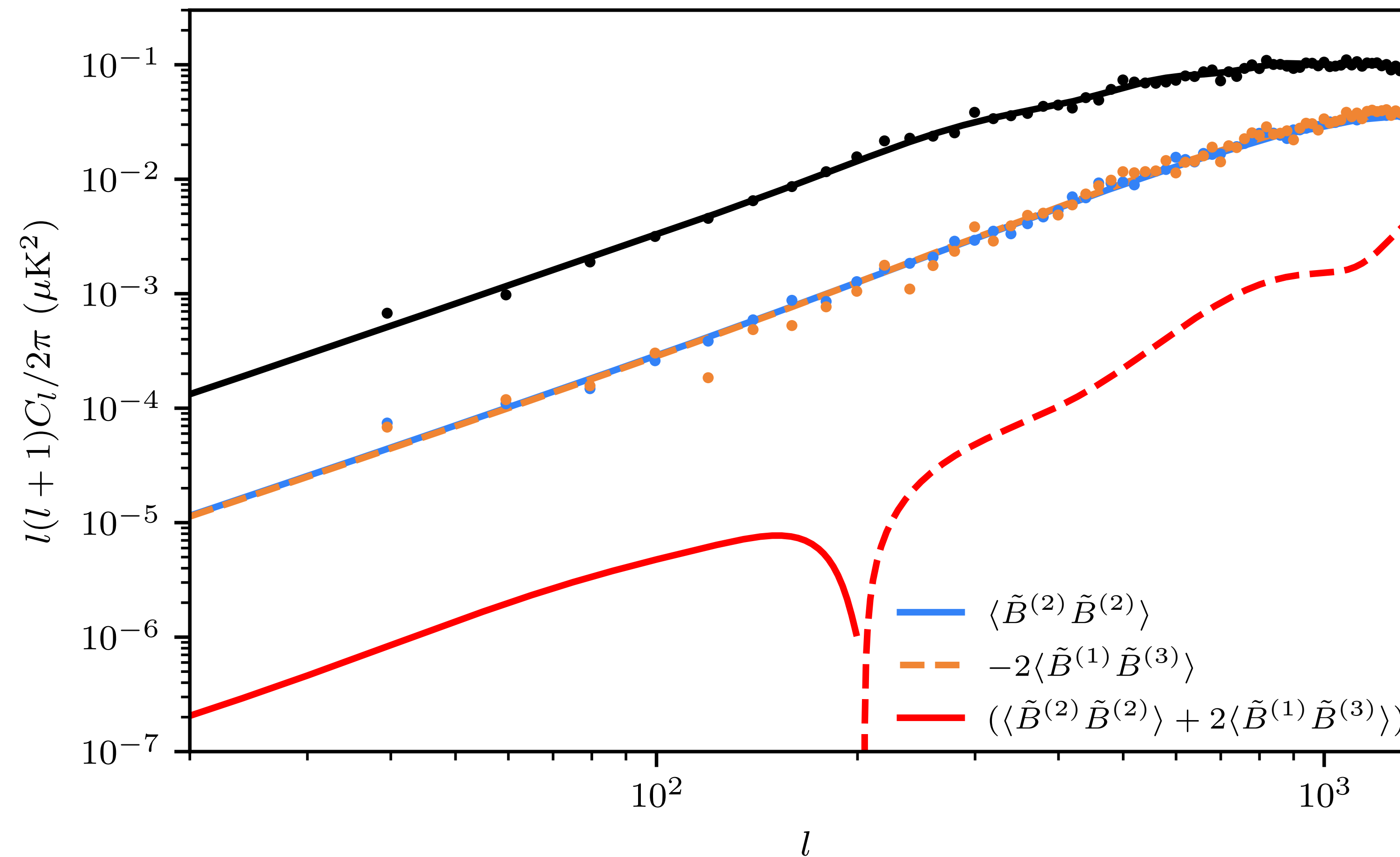
- Optimises strengths of LAT & SAT
- Analytically transparent (clear understanding of systematics)
- Template is assumed to track true B-modes very accurately

Non-perturbative template can also be built by deflecting observed E-modes directly:

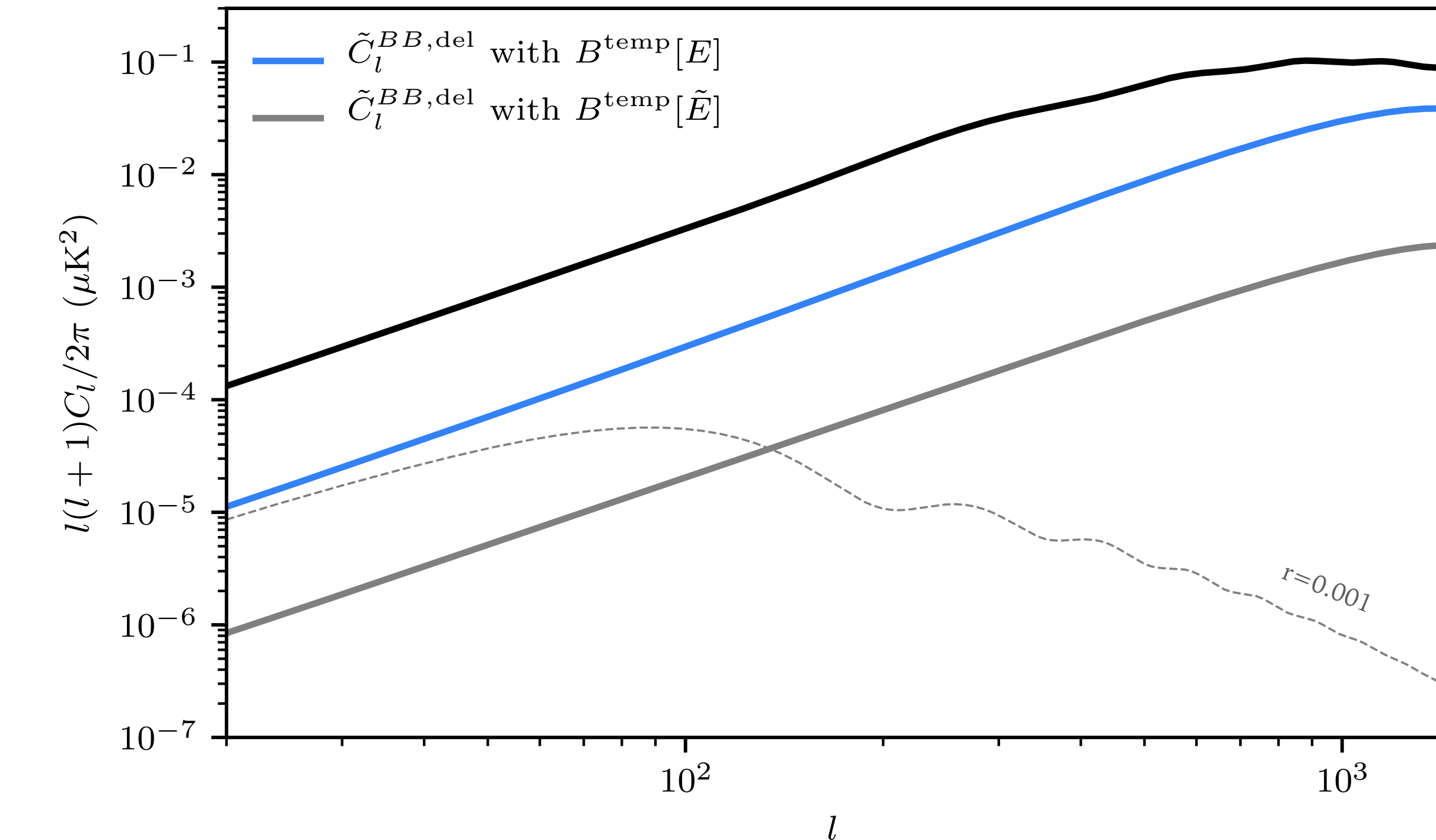
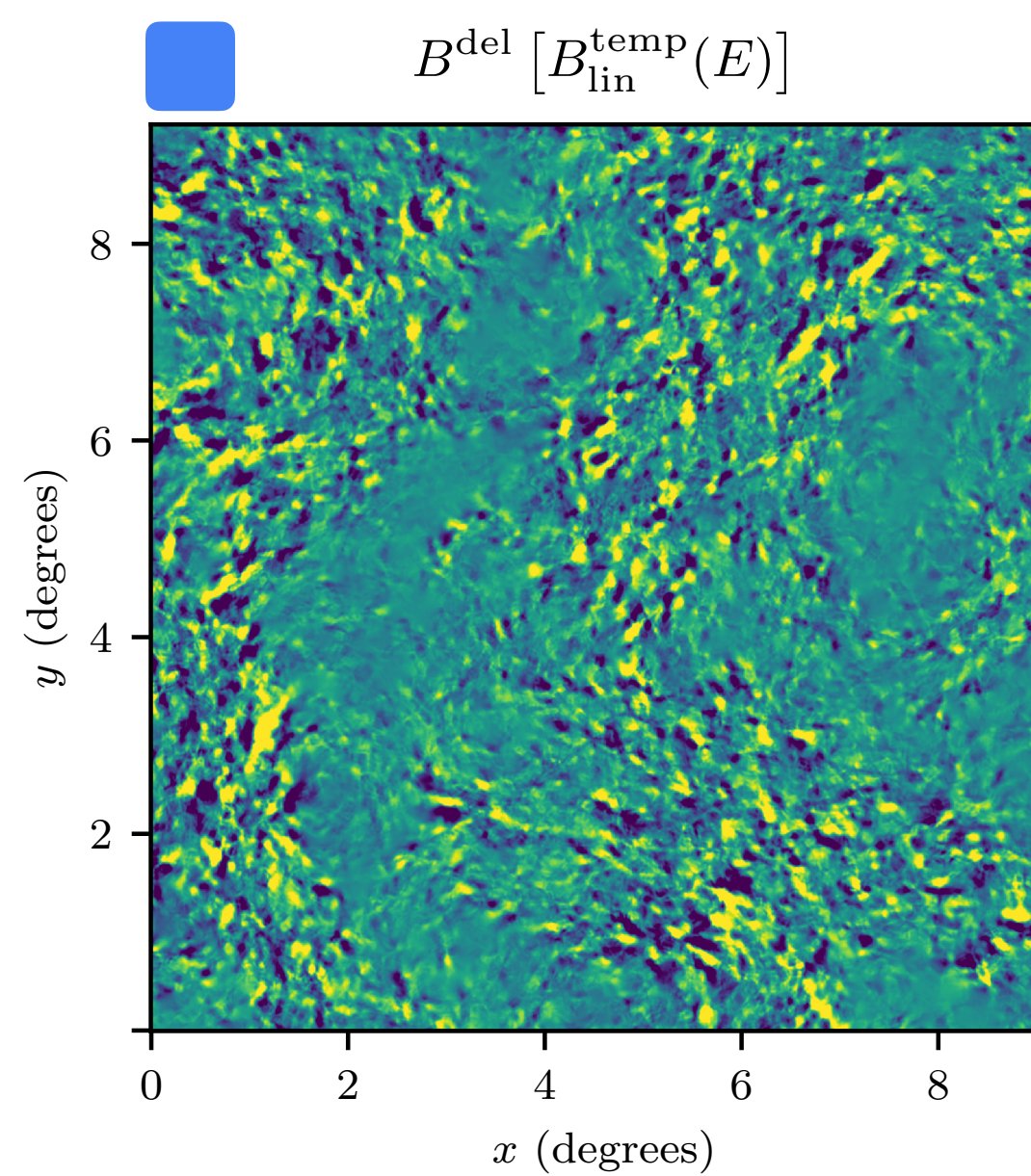
$$B_{\text{non-pert}}^{\text{temp}}(\mathbf{l}) = \mathcal{B}_{\mathbf{l}} \left[P^{E^{\text{obs}}}(\mathbf{x} + \nabla \hat{\phi}) \right]. \quad \text{e.g., Planck 18, POLARBEAR 19}$$

LIMITATIONS OF B-MODE DELENSING USING A TEMPLATE

- Corrections to the leading-order calculation of lensing B-mode power smaller than $O(1)\%$ because of extensive cancelations between large terms at higher orders.

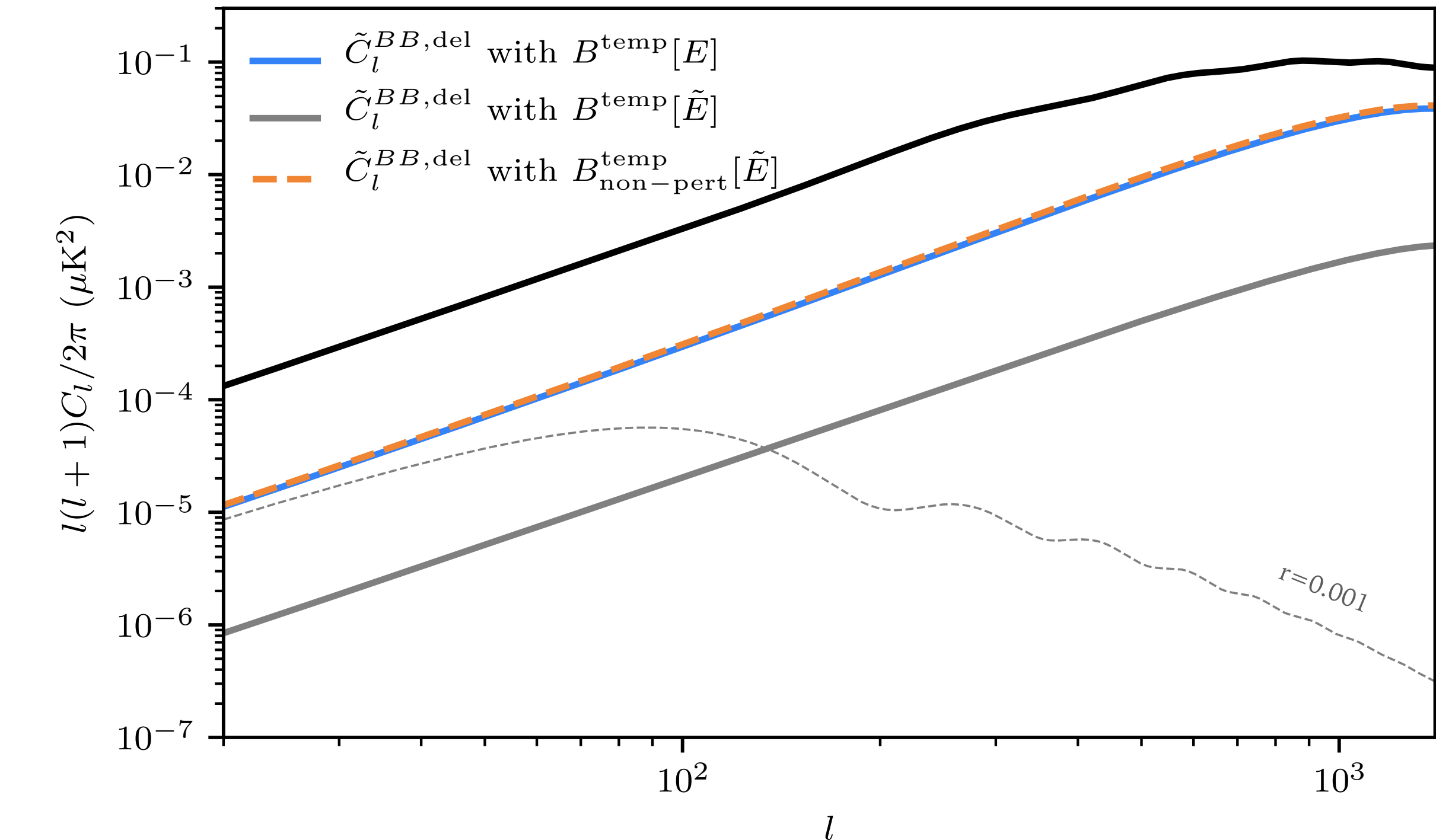
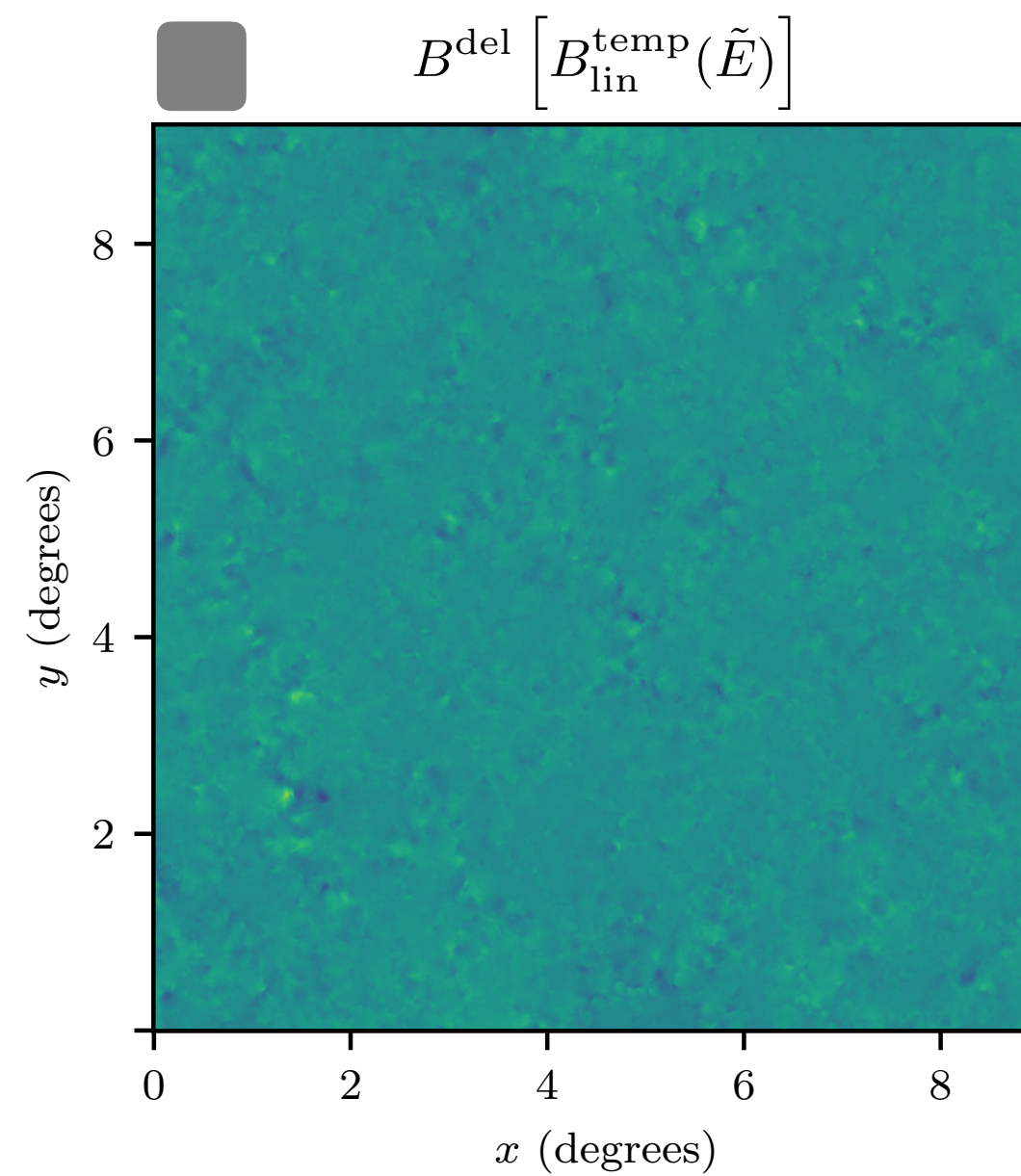
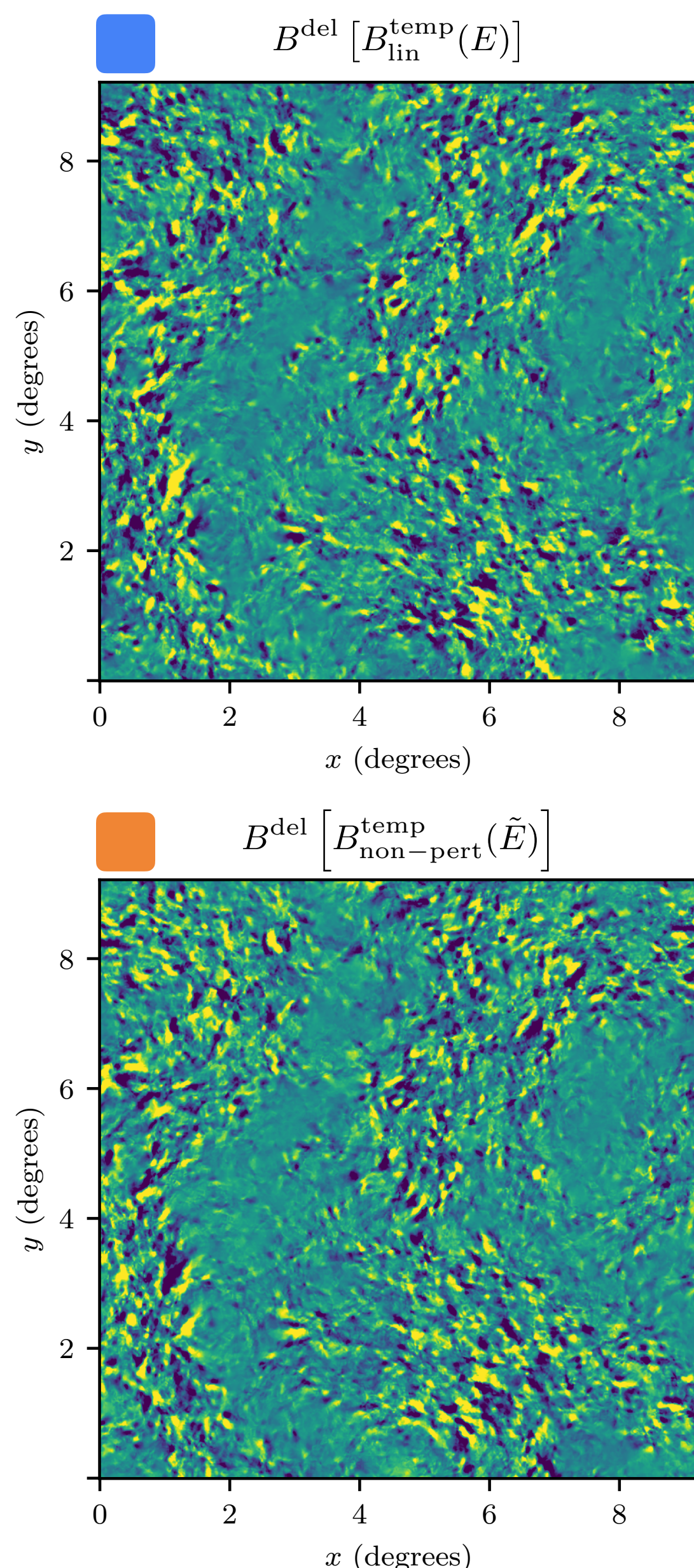


LIMITATIONS OF B-MODE TEMPLATE DELENSING: NOISELESS SCENARIO



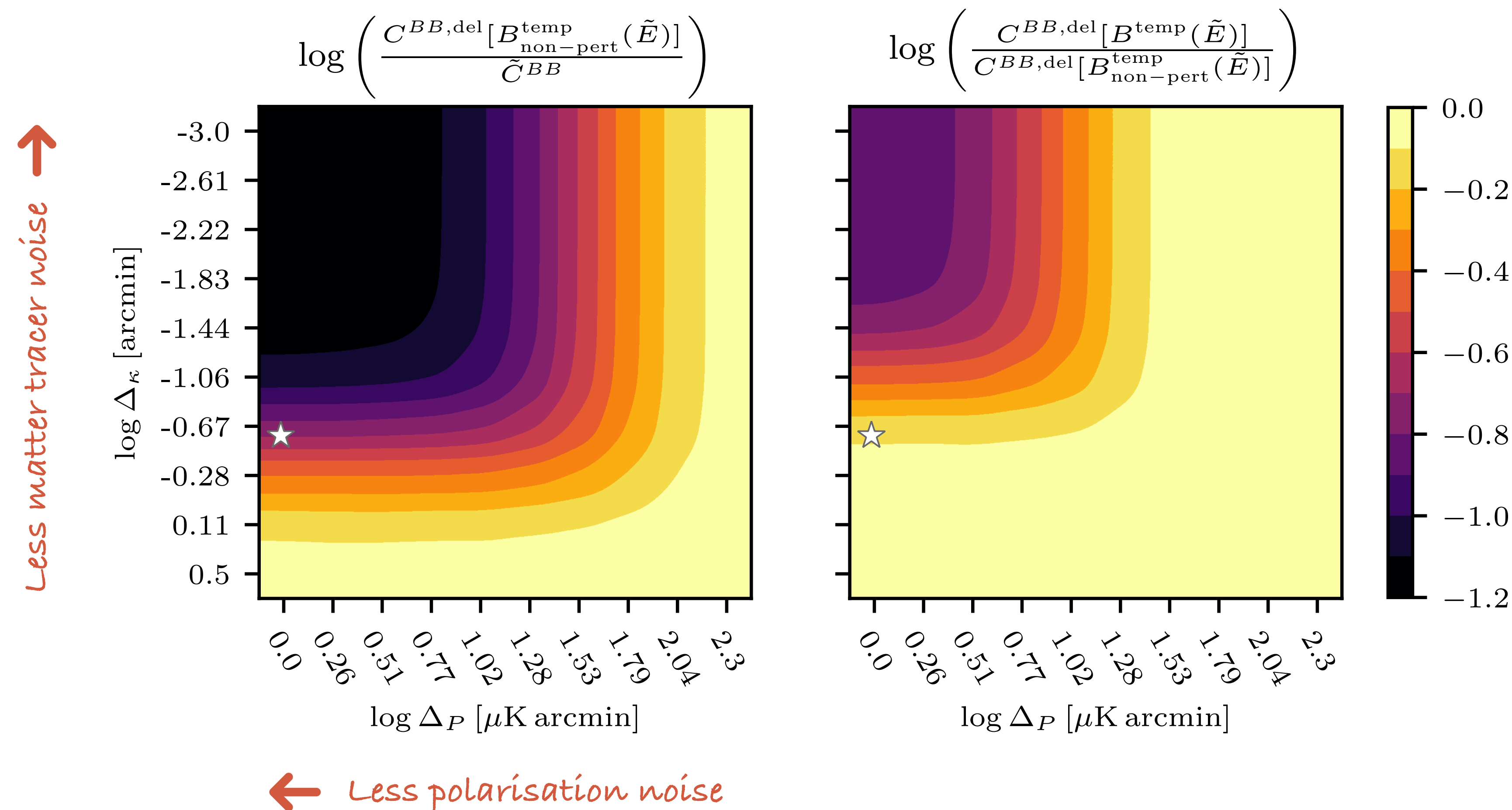
- Cancellations disappear if linear template is built from unlensed or delensed E-modes, hit delensing floor of $O(10)\%$

LIMITATIONS OF B-MODE TEMPLATE DELENSING: NOISELESS SCENARIO



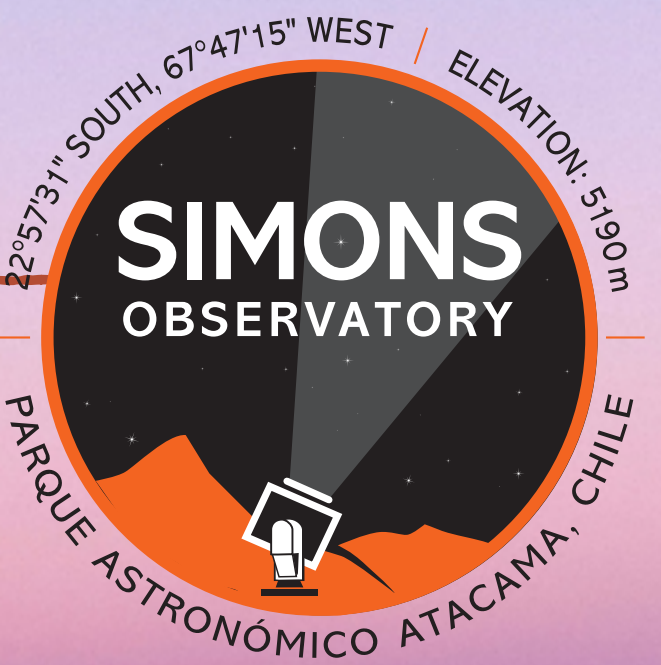
- Cancellations disappear if linear template is built from unlensed or delensed E-modes, hit delensing floor of $O(10)\%$
- New cancellations arise when the lensed E-modes are used in the linear template, so delensing floor is $O(1)\%$
- Advantage is lost when a non-perturbative template is built from lensed E-modes, so the delensing floor is also $O(10)\%$

LIMITATIONS OF B-MODE TEMPLATE DELENSING: REALISTIC CASE



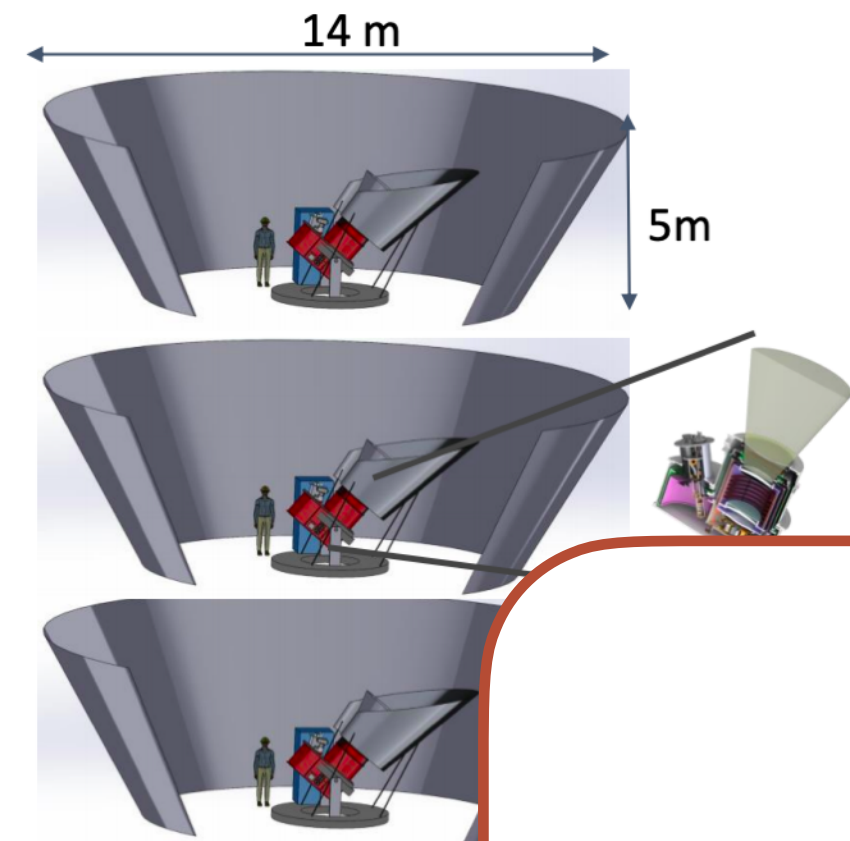
- With lensed E, advantageous to build gradient-order template even in realistic scenarios
- For CMB-S4, this removes $\sim 5\%$ more lensing power. Most transparent to systematics.

THE SIMONS OBSERVATORY (SO)



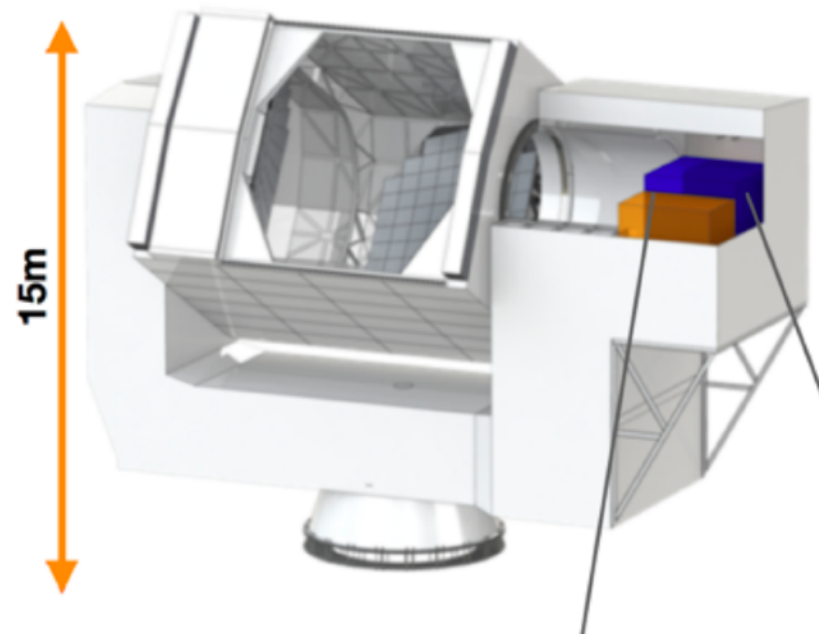
Credit: Deborah Kellner

THE SIMONS OBSERVATORY (SO)

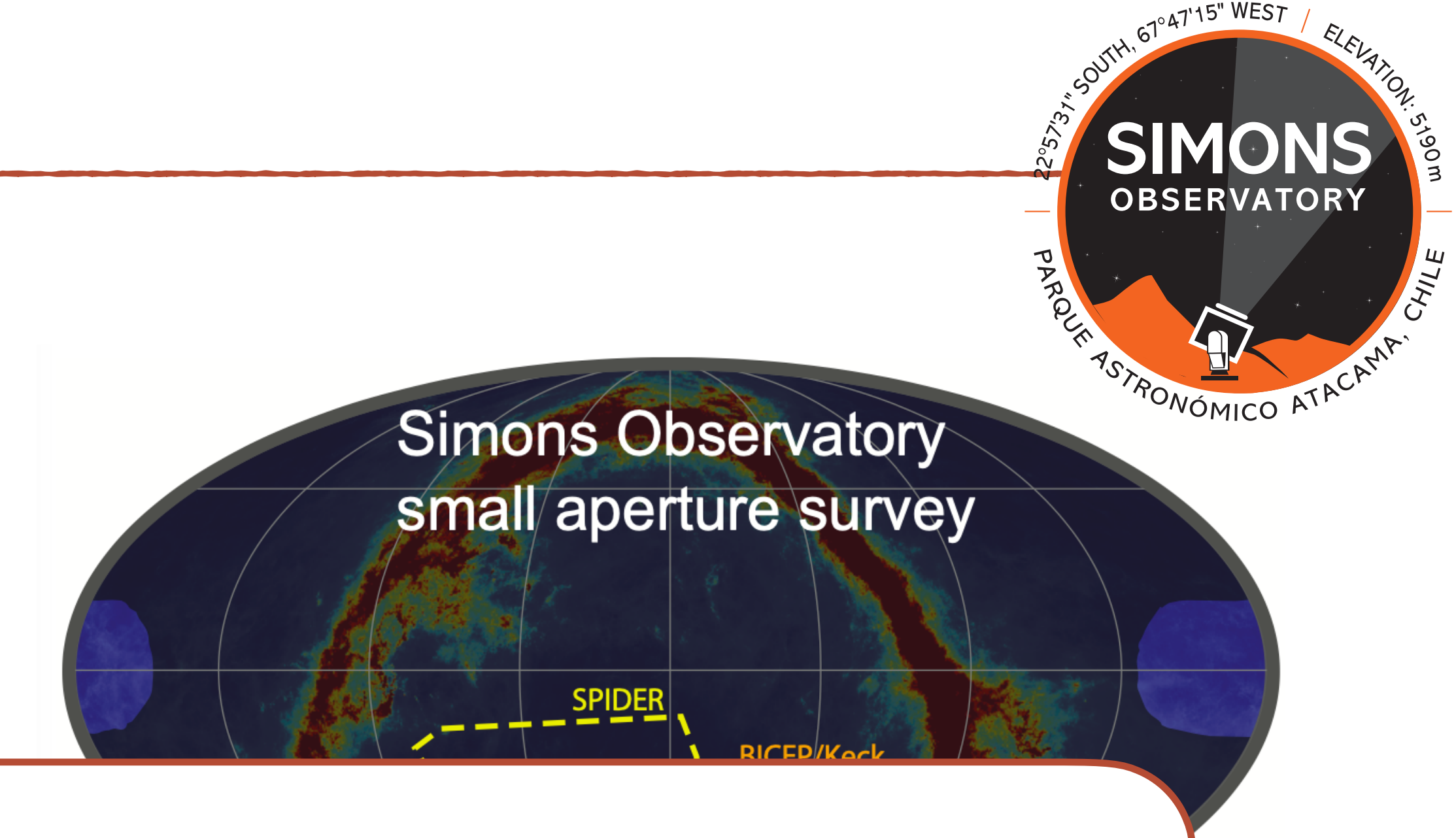


SATs ($f_{\text{sky}} = 0.1$)			
Freq. [GHz]	FWHM (')	Noise (baseline) [$\mu\text{K}\text{-arcmin}$]	Noise (goal) [$\mu\text{K}\text{-arcmin}$]
27	91	35	25
39	63	21	17
93	30	2.6	1.9
145	17	2.2	2.1

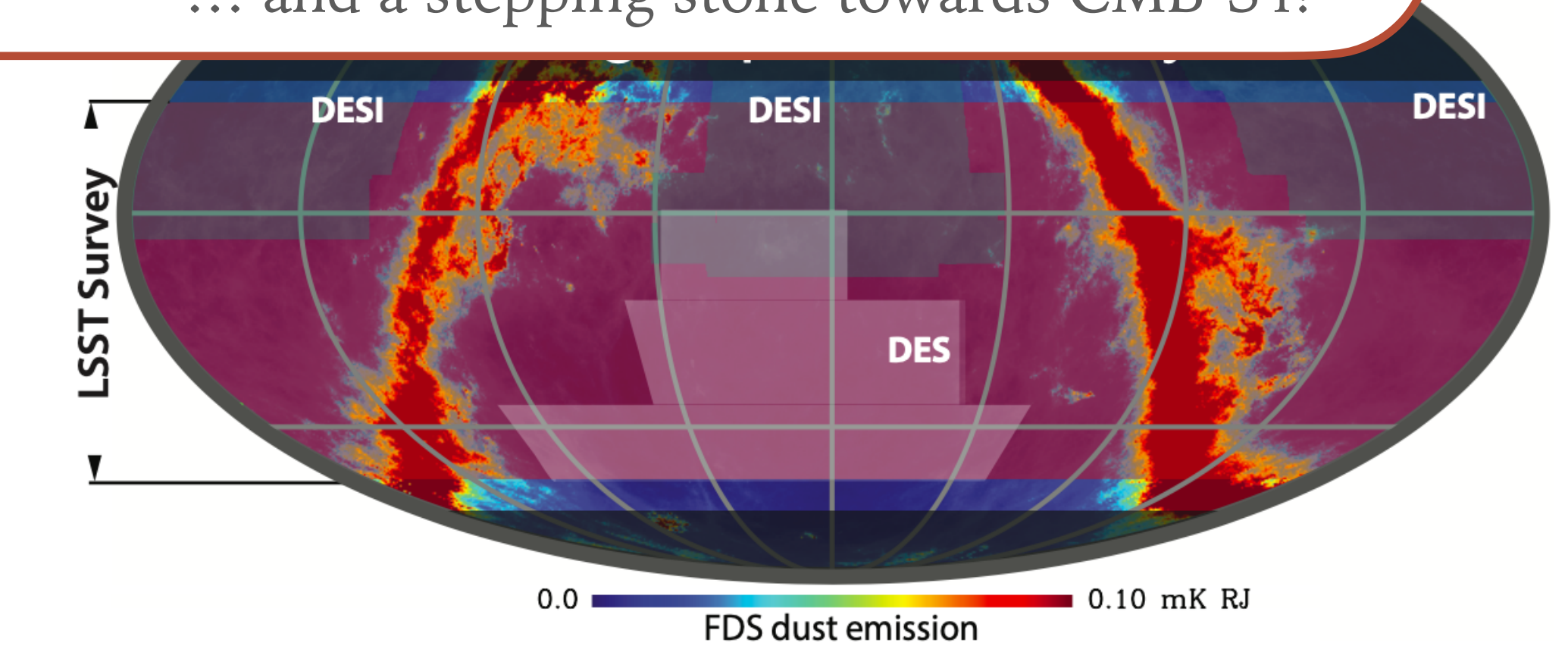
Early '21	Mid '22	Early '23	Mid '24
Testing and integration, optical validation	First light for both SAT + LAT	First science observations expected	Full science observations expected



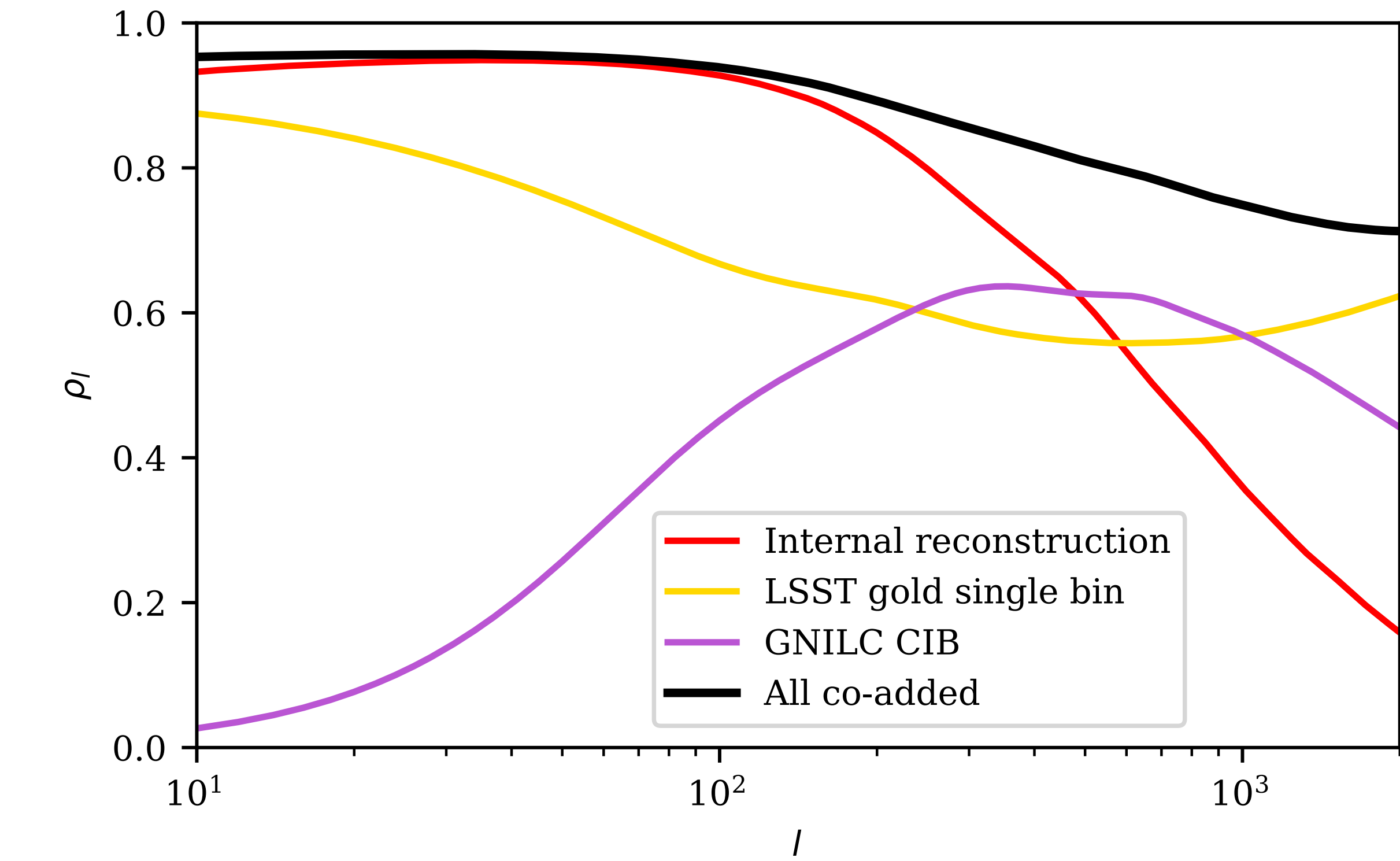
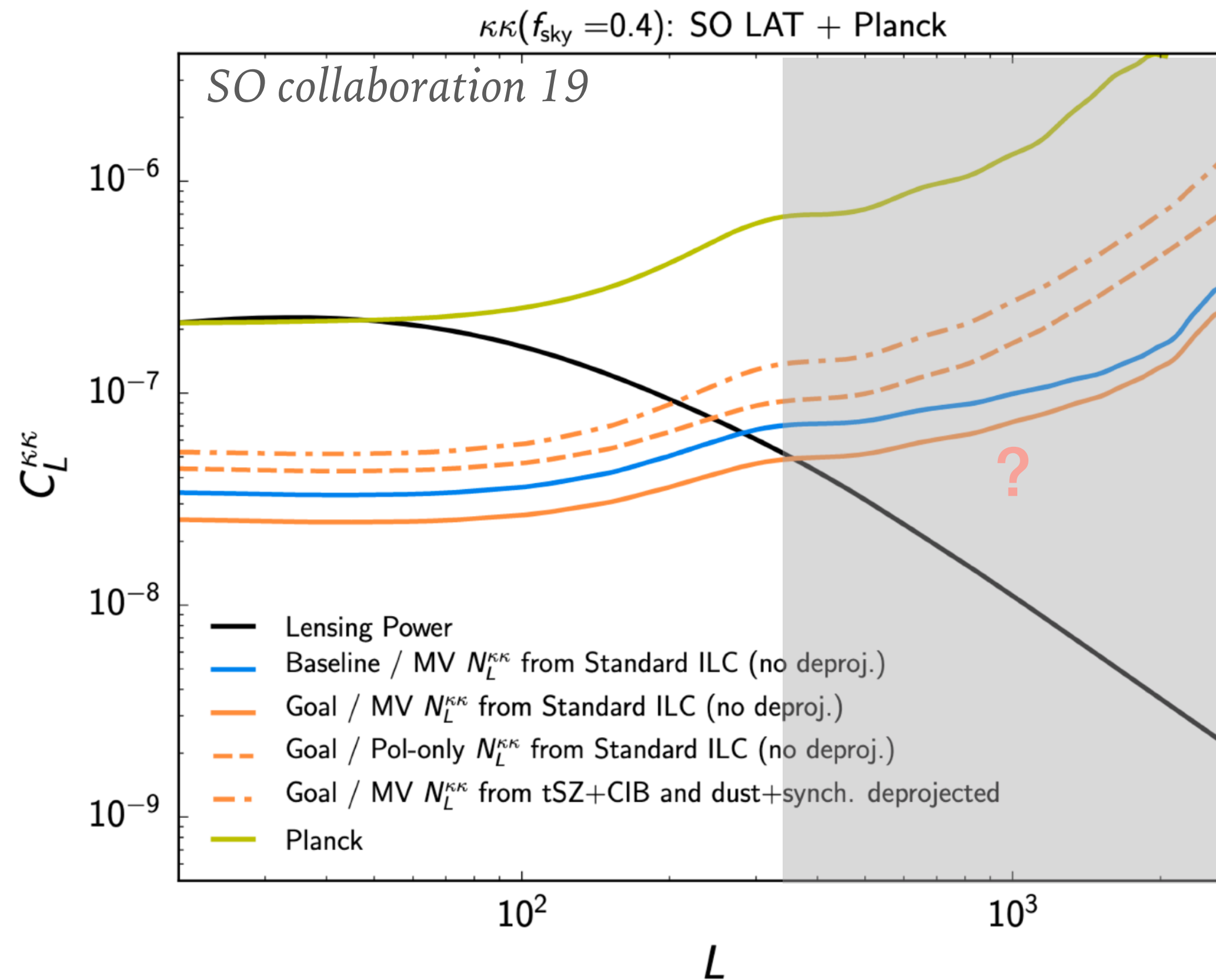
LAT ($f_{\text{sky}} = 0.4$)			
Freq. [GHz]	FWHM (')	Noise (baseline) [$\mu\text{K}\text{-arcmin}$]	Noise (goal) [$\mu\text{K}\text{-arcmin}$]
27	7.4	71	52
39	5.1	36	27
93	2.2	8.0	5.8
145	1.4	10	6.3
225	1.0	22	15
280	0.9	54	37



... and a stepping stone towards CMB-S4!



MULTI-TRACER DELENSING WITH SO



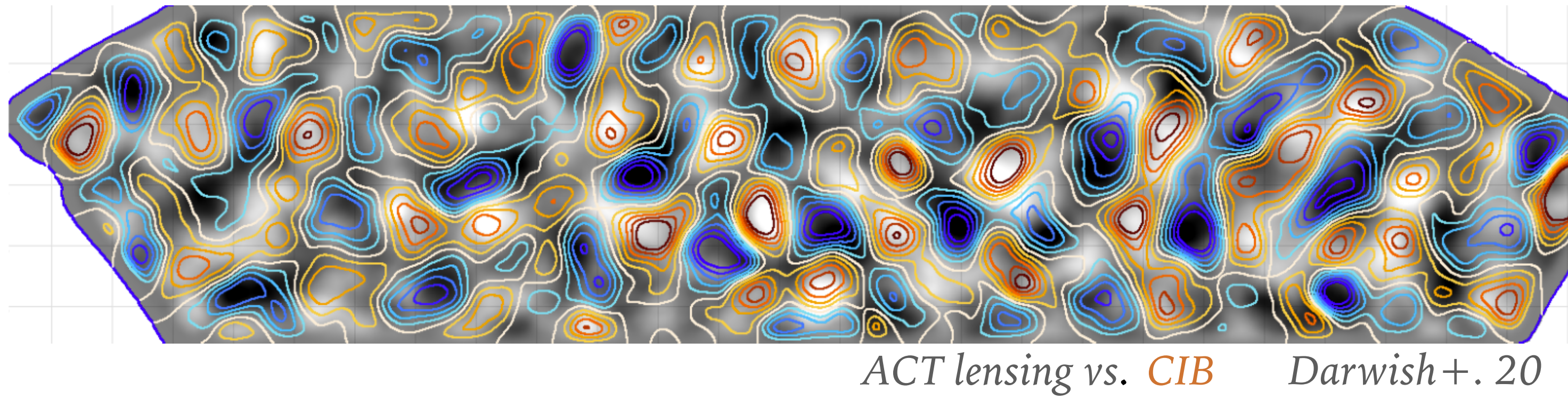
Combine internal reconstructions with external tracers of the LSS to get small-scale lenses at high z

Sherwin & Schmittfull 15, Manzotti 18 ...

ASIDE - THE COSMIC INFRARED BACKGROUND (CIB)

The CIB: emission from UV-heated dust in star-forming galaxies

Highly correlated with CMB lensing on the (arcminute) scales we need
Sherwin & Schmittfull 15



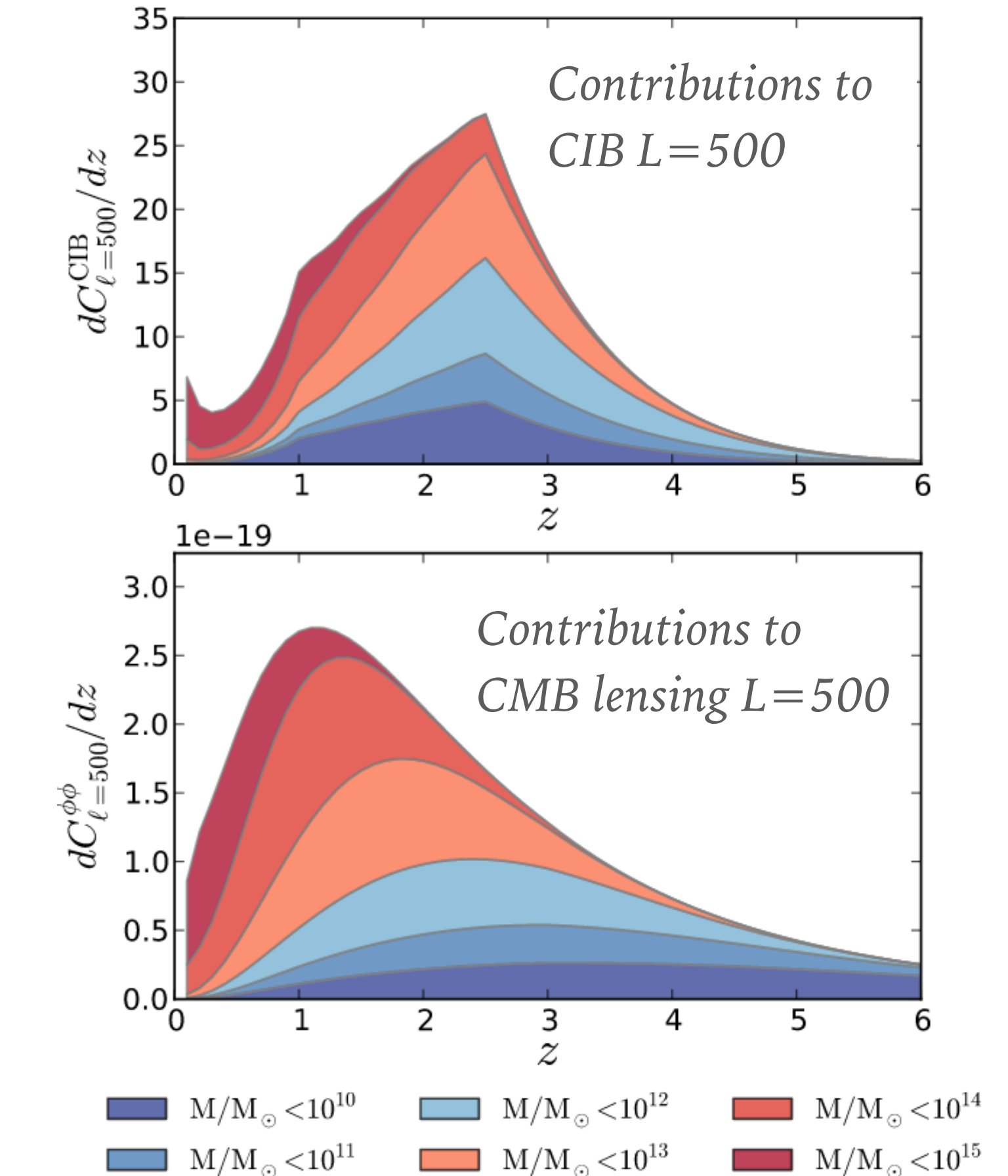
Used in:

- First demonstration of delensing in general
- First demonstration of B-mode delensing
- First improvement on $\sigma(r)$ from delensing

Larsen + 16

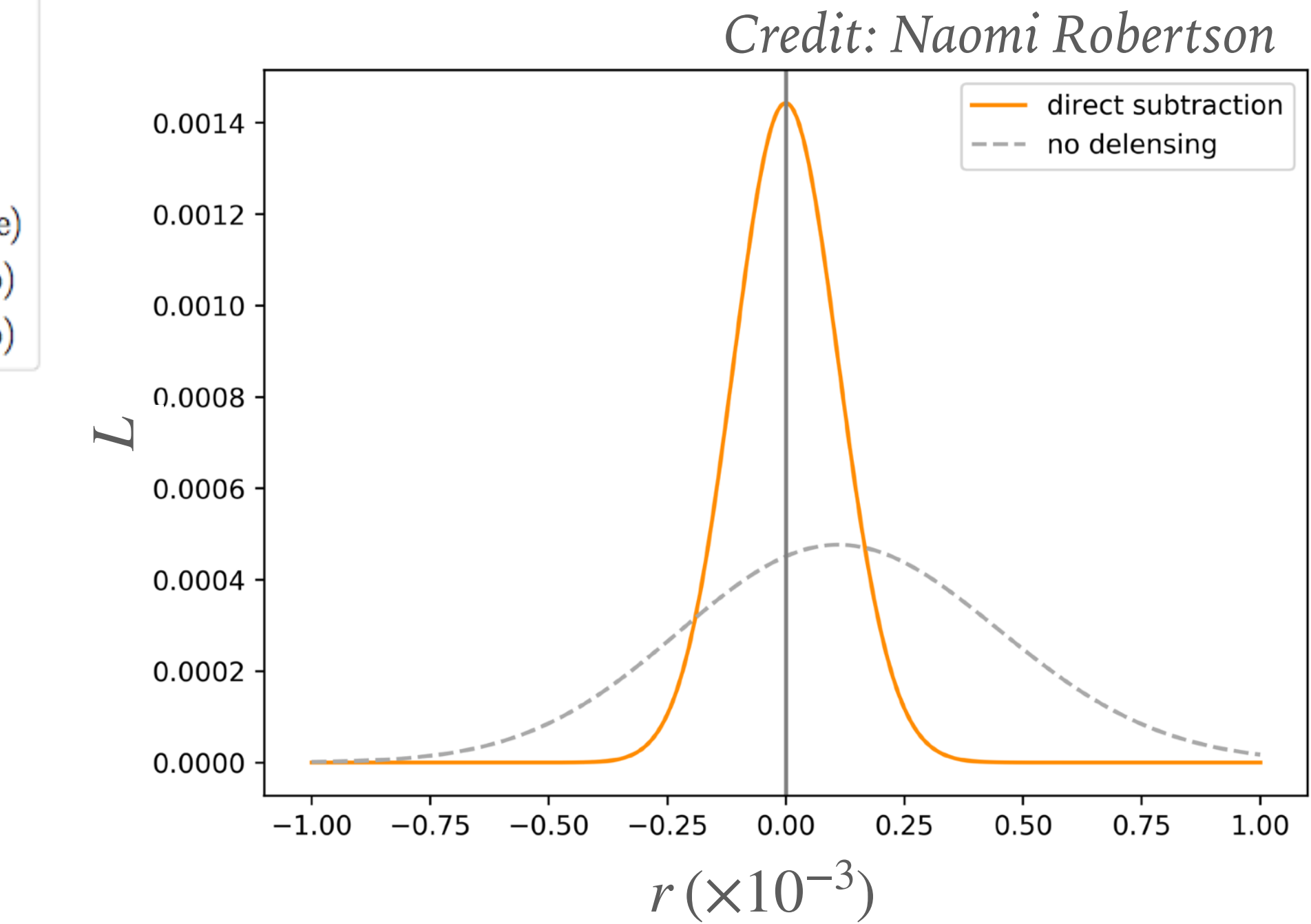
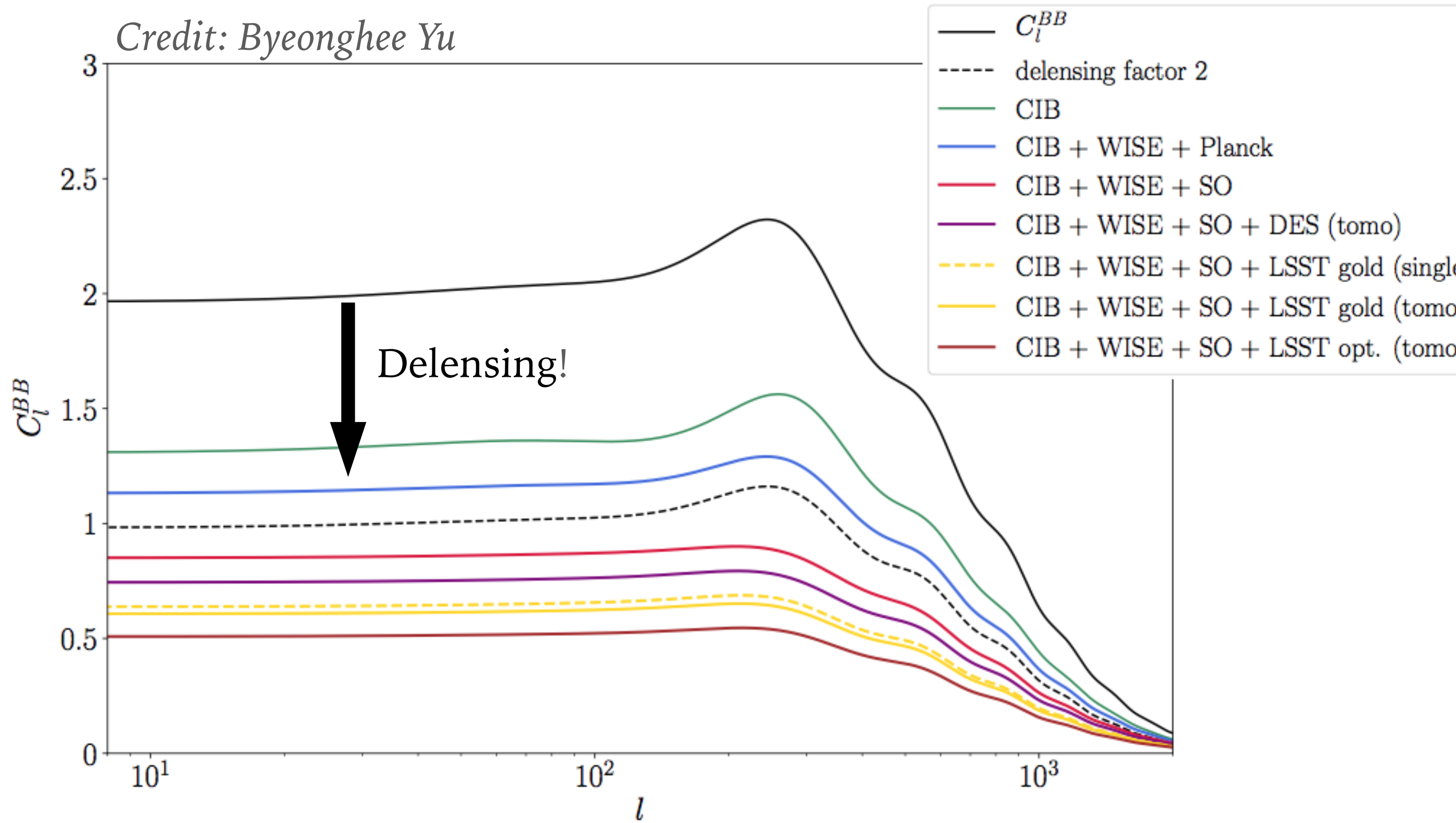
SPT 17

SPT + BICEP/Keck 20



Planck 13 XVIII

DELENSING WITH SO

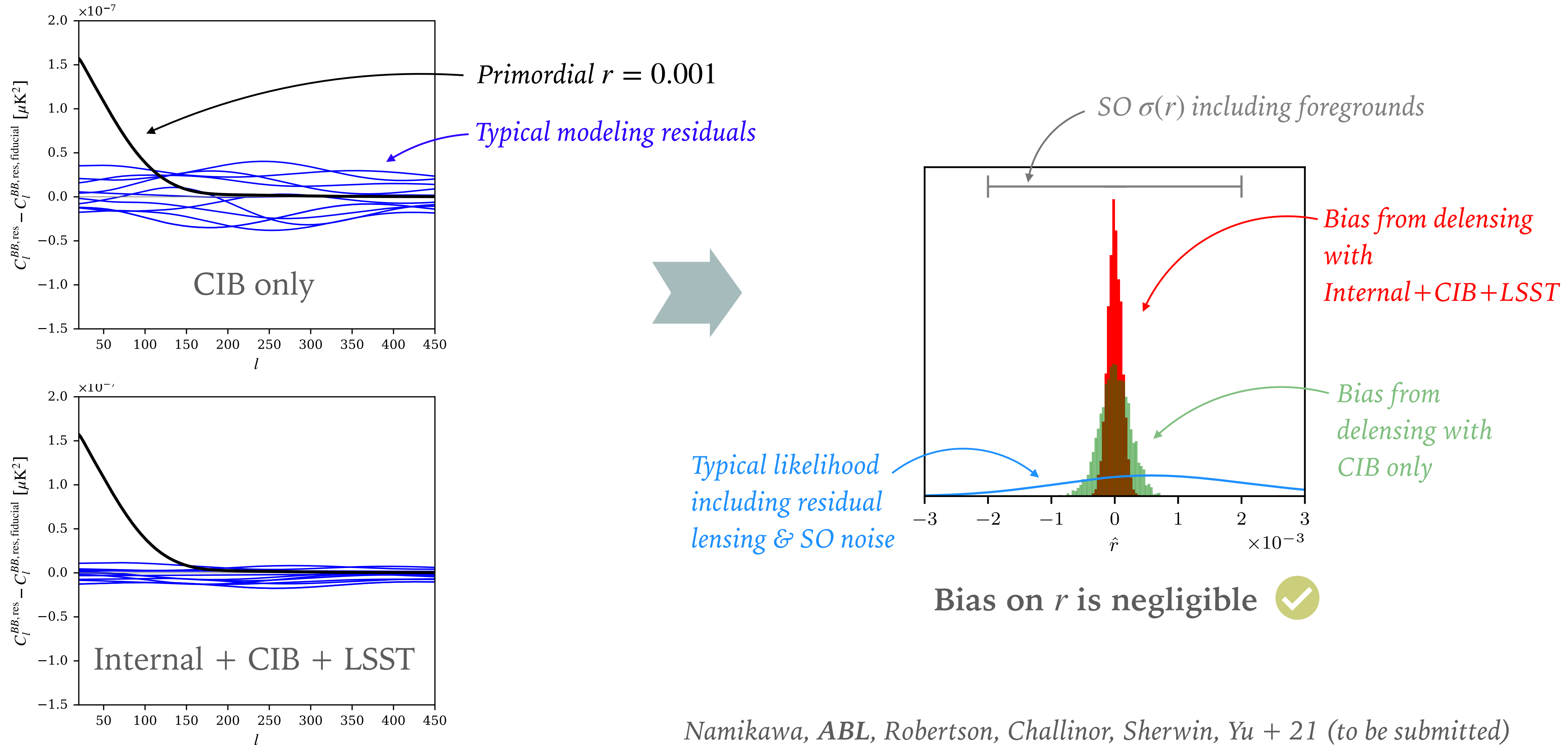


Close to idealised performance on realistic simulations including inhomogeneous noise and masking

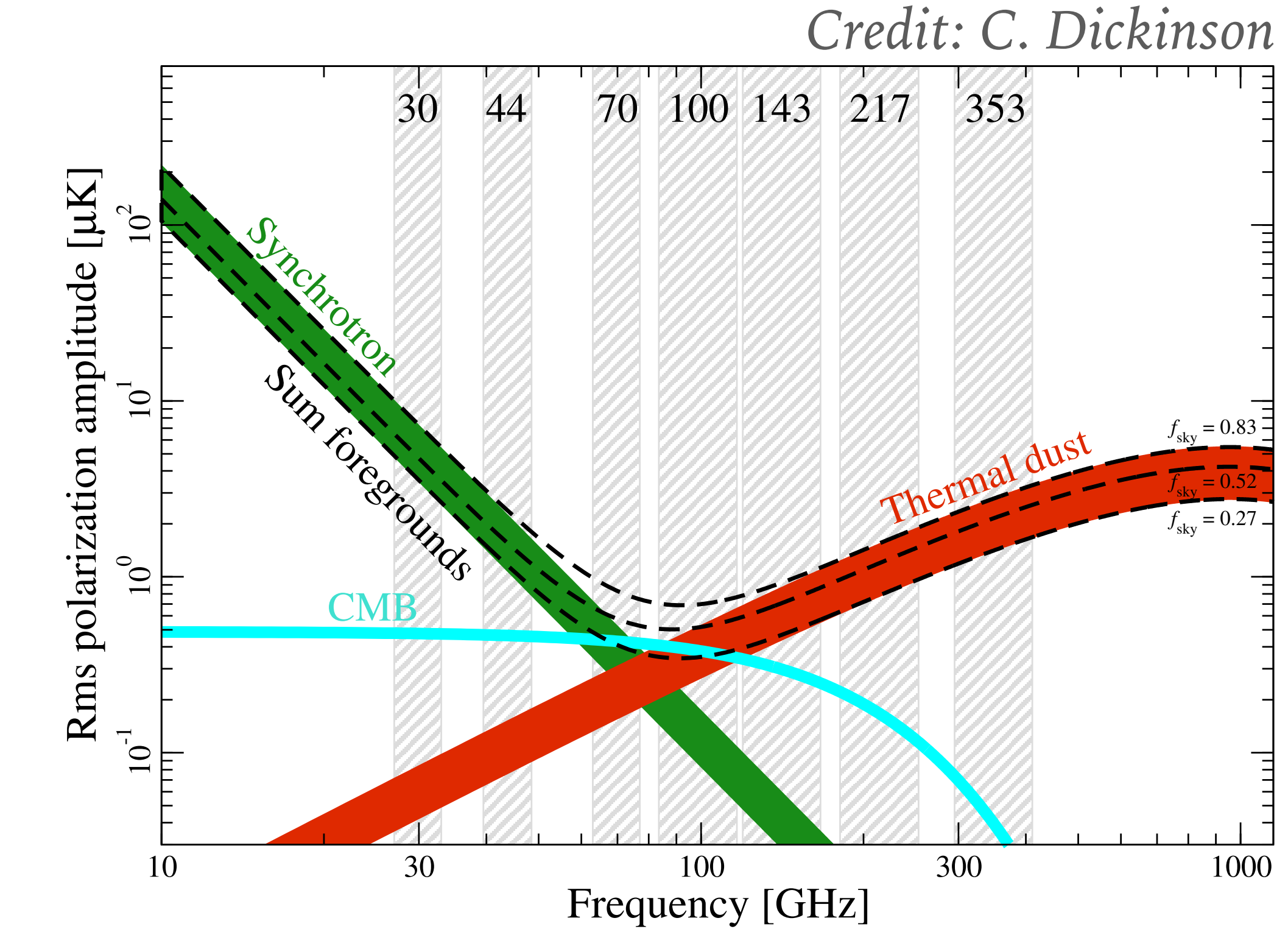
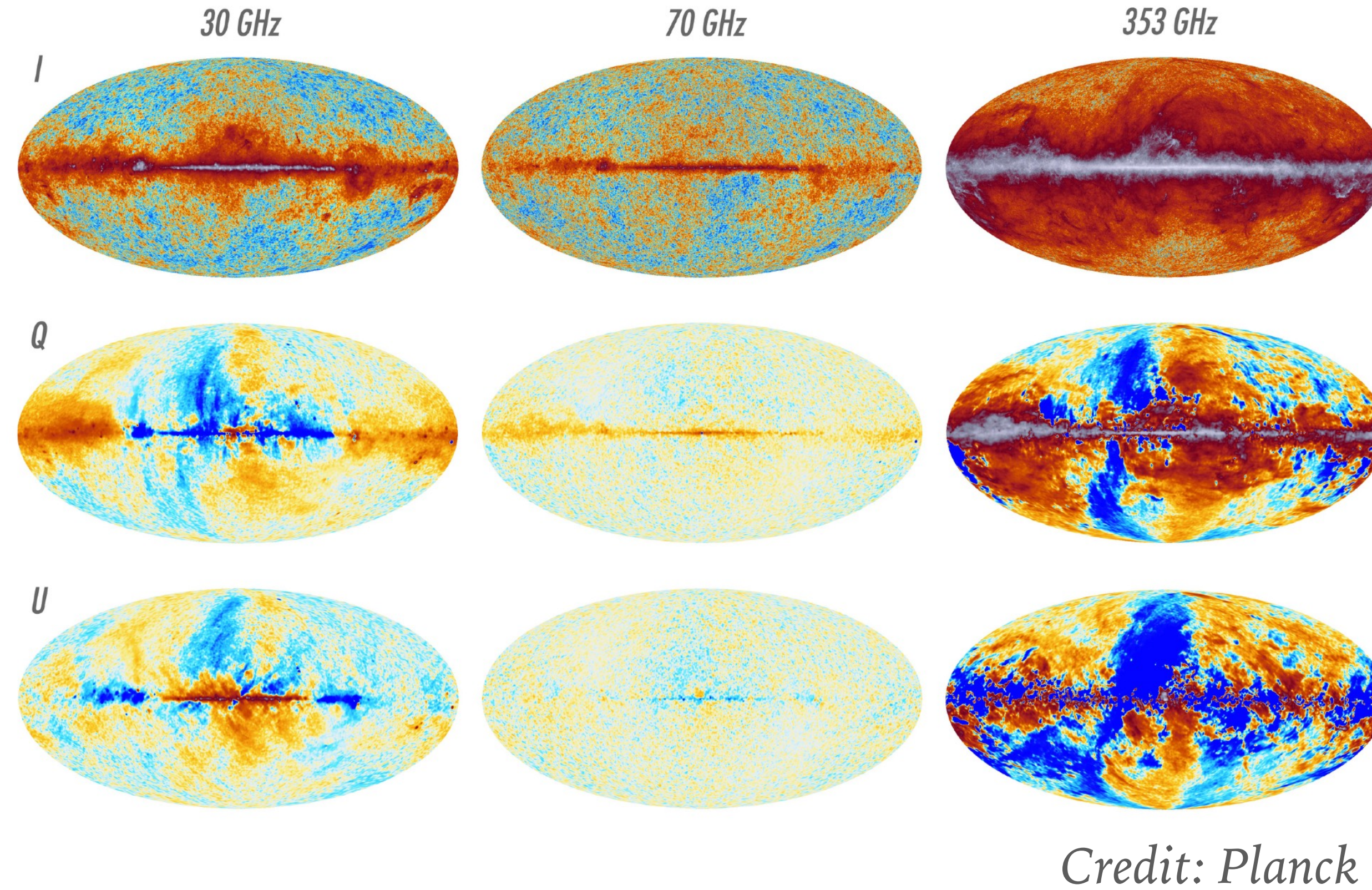
Currently $\sigma(r) = 0.044$ (Planck + BICEP/Keck), SO forecast after delensing $\sigma(r) = 0.003$

MULTITRACER DELENSING WITH SO - UNCERTAINTIES ON EXTERNAL TRACER SPECTRA

Internal reconstructions remove large lenses, so modeling residuals “flatten out”



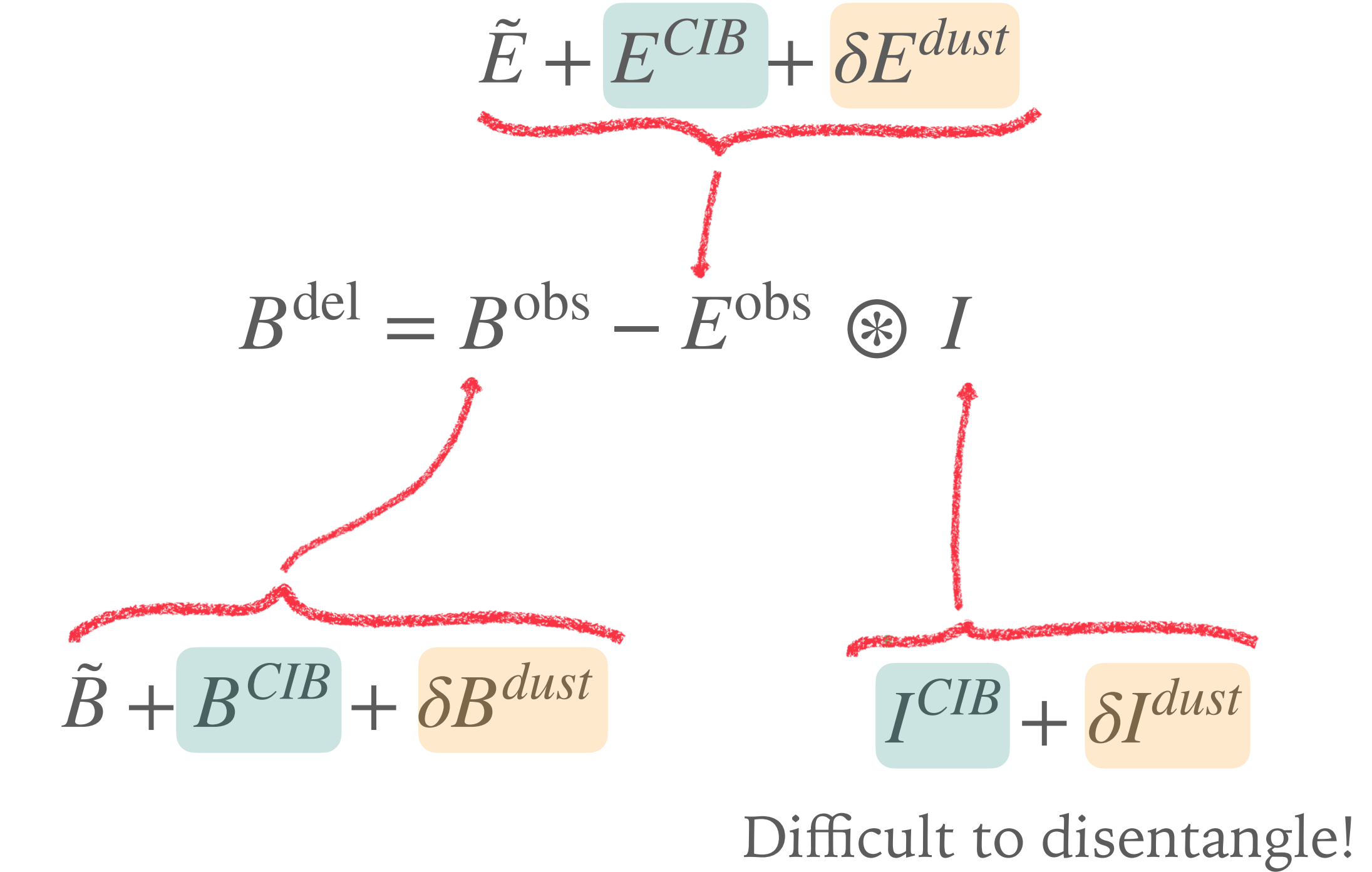
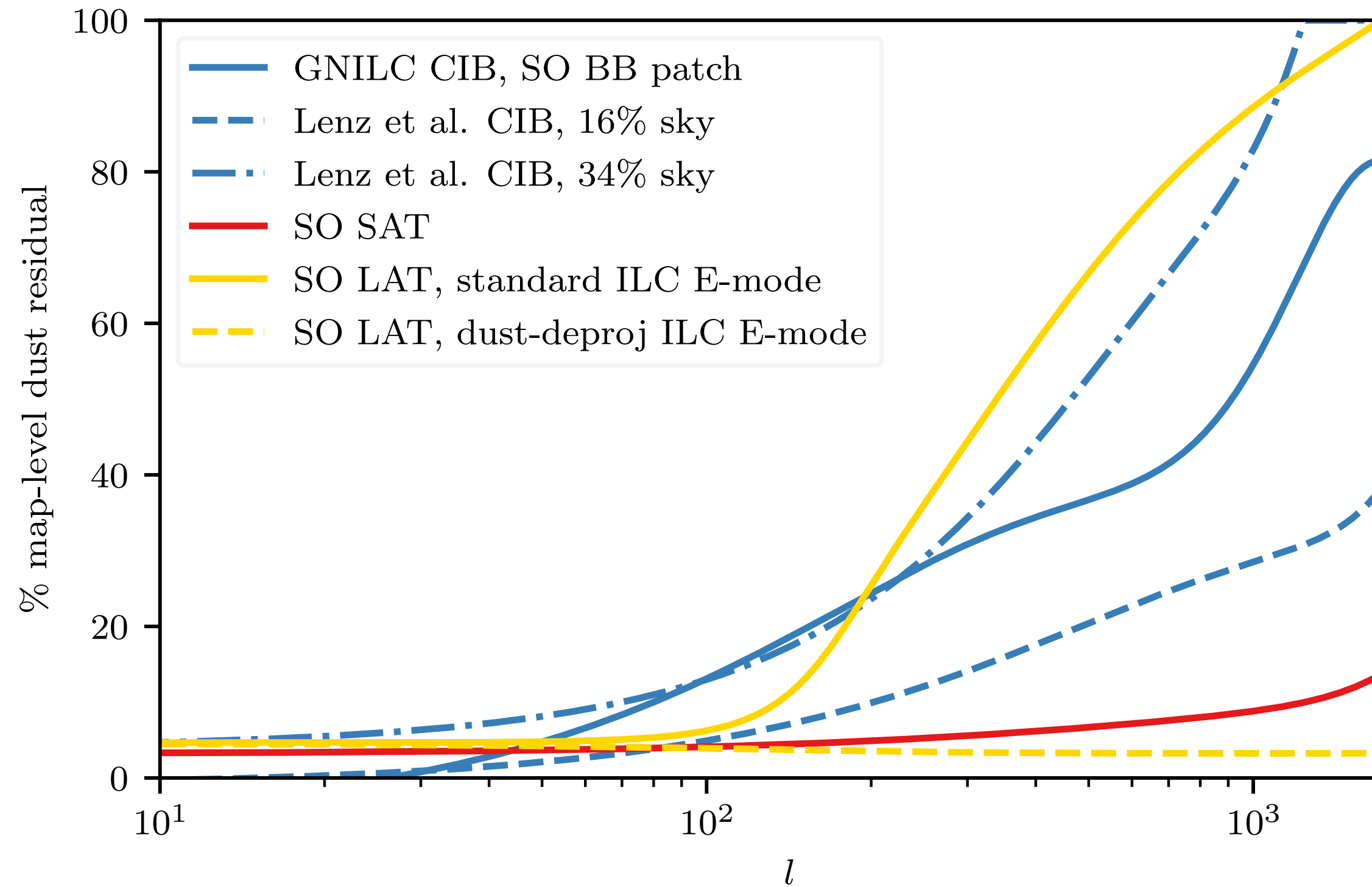
DELENSING BIASES FROM FOREGROUNDS



Negligible bias from internal delensing of CMB-S4 after foreground cleaning D. Beck + 20

... but what about CIB-delensing?

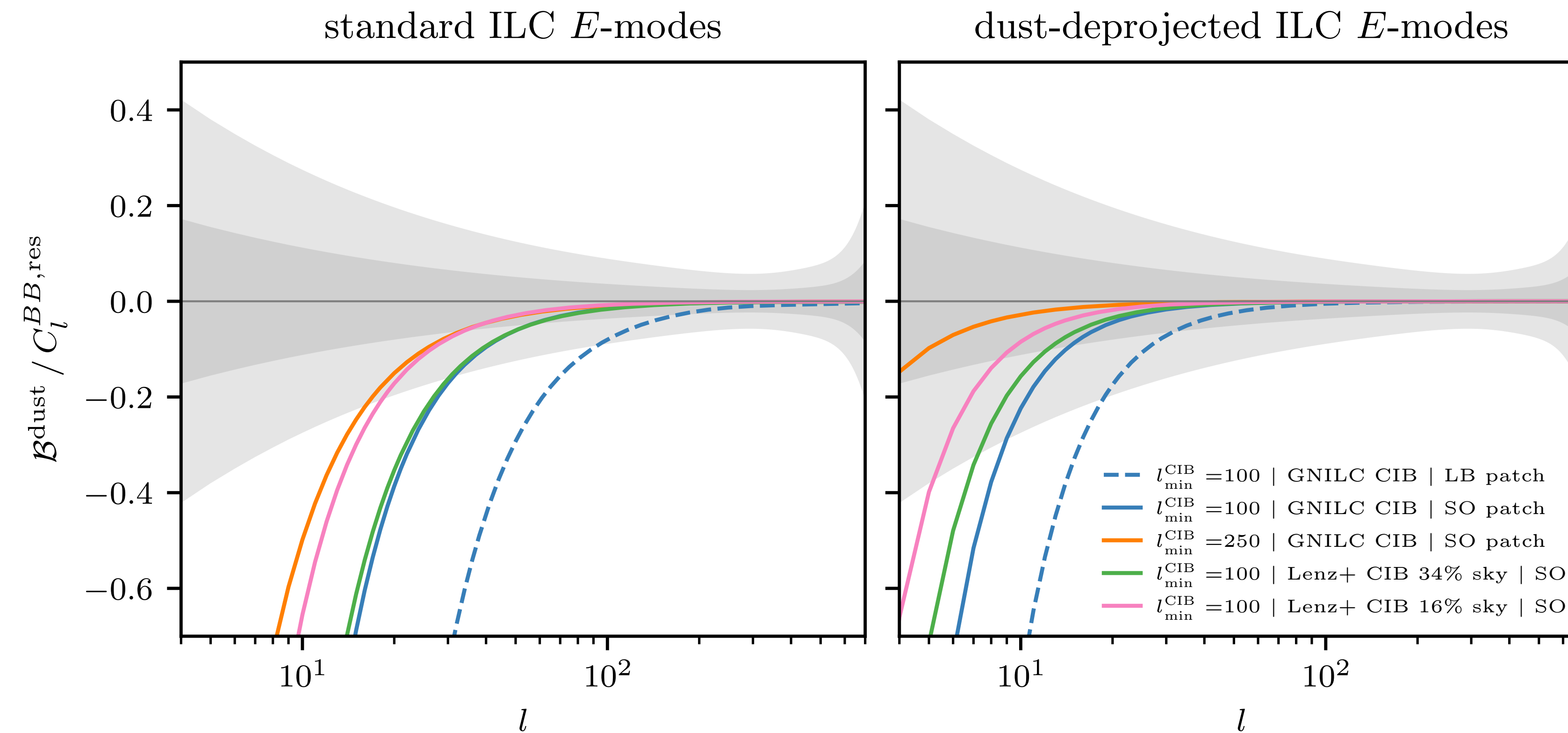
DELENSING WITH THE CIB — POSSIBLE BIASES



The power spectrum of delensed B-modes is then biased:

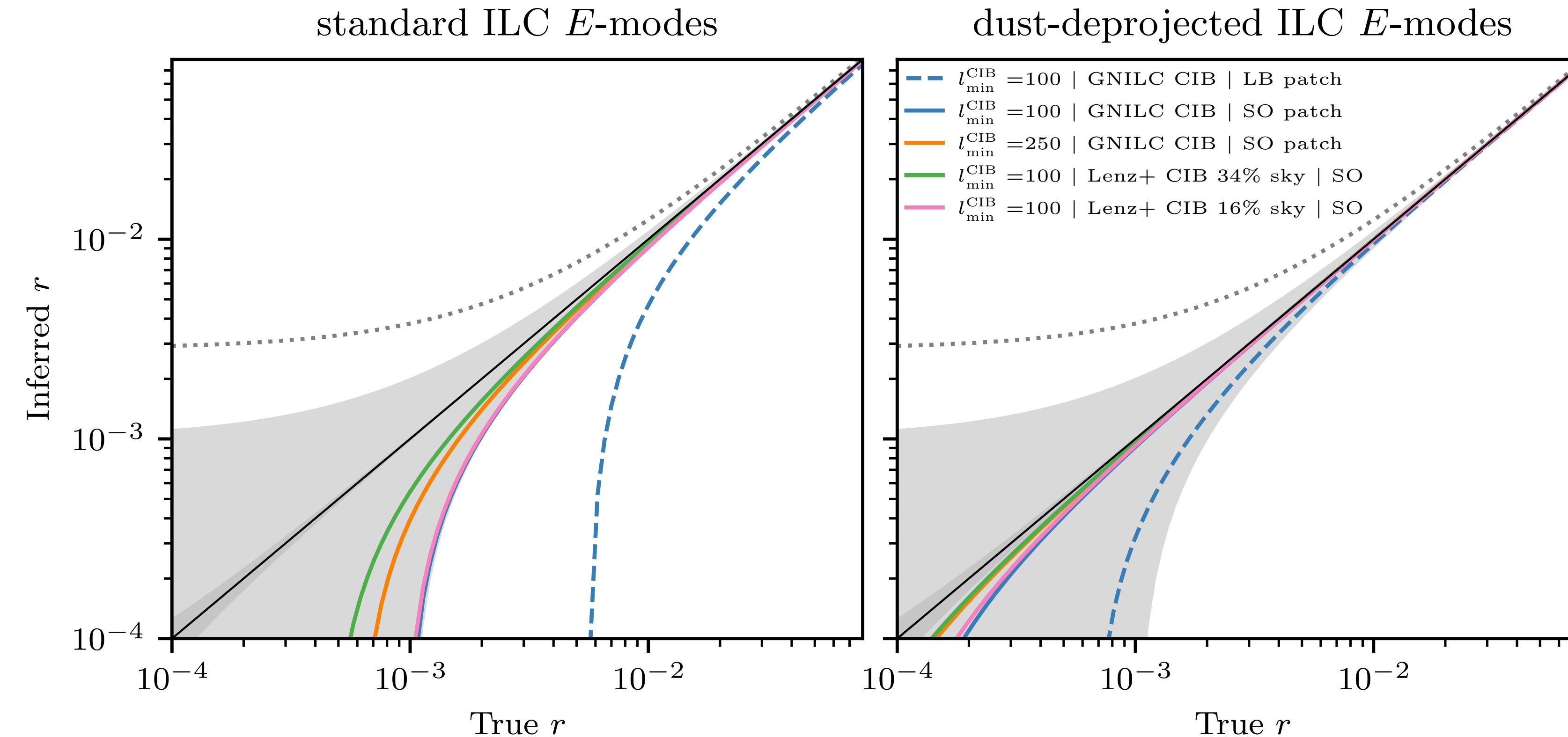
$$C_{\ell}^{BB,\text{del}} \supset \langle B_{100\text{GHz}}^{\text{dust}} E_{100\text{GHz}}^{\text{dust}} I_{353\text{GHz}}^{\text{dust}} \rangle, \langle B_{100\text{GHz}}^{CIB} E_{100\text{GHz}}^{CIB} I_{353\text{GHz}}^{CIB} \rangle \dots$$

DELENSING SO WITH THE CIB — BIAS FROM RESIDUAL GALACTIC DUST



- Negative bias dominated by $\langle B^{\text{dust}} E^{\text{dust}} I^{\text{dust}} \rangle$
- Can be mitigated by nulling dust contribution to E-modes, with only small penalty in delensing efficiency
- Small on scales probed from the ground

DELENSING SO WITH THE CIB — BIAS FROM RESIDUAL GALACTIC DUST

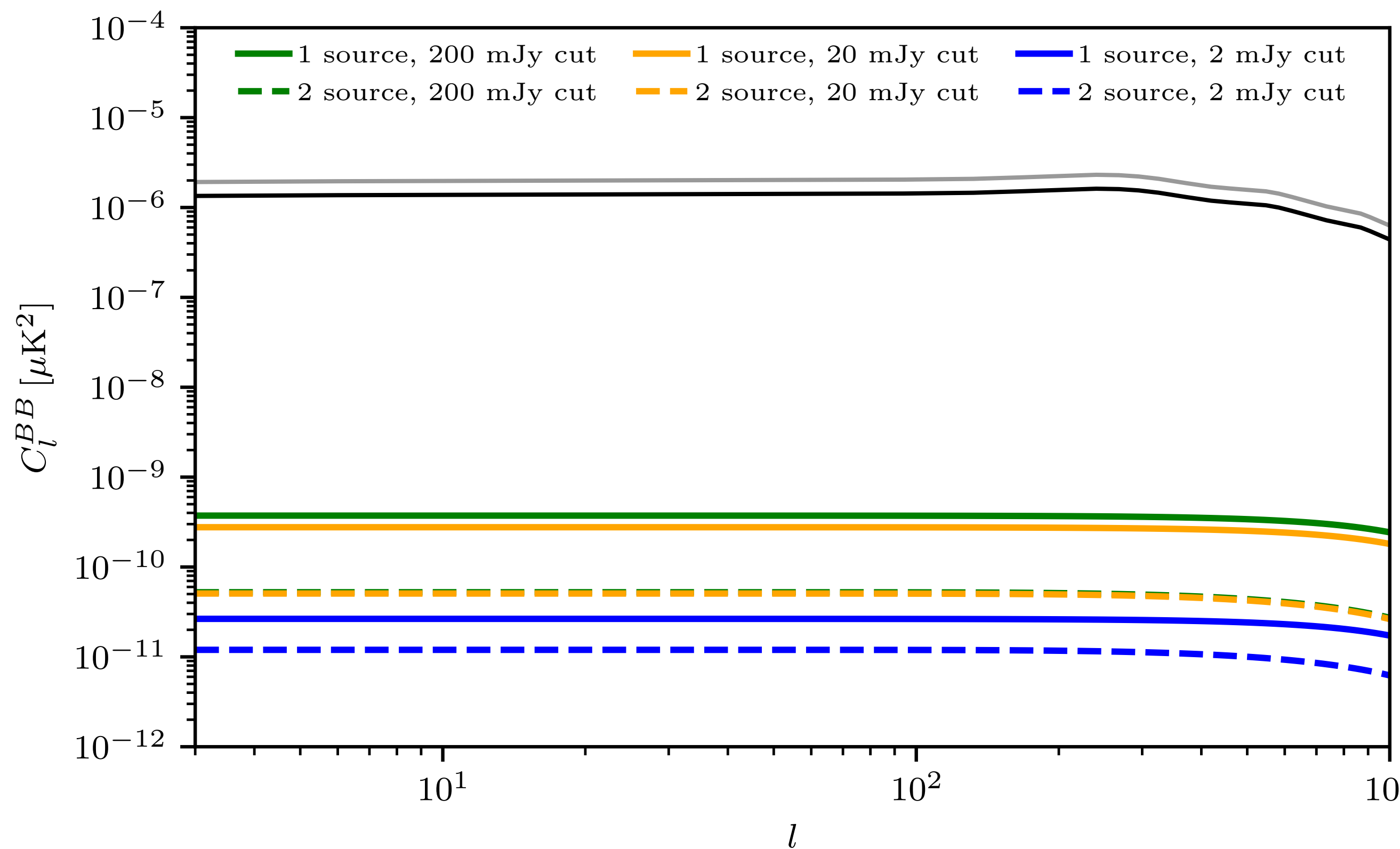


- Bias leads to underestimation of r
- Can be mitigated by nulling dust contribution to E-modes, with only small penalty in delensing efficiency
- Small on scales probed from the ground

DELENSING WITH THE CIB — BIAS FROM CIB BI- & TRISPECTRUM

In a minimal analytic model with uncorrelated source polarisation angles,

$$\begin{aligned} \mathcal{B}_l^{BEI} = & 2p^2 G_{353 \text{ GHz}} G_{145 \text{ GHz}}^2 \int \frac{d^2 l'}{(2\pi)^2} \frac{\mathbf{l}' \cdot (\mathbf{l} - \mathbf{l}')}{|\mathbf{l} - \mathbf{l}'|^2} W^E(\mathbf{l}') W^I(|\mathbf{l} - \mathbf{l}'|) \sin^2 2(\psi_{\mathbf{l}'} - \psi_{\mathbf{l}}) \\ & \times \int dz \left(\frac{I^{\text{CIB}}[145(1+z) \text{ GHz}]}{I^{\text{CIB}}[353(1+z) \text{ GHz}]} \right)^2 \left[S_{353 \text{ GHz}}^{(3)}(z) + \frac{H(z)}{cr^2(z)} S_{353 \text{ GHz}}^{(2)}(z) S_{353 \text{ GHz}}^{(1)}(z) P_g(|\mathbf{l} - \mathbf{l}'|/r(z); z) \right] \end{aligned}$$

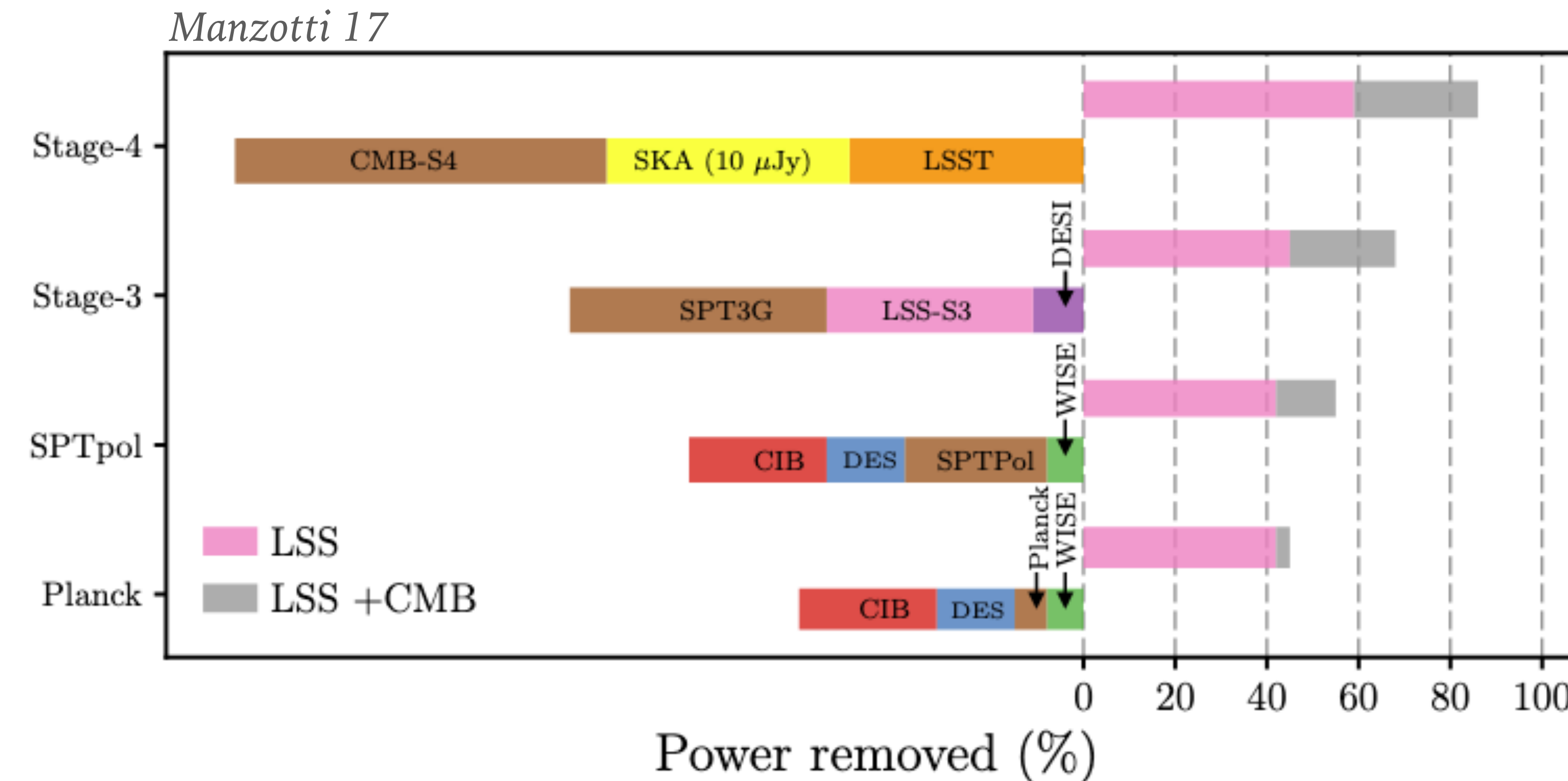


where $S_{\nu}^{(n)}(z) \equiv \int_{s_{\min}}^{s_{\max}} dS S^n \frac{d^2 N}{dS dz d\Omega}(z, \nu)$

and $\langle B^{\text{CIB}} E^{\text{CIB}} T^{\text{CIB}} \rangle \gg \langle E^{\text{CIB}} T^{\text{CIB}} E^{\text{CIB}} T^{\text{CIB}} \rangle$
for expected flux cuts.

Hence, negligible for any implementation of
CIB-delensing

INTERNAL DELENSING



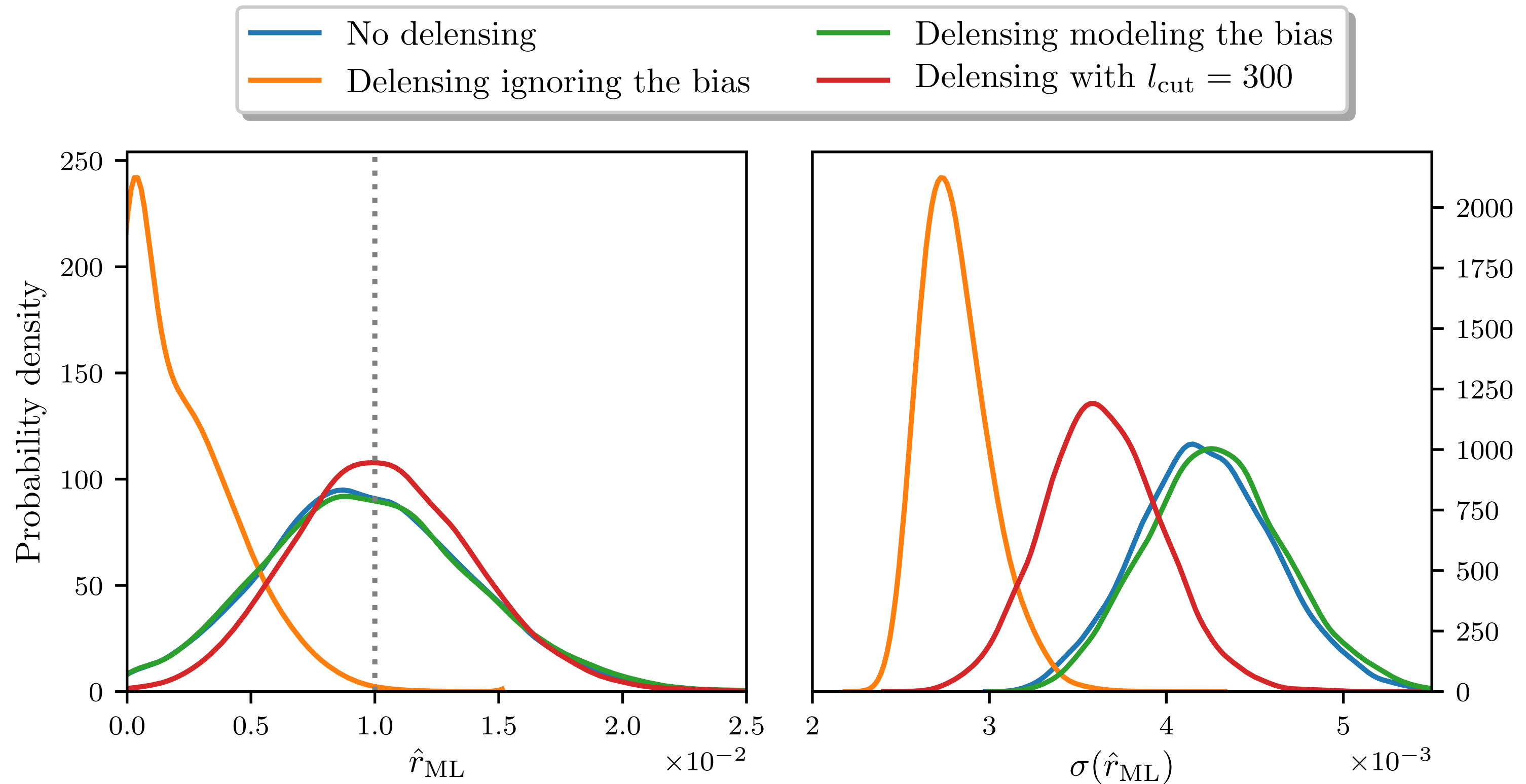
Soon dominated by internal lensing reconstructions based on CMB polarisation (mainly EB correlations)

Maximum-a-posteriori (MAP) $\hat{\phi}$ reconstruction will supersede QEs Hirata & Seljak 03, Carron & Lewis 17

Delensing with MAP $\hat{\phi}$ and Bayesian lensing reconstruction both recently demonstrated on data!

INTERNAL DELENSING BIAS

- Overlap in modes between B in EB estimator and B -modes to be delensed causes spurious suppression of delensed power spectrum and its variance *Teng et al. 11, Namikawa & Nagata 14*
- Could this lower variance translate to improved constraints on r ? **NO**



- Primordial signal is suppressed by a larger fraction than the “noise”
- Preferable to avoid by masking overlapping modes (small impact on S/N) than renormalising/modeling

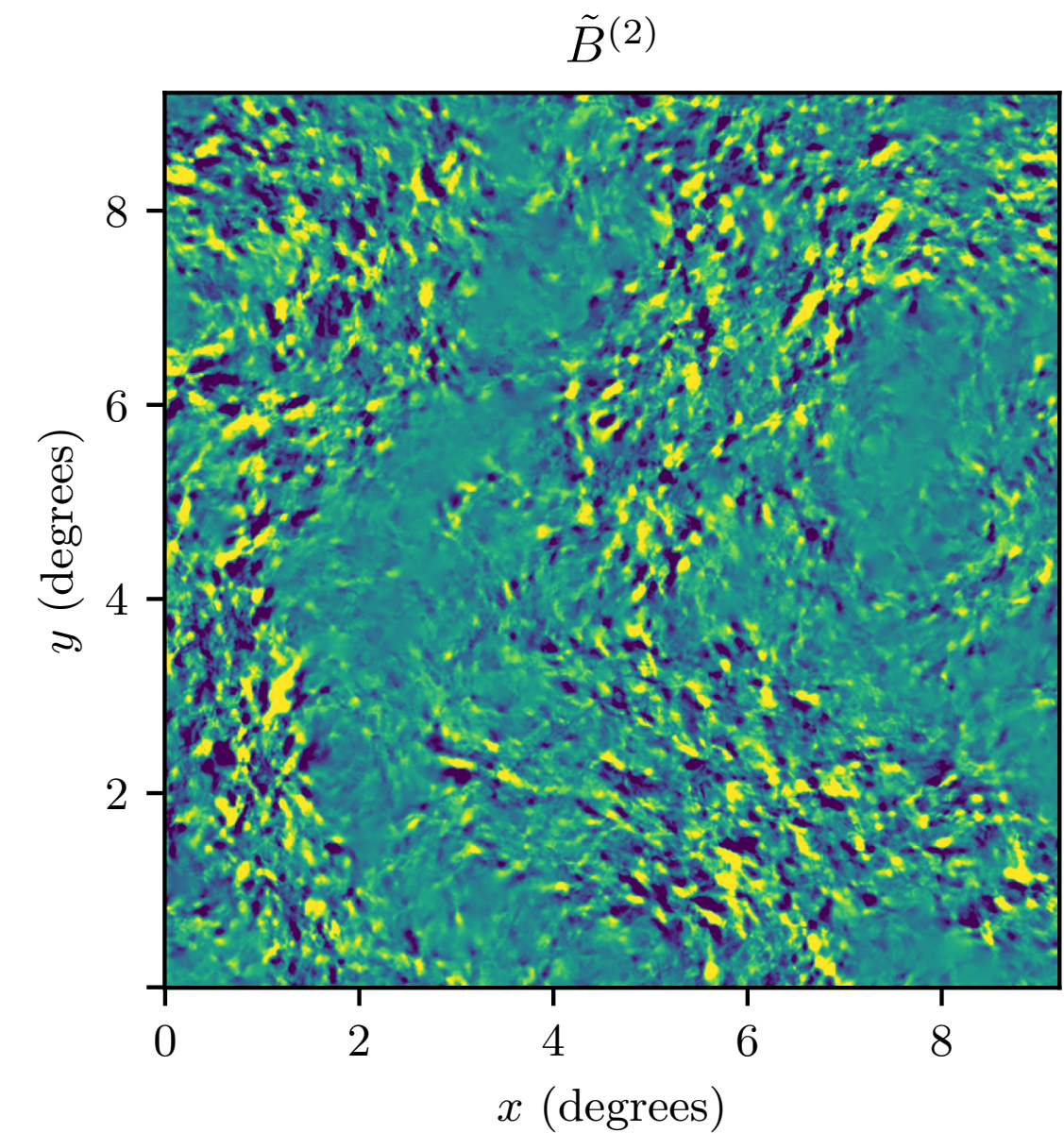
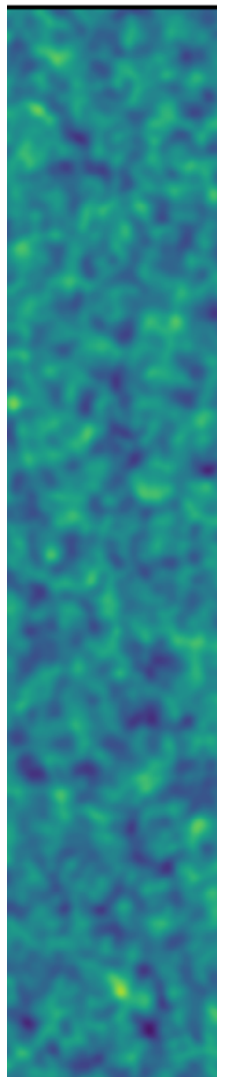
CONCLUSIONS

- **CMB lensing spectra** probes anything affecting growth of structure (including Σm_ν). Great synergy with Stage-4 LSS surveys
- Polarization-based reconstructions very clean and easy to model. Temperature can be biased by extragalactic foregrounds, but can be mitigated
- Primordial B-modes probe inflation/alternatives via the tensor-to-scalar ratio, r
- **Delensing B-modes** is essential for CMB-S3 & CMB-S4 r targets
 - First-order lensing B-mode template built from lensed E is effectively optimal beyond CMB-S4 & transparent to systematics
 - For SO, multi-tracer delensing removes $\sim 70\%$ of power, halves $\sigma(r)$
 - LSS tracers great for delensing (even CMB-S3). CIB particularly useful, but deproject galactic dust to avoid bias
 - Internal delensing biases, with us for the foreseeable future — better to mask overlapping modes than to model

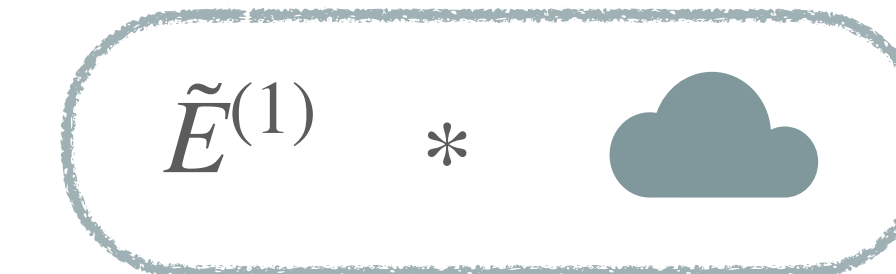
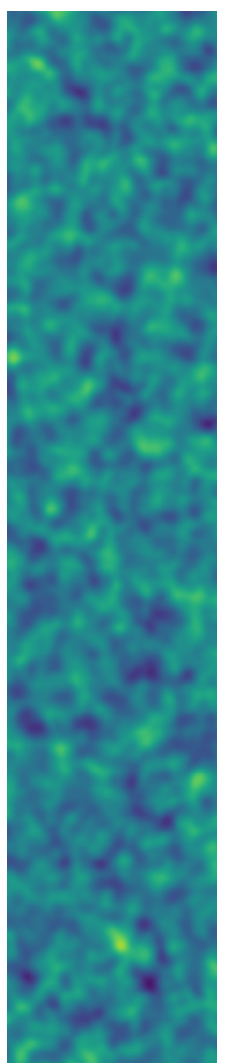
Thank you very much for having me!
a.baleatolizancos@berkeley.edu

BACK-UP SLIDES

WHY THE CANCELLATIONS IN $B^{\text{del}}[B_{\text{lin}}^{\text{temp}}(\tilde{E})]$?

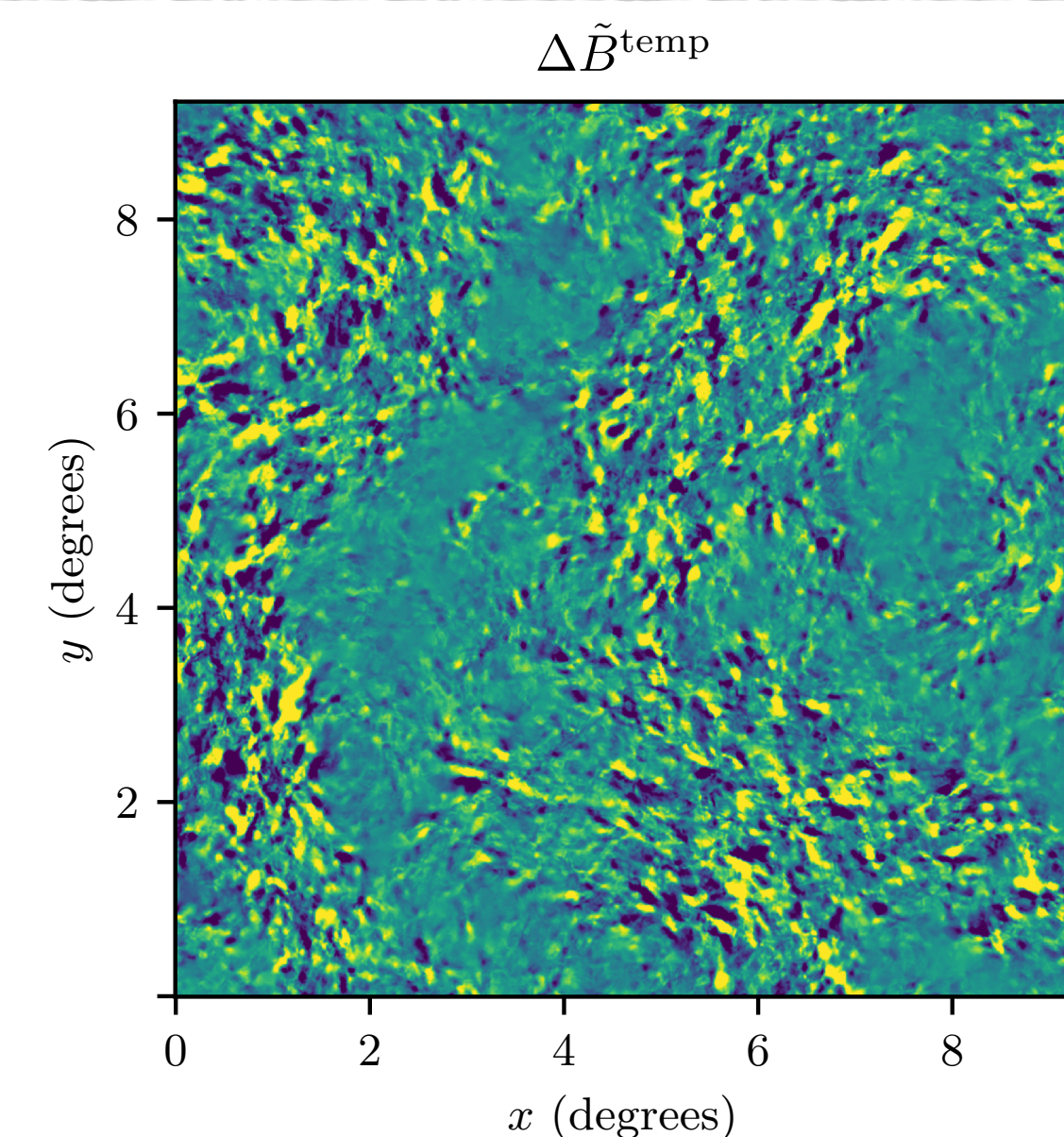


E-mode at
emission



$\tilde{E}^{(1)}$

Template-making



WHY THE LARGE FLOOR IN $B^{\text{del}}[B_{\text{non-pert}}^{\text{temp}}(\tilde{E})]?$

$$\tilde{B}_{\text{non-pert}}^{\text{temp}}(\mathbf{l}) = \tilde{B}^{(1)}(\mathbf{l}) + \Delta\tilde{B}^{\text{temp}}(\mathbf{l}) + \tilde{B}^{(2)}(\mathbf{l}) + O(\phi^3).$$

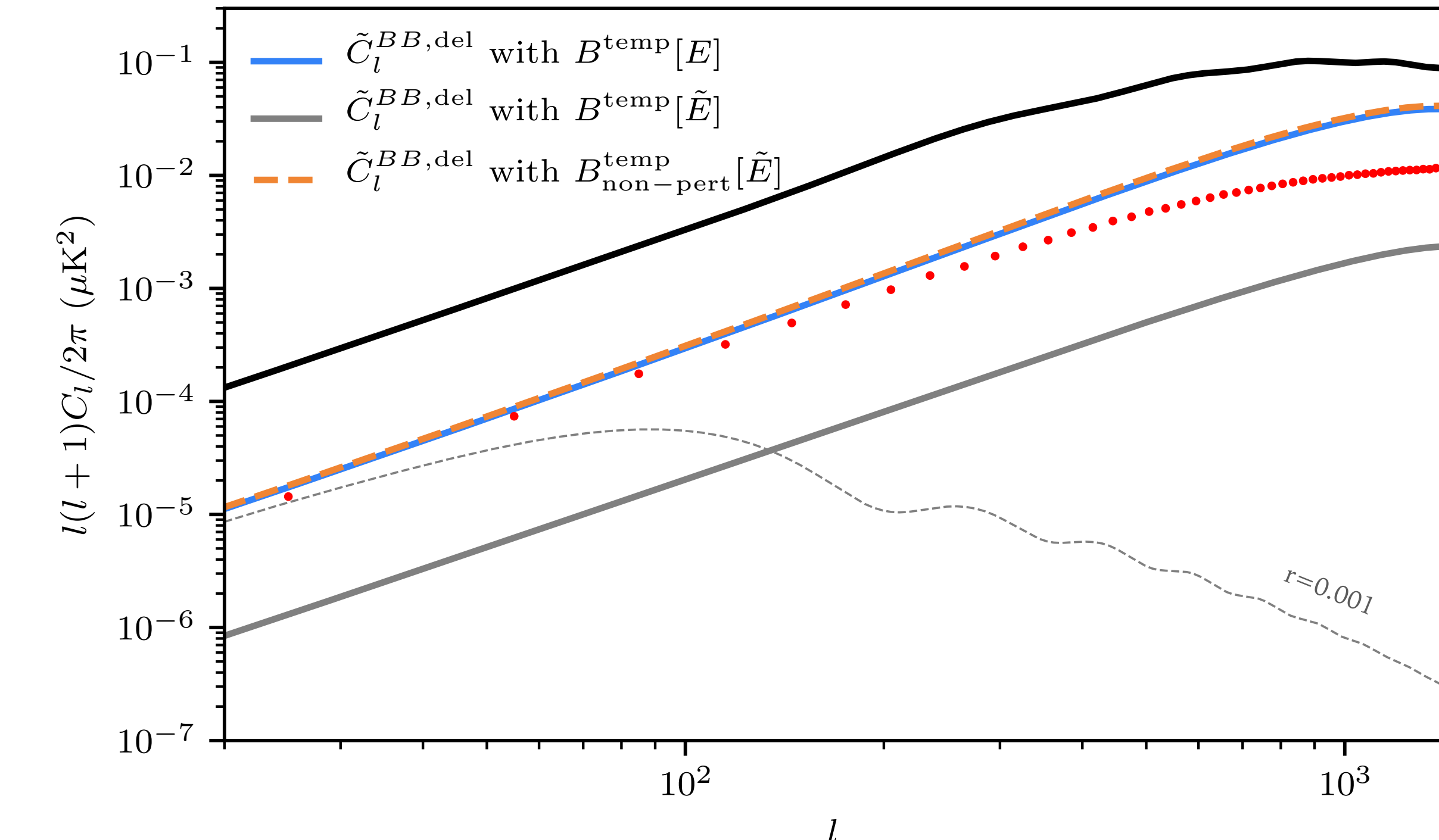
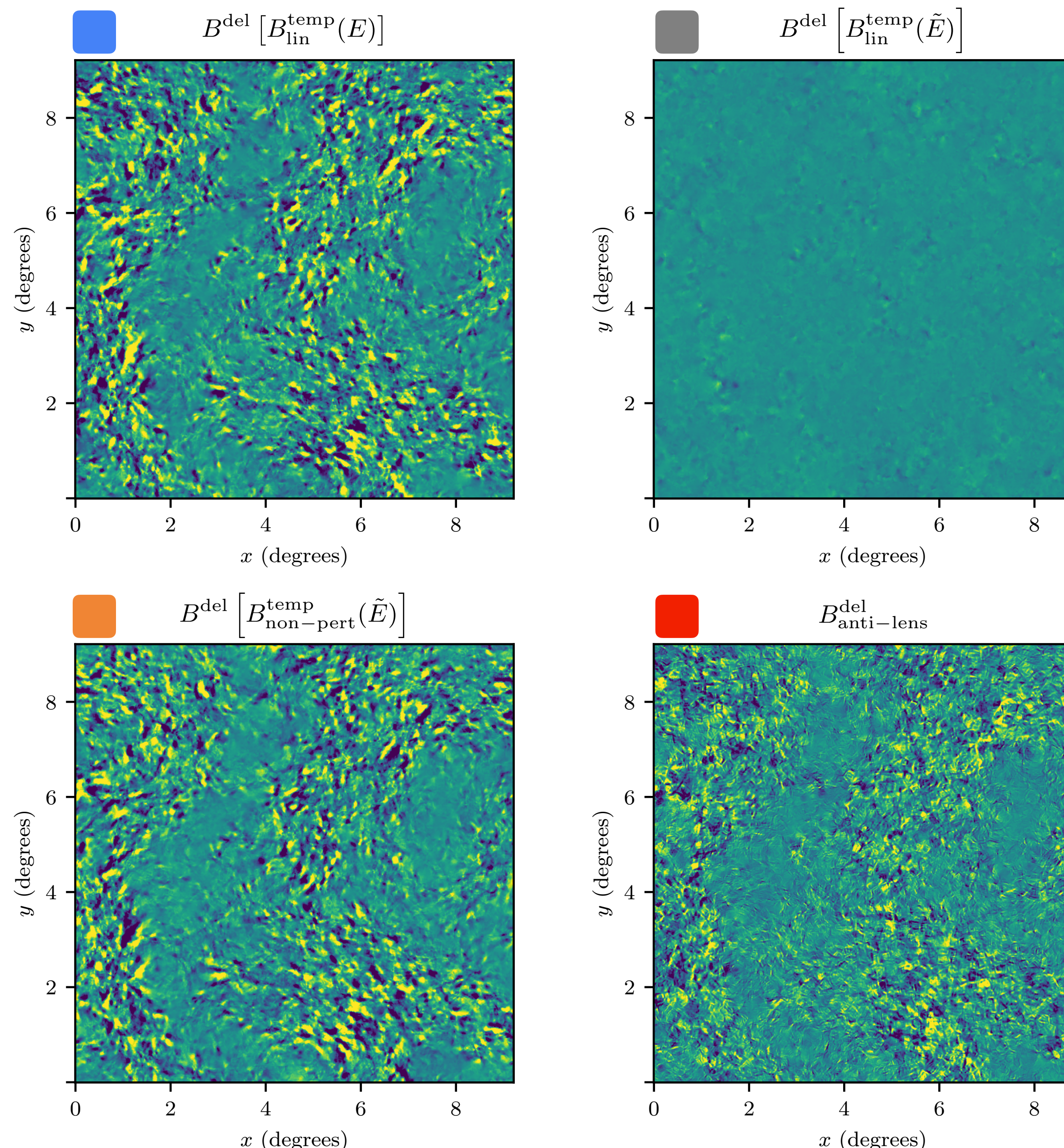
When subtracting this off of observations,

$$B^{\text{del}} = B^{\text{obs}} - \tilde{B}_{\text{non-pert}}^{\text{temp}} = (\cancel{\tilde{B}^{(1)}(\mathbf{l})} + \cancel{\tilde{B}^{(2)}(\mathbf{l})} + O(\phi^3)) - (\cancel{\tilde{B}^{(1)}(\mathbf{l})} + \underline{\Delta\tilde{B}^{\text{temp}}(\mathbf{l})} + \cancel{\tilde{B}^{(2)}(\mathbf{l})} + O(\phi^3)).$$

So the power spectrum of delensed B-modes has a large floor:

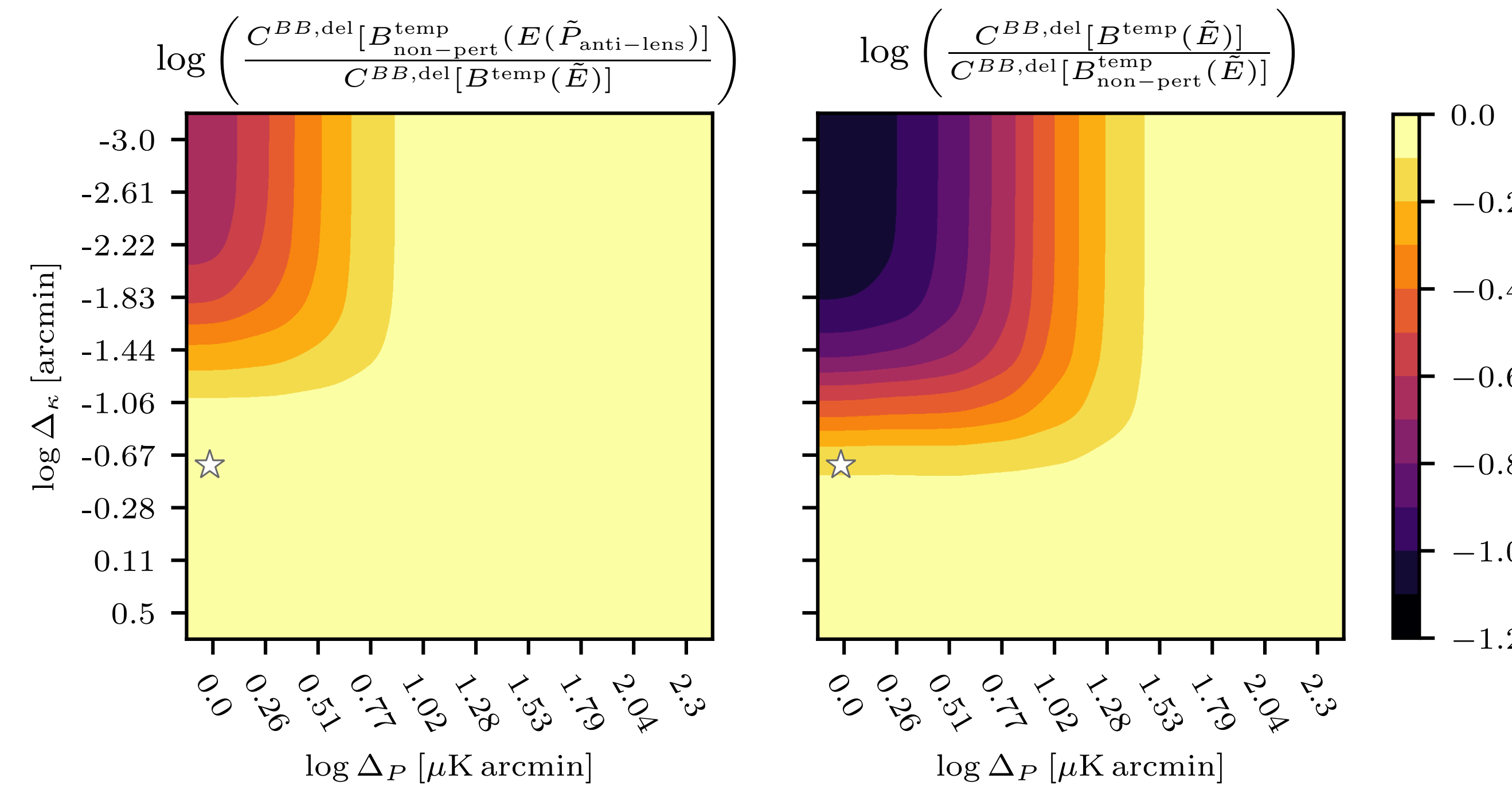
$$\langle |B^{\text{del}}|^2 \rangle \approx \langle |\Delta\tilde{B}^{\text{temp}}|^2 \rangle \sim O(0.1 \tilde{C}^{BB}).$$

LIMITATIONS OF B-MODE TEMPLATE DELENSING: NOISELESS SCENARIO



- Cancellations disappear if linear template is built from unlensed or delensed E-modes, hit delensing floor of $O(10)\%$
- New cancellations arise when the lensed E-modes are used in the linear template, so delensing floor is $O(1)\%$
- Advantage is lost when a non-perturbative template is built from lensed E-modes, so the delensing floor is also $O(10)\%$

ADDITIONAL SLIDES



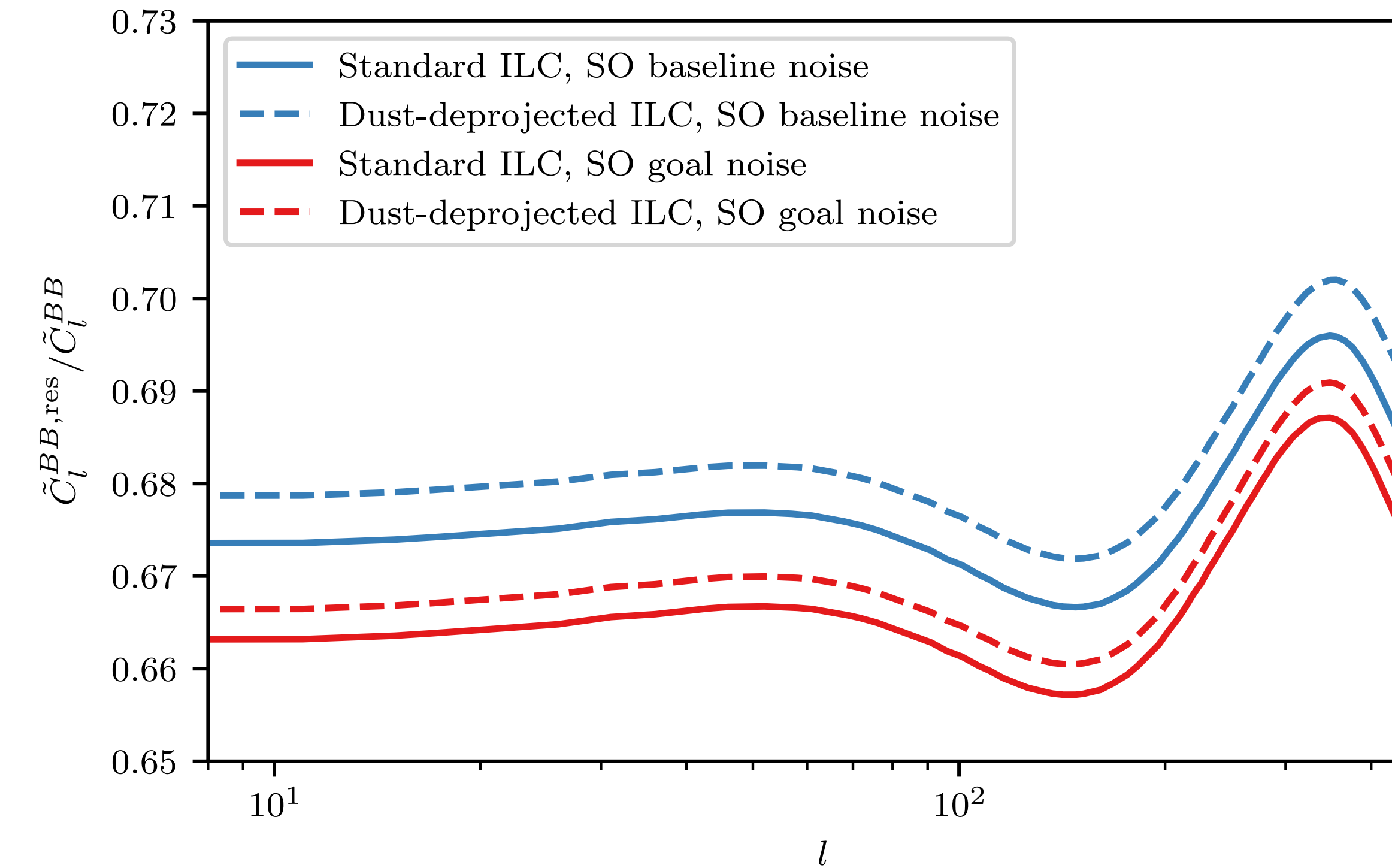
Left panel numerator:

1. *Observe QU, extract E*
2. *Anti-lens these observations*
3. *Extract E-modes*
4. *Form non-perturbative template*
5. *Delens*

... but less clear what's happening to primordial B-modes.

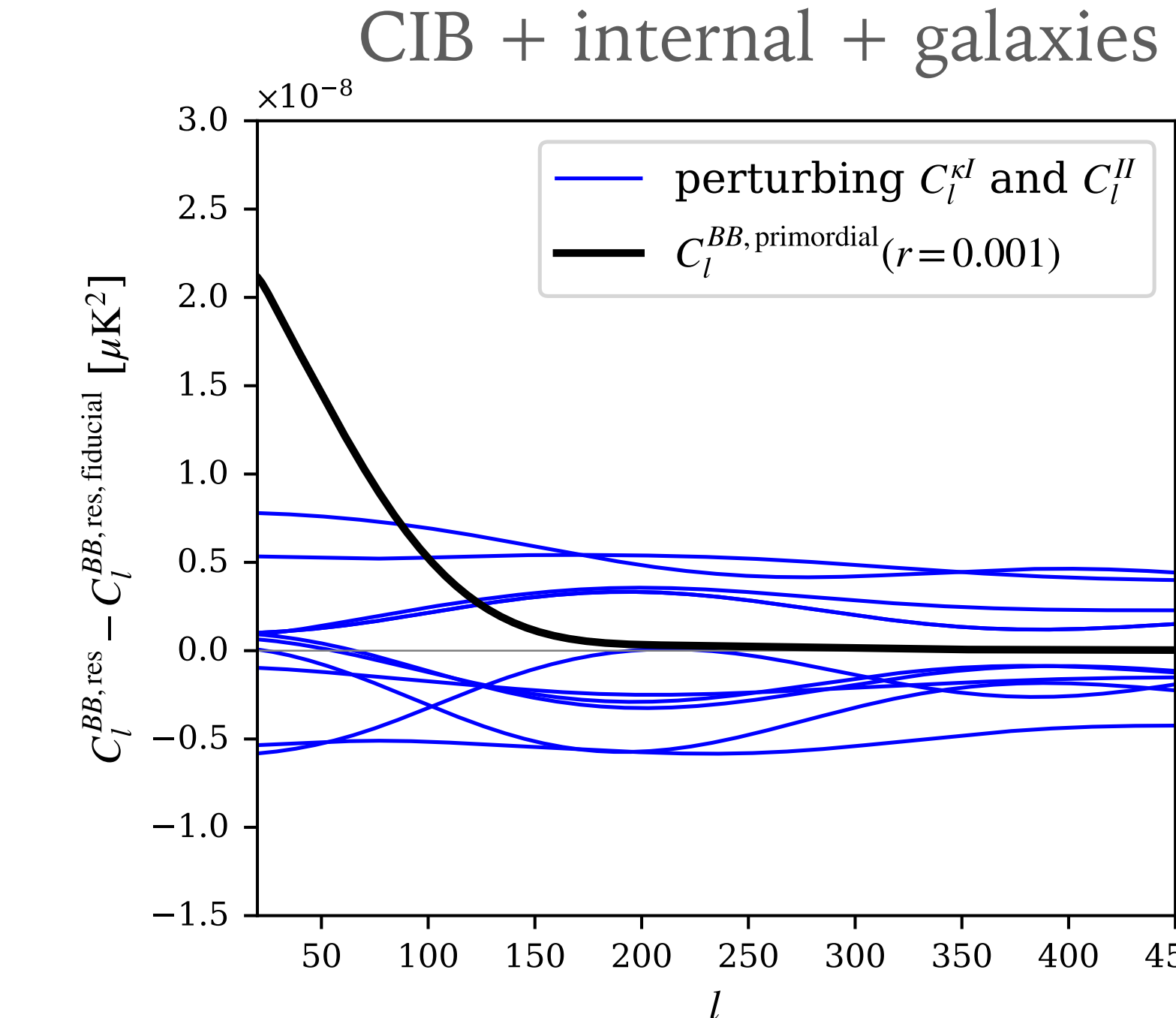
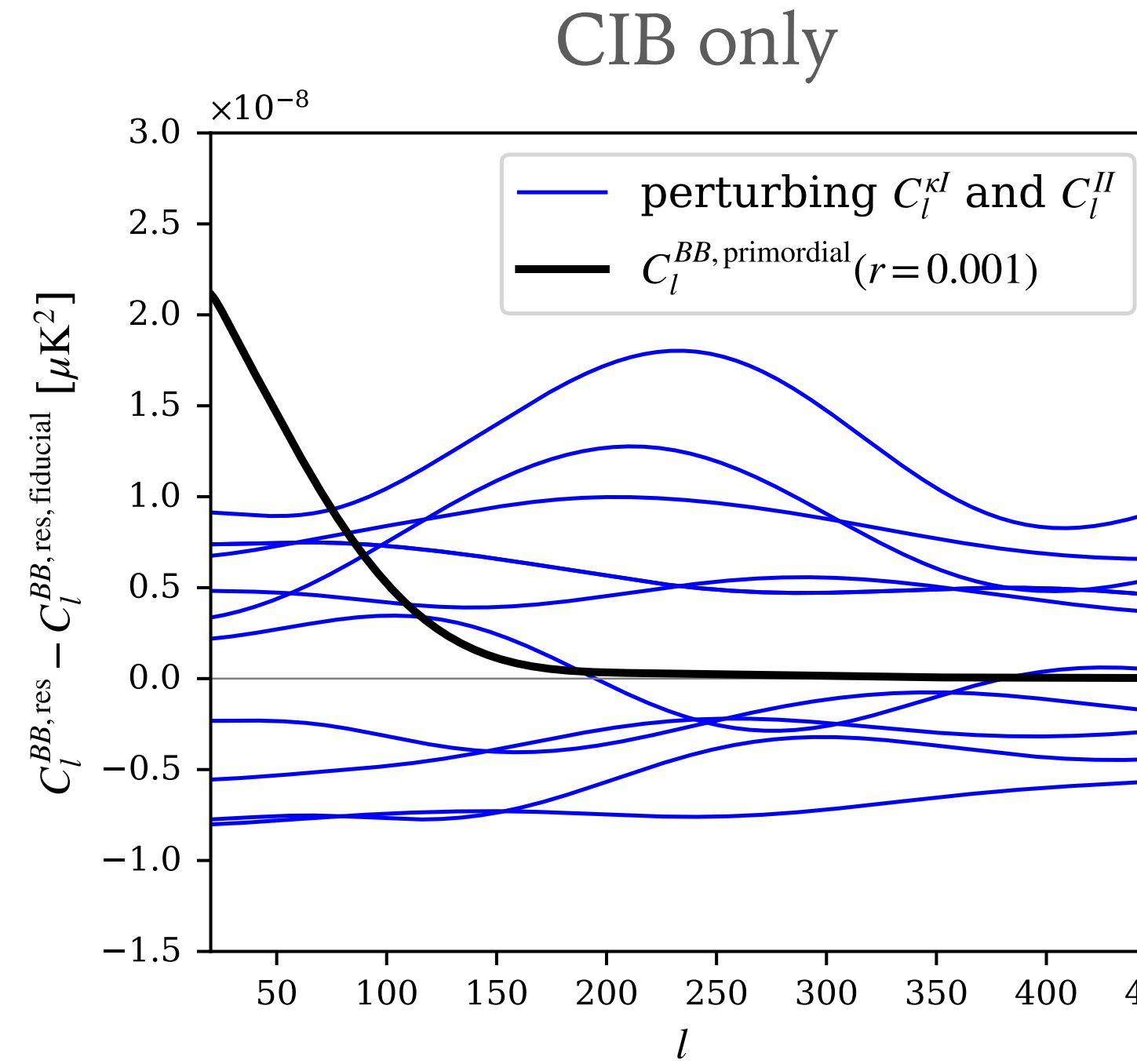
ADDITIONAL SLIDES

Small degradation in delensing efficiency from deprojecting dust from LAT E-modes



CHALLENGES TO MULTI-TRACER DELENSING

- Uncertainties in measurements of tracer auto- and cross- spectra:



Flat enough to
marginalise over
amplitude parameter!

T. Namikawa, ABL, N. Robertson, A Challinor, B. Sherwin & B. Yu 21 (to be submitted)

- The impact of foregrounds

RECAP OF B-MODE DELENSING

Schematically:

$$\langle |B^{obs} - E^{obs}\hat{\phi}|^2 \rangle = \langle |B^{obs}|^2 \rangle - 2 \langle B^{obs}E^{obs}\hat{\phi} \rangle + \langle E^{obs}\hat{\phi}E^{obs}\hat{\phi} \rangle:$$



delensing: $\langle \tilde{B}(E, \phi)\tilde{E}\phi \rangle_c$



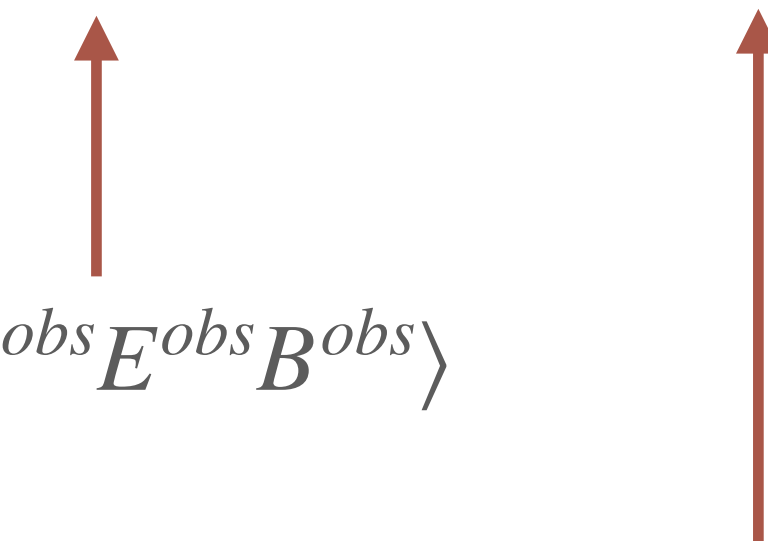
= residual lensing + experimental noise

INTERNAL DELENSING BIAS

Schematically:

$$\langle |B^{obs} - E^{obs}\hat{\phi}|^2 \rangle = \langle |B^{obs}|^2 \rangle - 2\langle B^{obs}E^{obs}\hat{\phi} \rangle + \langle E^{obs}\hat{\phi}E^{obs}\hat{\phi} \rangle:$$

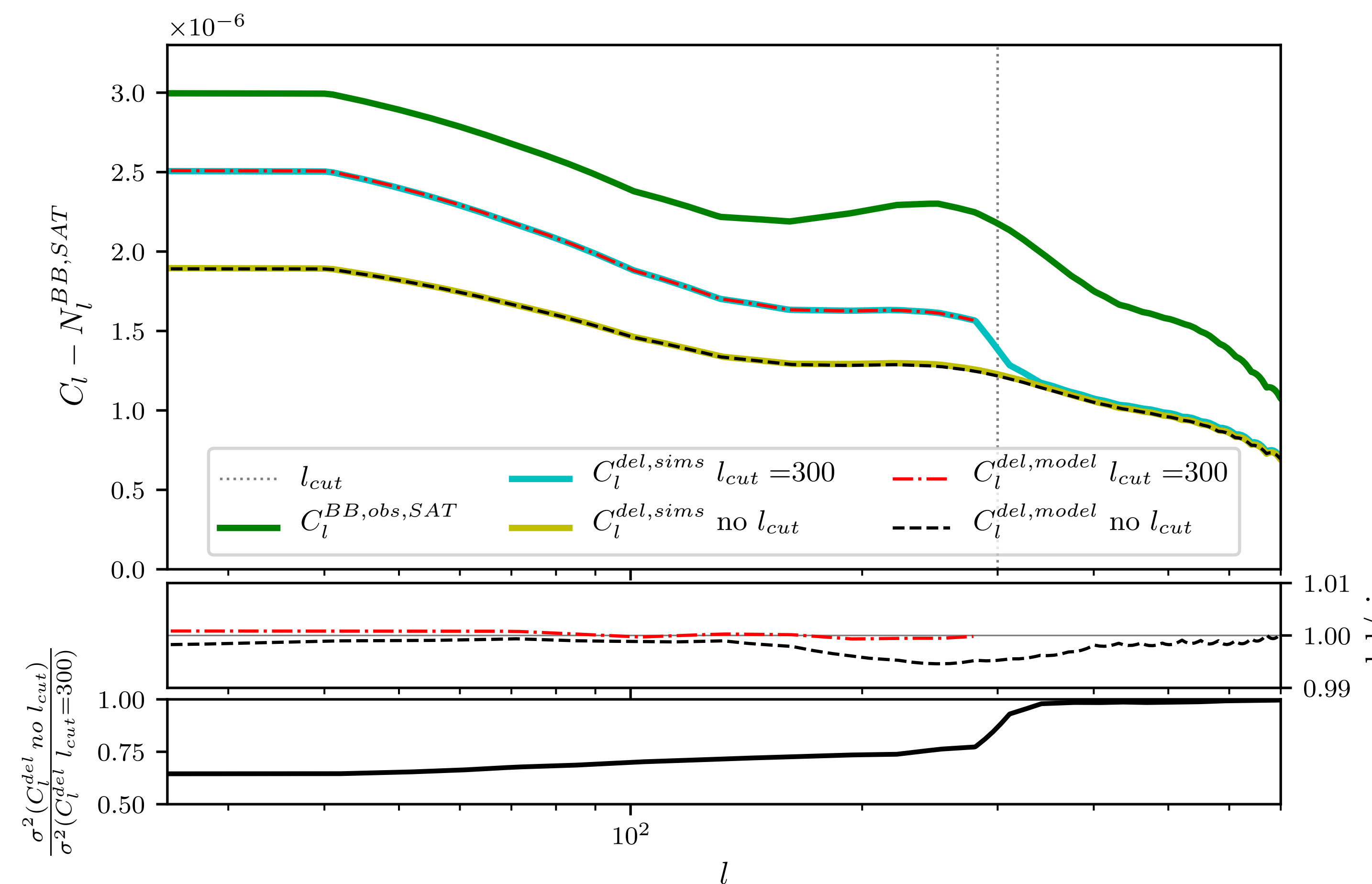
$$\hat{\phi} = \hat{\phi}^{EB}(E, B)$$

$$\begin{aligned} & \langle B^{obs}E^{obs}E^{obs}B^{obs} \rangle \\ & \langle E^{obs}E^{obs}B^{obs}E^{obs}E^{obs}B^{obs} \rangle \end{aligned}$$


- Suppression of power beyond a simple removal of lensing
- Bias is *local* — avoid by removing overlapping modes

Teng+11, Namikawa & Nagata 14

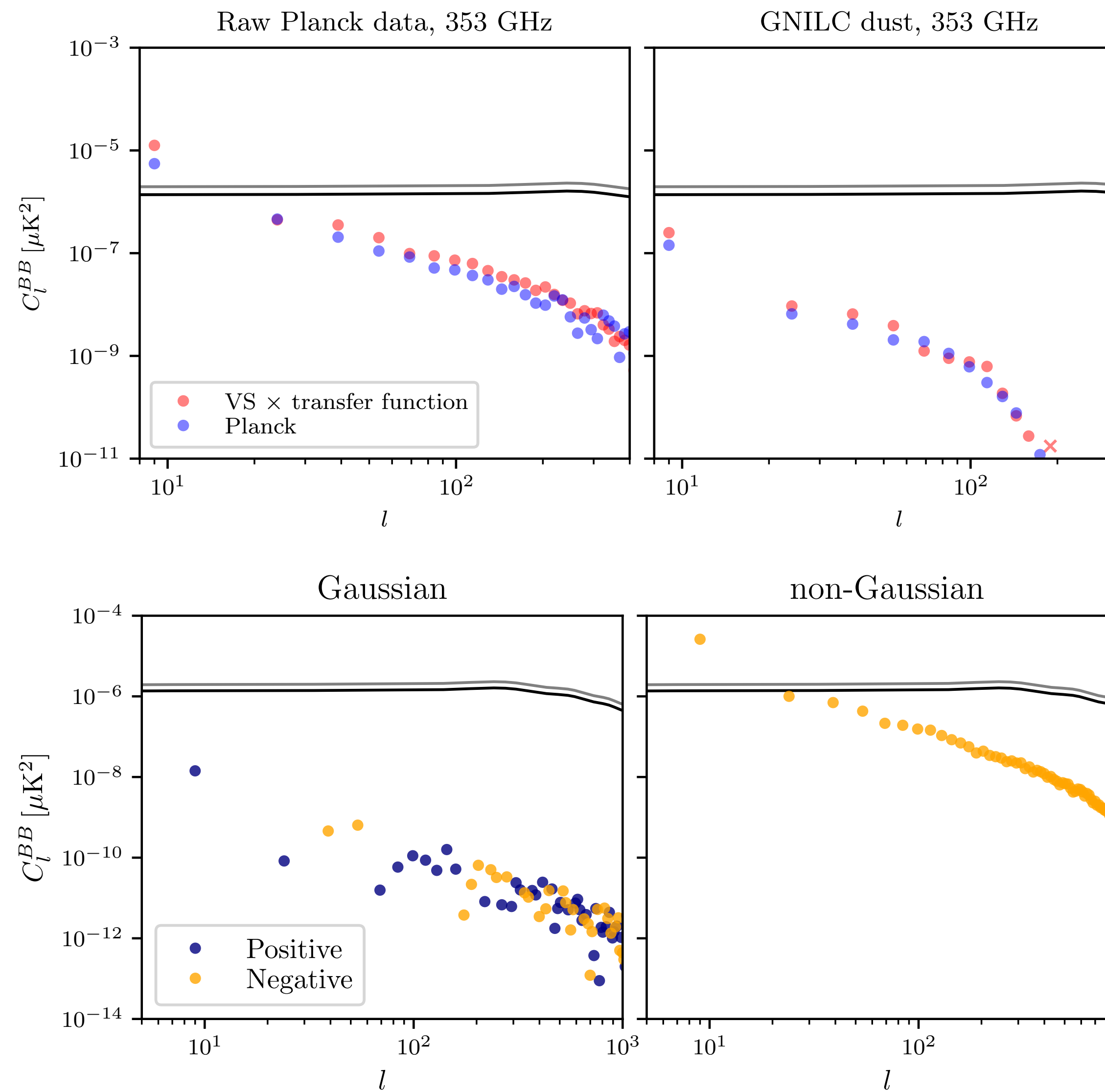
INTERNAL DELENSING BIAS



Variance of delensed spectrum is reduced!

$$\text{Model: } \frac{C_l^{BB,\text{del},\text{biased}}}{(D_l - 1)^2} = C_l^{BB,\text{del},\text{unbiased}} + \left(\frac{D_l}{D_l - 1} \right)^2 \left[C_l^W + N_l^{BB,\text{LAT}} + N_l^{BB,\text{SAT}} \left(\frac{2}{D_l} - 1 \right) - \frac{2}{D_l} N_l^X \right], \quad 0 < D_l < 1$$

ADDITIONAL SLIDES



ADDITIONAL SLIDES

Pearson + 14

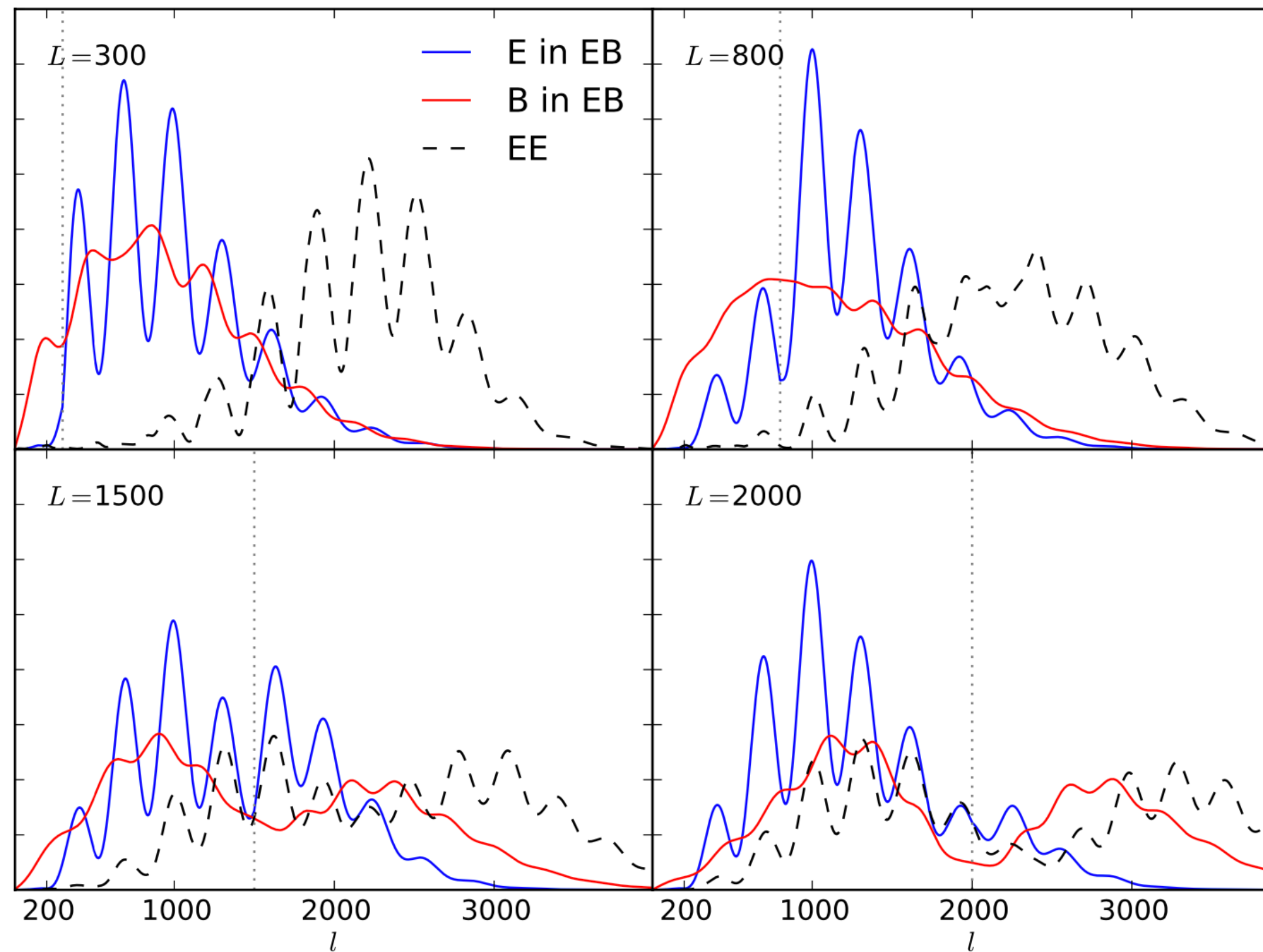


Figure 56. Contributions from CMB scales (ℓ) to lensing reconstruction on four lensing scales (L). The EB estimator is expected to be the main channel for lensing science with CMB-S4. On degree and sub-degree scales, $L = 300$ and 800 , the estimator uses E and B modes at $\ell \sim 1000$. On scales of several arcmin, $L = 1500$ and 2000 , the estimator uses B modes on significantly smaller scales. Figure taken from [557].

ADDITIONAL SLIDES

McCarthy & Madhavacheril 20

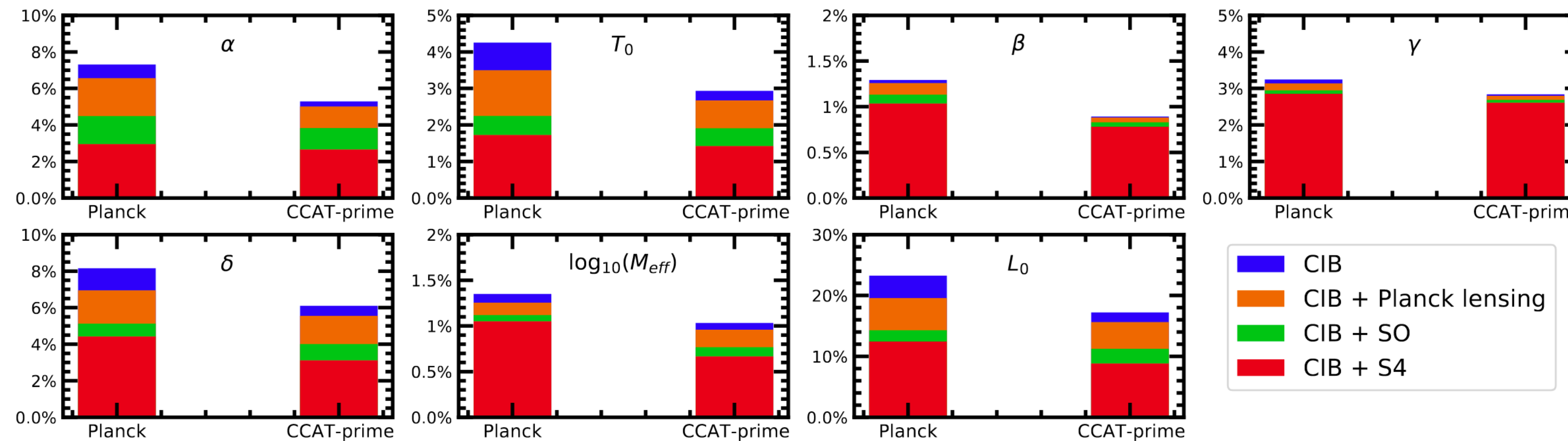
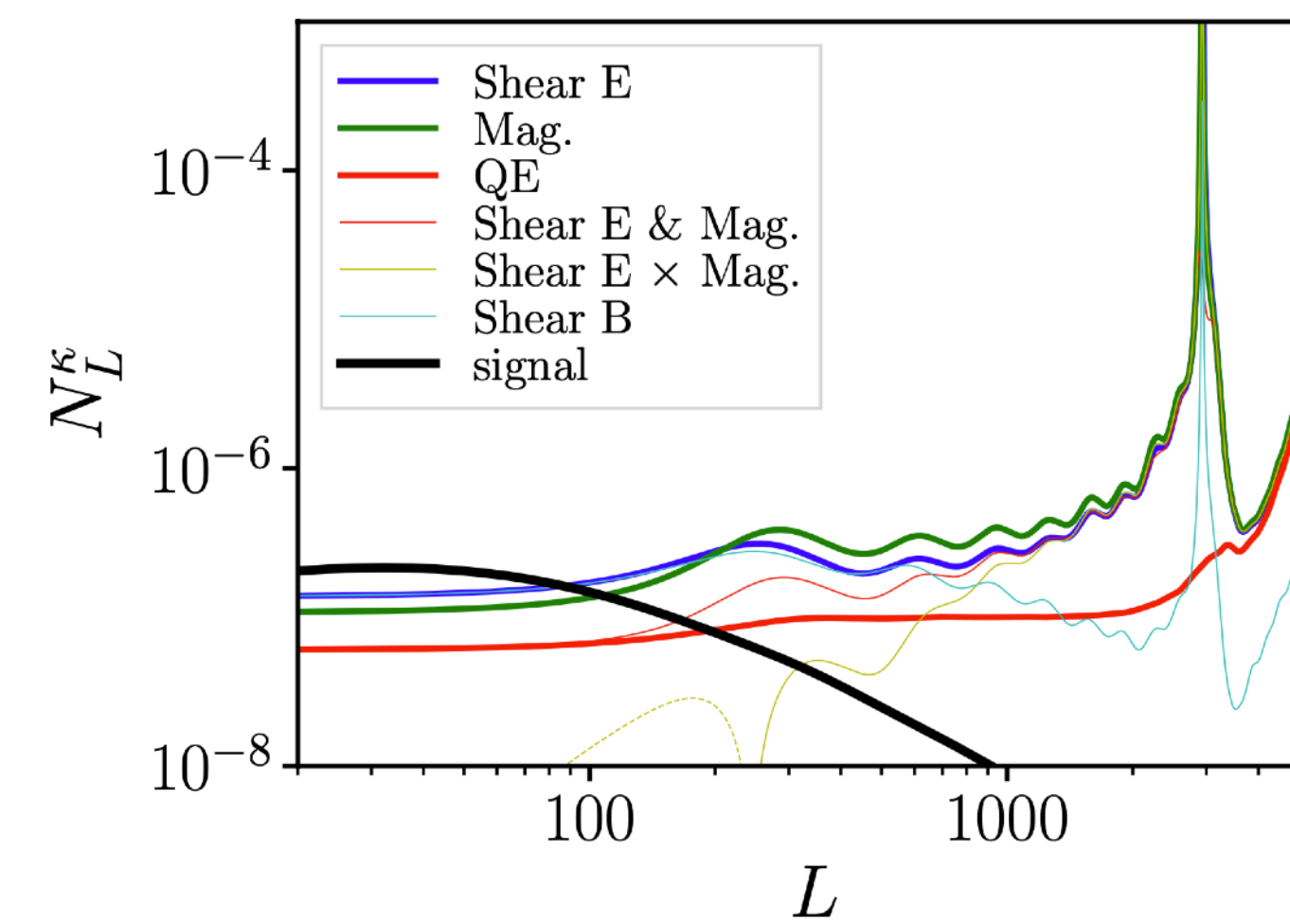
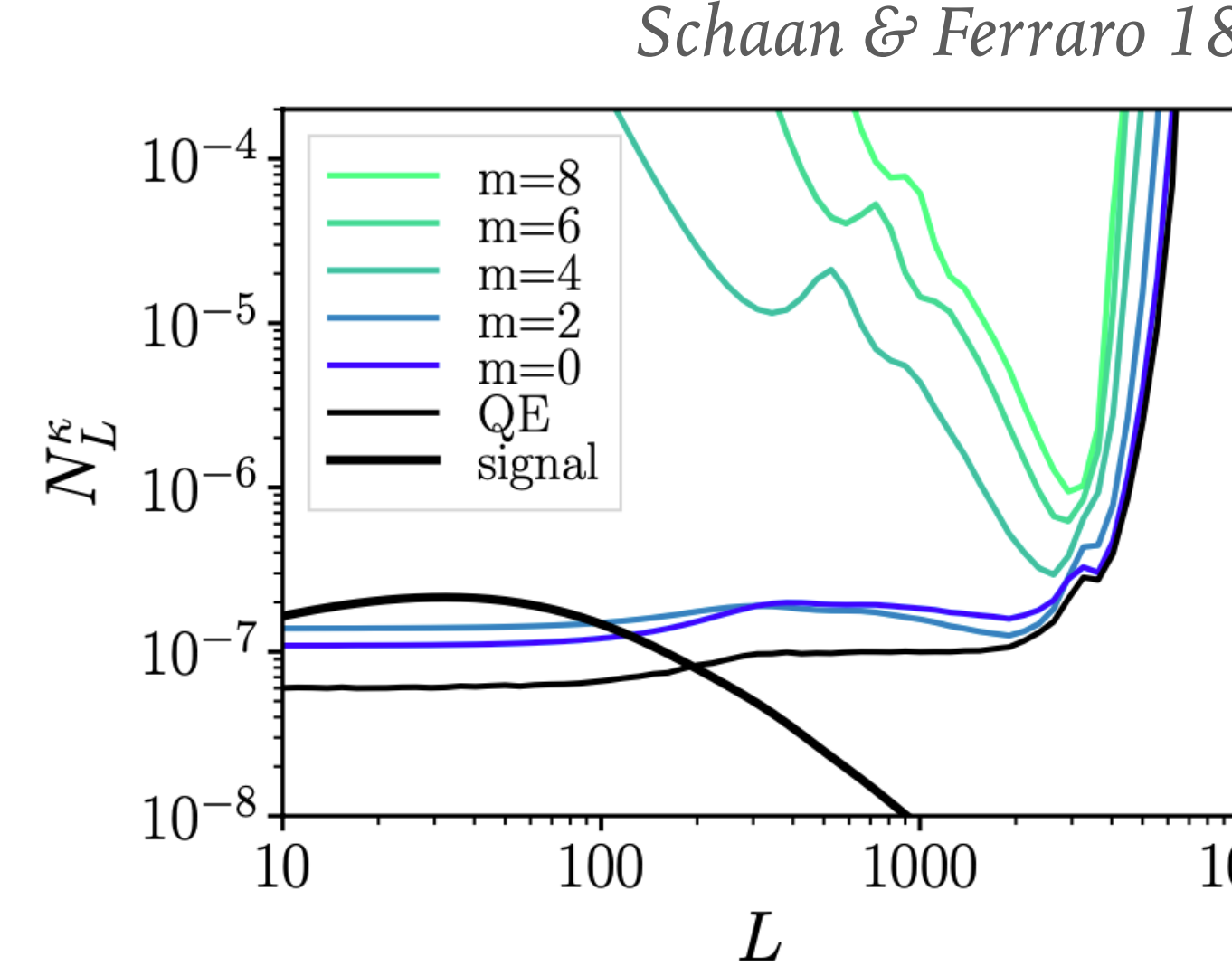
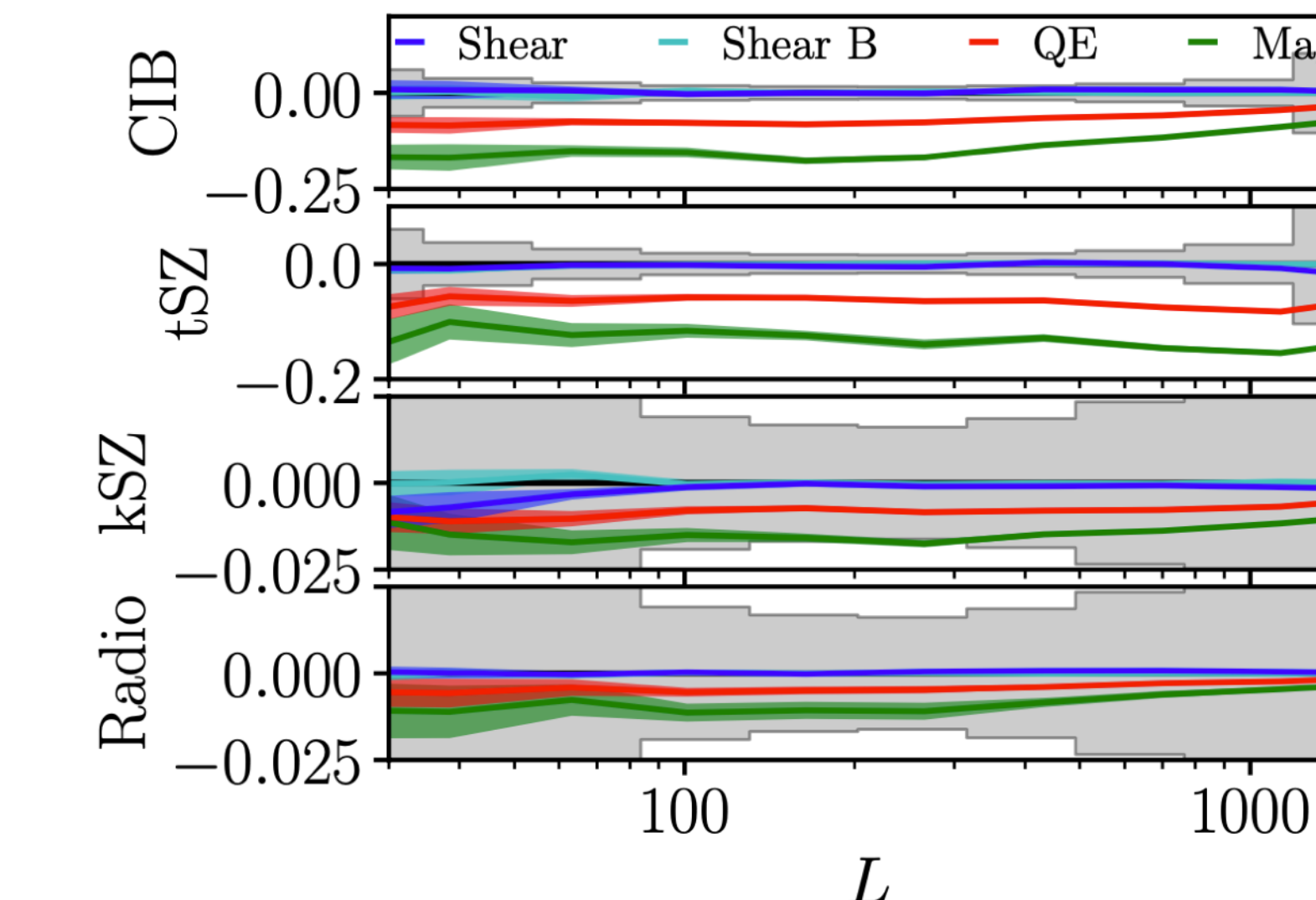


FIG. 6: Percentage constraints on various CIB halo model parameters and their improvement with the incorporation of CMB lensing, for the CIB as measured by *Planck* and by CCAT-prime. We show improvements when including lensing reconstruction from *Planck* itself or from a future Simons Observatory-like or CMB-S4-like survey configuration.

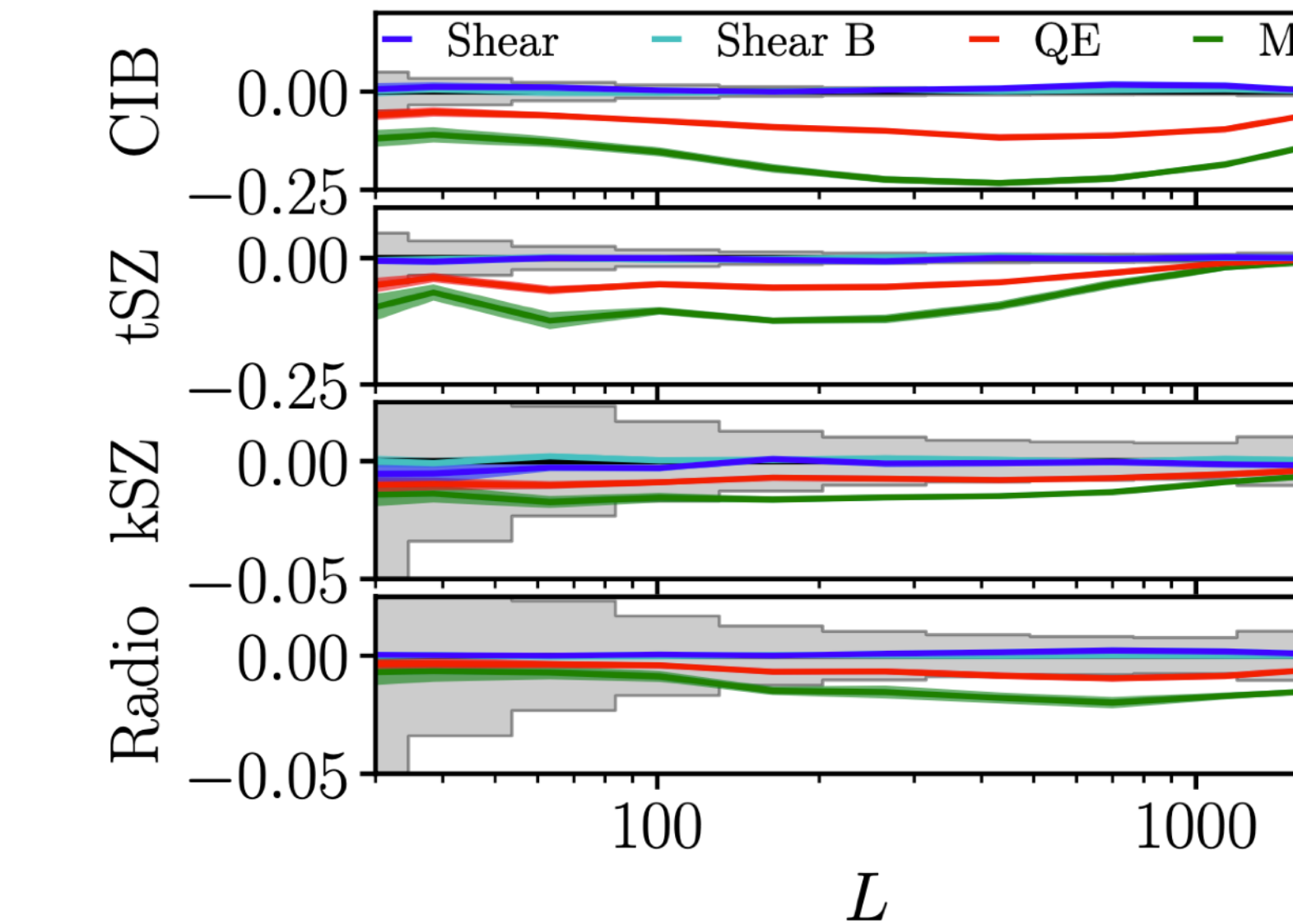
ADDITIONAL SLIDES



Relative Bias on $C_L^{\kappa_{\text{CMB}}}$: Primary



Relative Bias on $C_L^{\kappa_{\text{CMB}} \times \text{LSST}}$



ADDITIONAL SLIDES

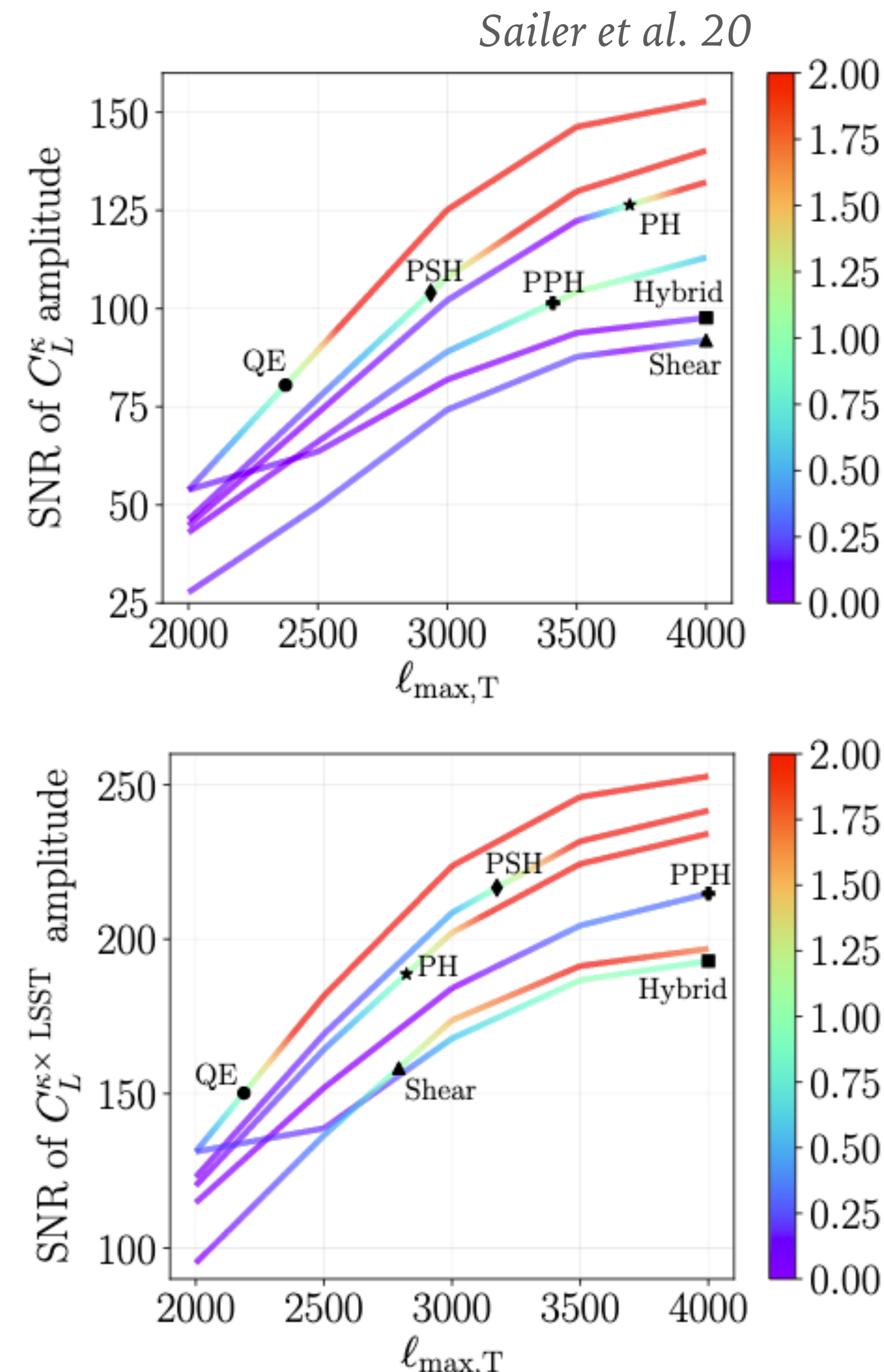


Figure 6. Total signal-to-noise of the lensing amplitude (top) and the cross correlation with LSST (bottom). The black markers denote the highest $\ell_{\max, T}$ where the bias is less than 1σ . We find that the Profile Hardened (PH) estimator reconstructs the lensing amplitude with the highest signal to noise: a $\sim 50\%$ improvement over the standard QE. We find that the Point Source Hardened (PSH) and Point source and Profile Hardened (PPH) reconstruct the cross with similar SNRs: a $\sim 50\%$ improvement over the standard QE. The Hybrid estimator is a combination of Shear and QE, and is described in greater detail in Appendix B. We note that the color-scale saturates at 2σ , and that the bias to the standard QE can be $> 10\sigma$ at $\ell_{\max, T} \gtrsim 3000$.

ADDITIONAL SLIDES

arXiv:1309.5383

- $\sum m_\nu < 0.72 \text{ eV}$ Planck TT+lowP ;
- $\sum m_\nu < 0.21 \text{ eV}$ Planck TT+lowP+BAO ;
- $\sum m_\nu < 0.49 \text{ eV}$ Planck TT, TE, EE+lowP ;
- $\sum m_\nu < 0.17 \text{ eV}$ Planck TT, TE, EE+lowP+BAO .

SO forecasting paper

We show the anticipated constraints as a function of sky area in Fig. 28. Here we include foreground cleaning with explicit tSZ deprojection for temperature and dust deprojection for polarization (Deproj-1), since these foregrounds could potentially cause the largest systematic effects (see Sec. 5.5 below). We forecast

$$\begin{aligned} \sigma(\sum m_\nu) &= 33 \text{ meV} & \text{SO Baseline + DESI-BAO ,} \\ \sigma(\sum m_\nu) &= 31 \text{ meV} & \text{SO Goal + DESI-BAO ,} \end{aligned} \quad (16)$$

for $\sigma(\tau) = 0.01$ – i.e., for current measurements of τ . The

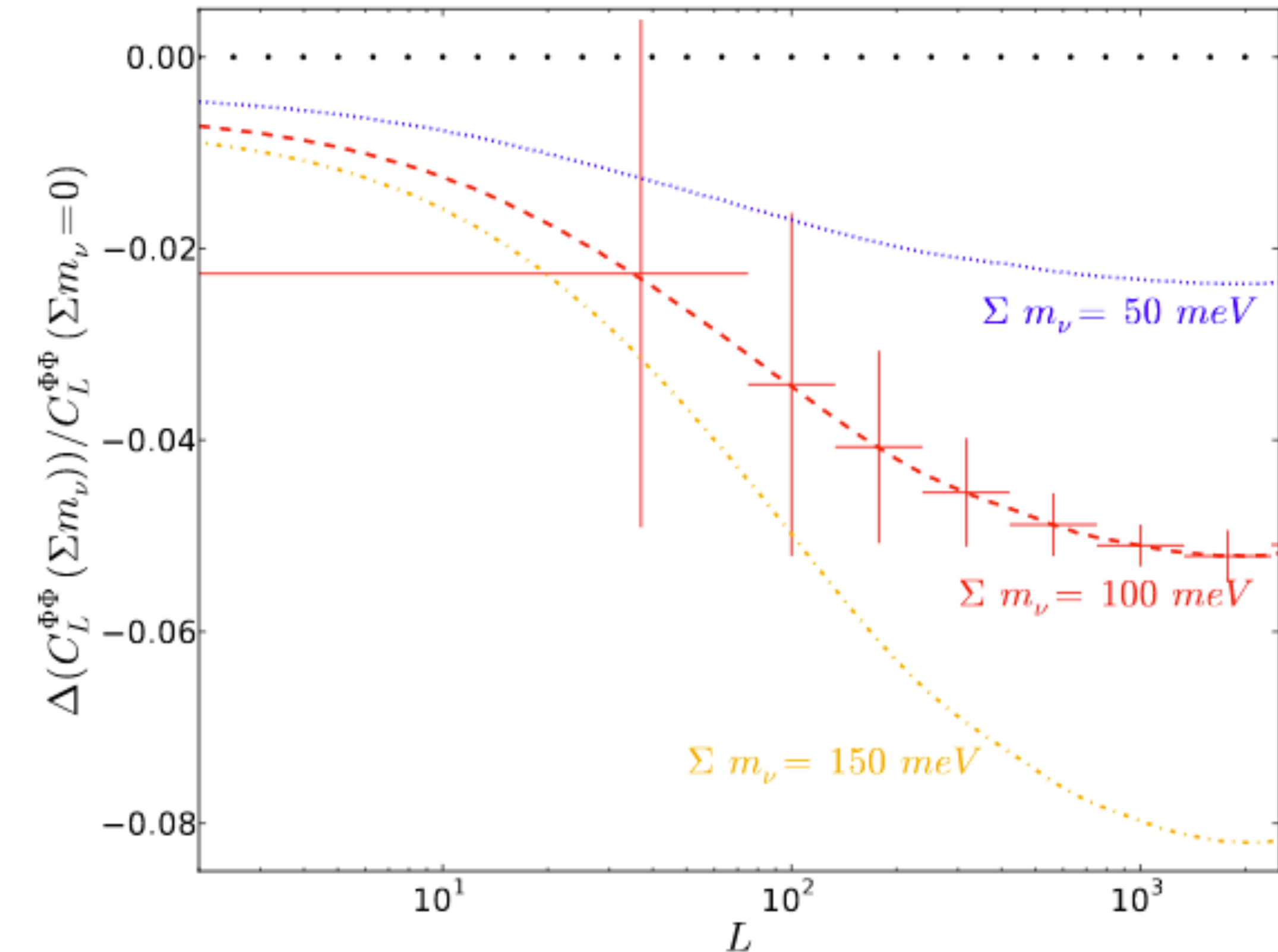
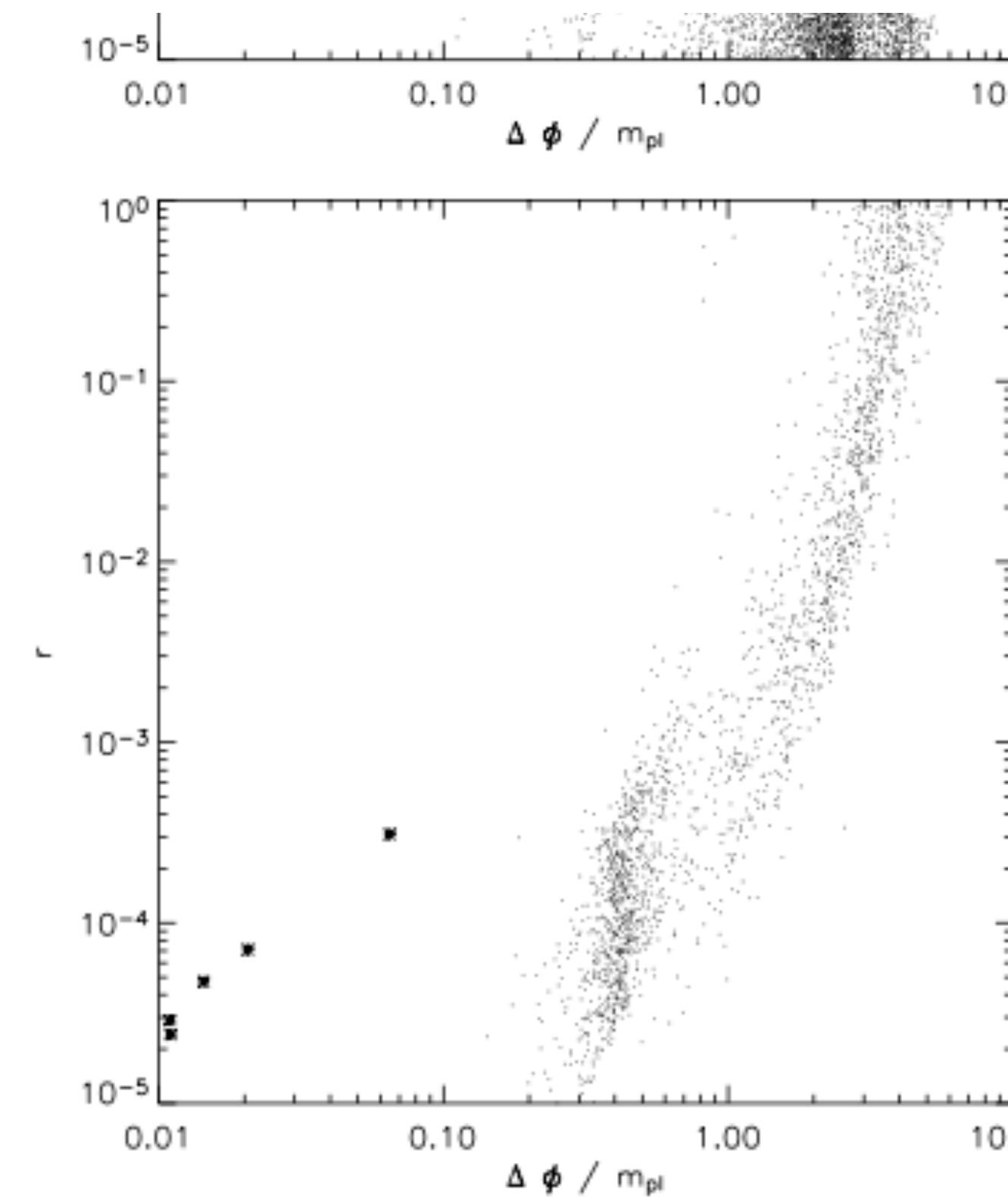


Figure 5. The effect of massive neutrinos on the CMB lensing potential power spectrum $C_L^{\Phi\Phi}$. The fractional change in $C_L^{\Phi\Phi}$ for a given value of $\sum m_\nu$ is shown relative to the case for zero neutrino mass. Projected constraints on $C_L^{\Phi\Phi}$ for a Stage-IV CMB experiment are shown for $\sum m_\nu = 100 \text{ meV}$. Here we have approximated all of the neutrino mass to be in one mass eigenstate and fixed the total matter density $\Omega_m h^2$ and H_0 . The 1σ constraint for $\sum m_\nu$ is approximately 45 meV for lensing alone and drops to 16 meV when combined with other probes.

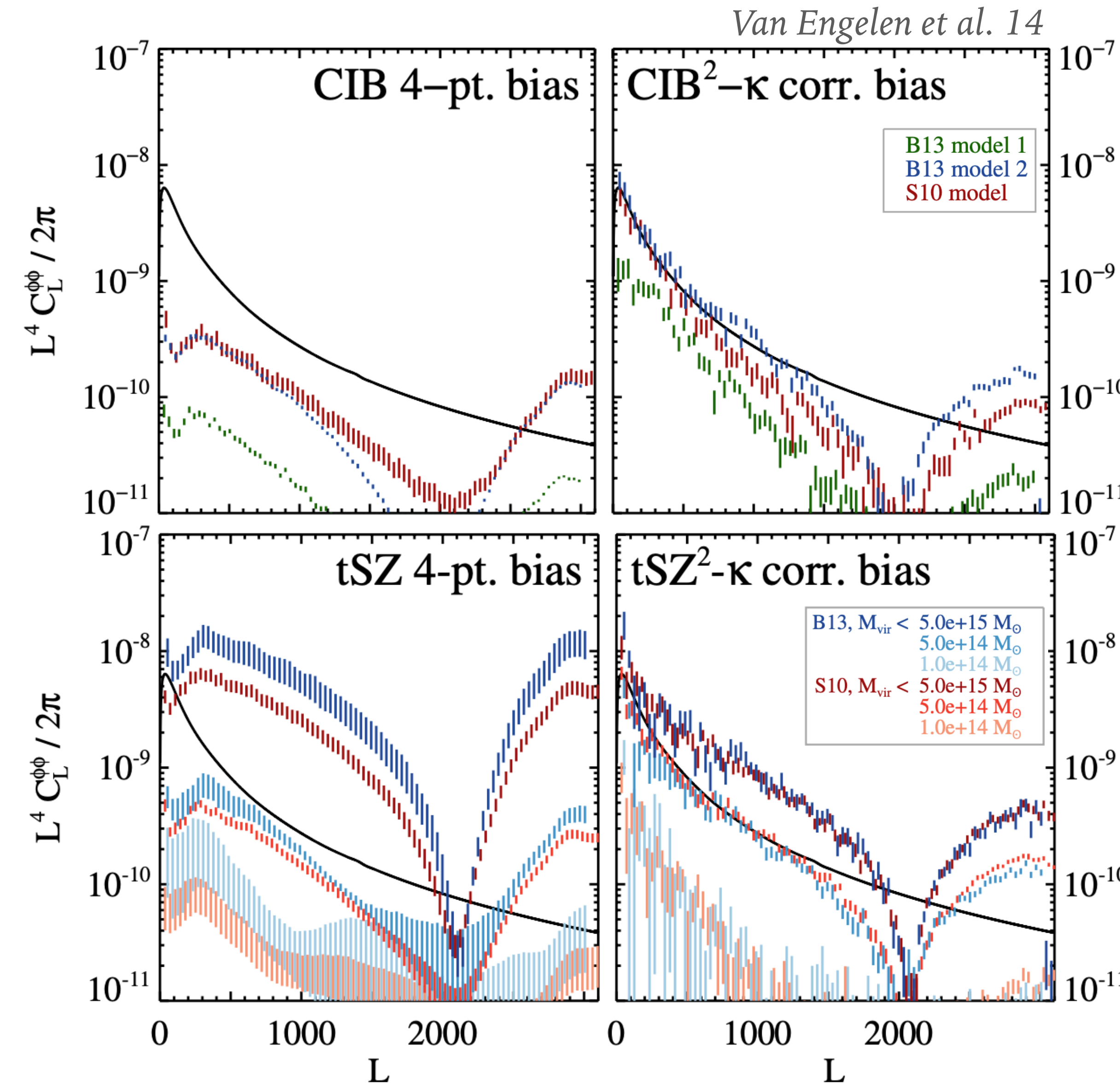
ADDITIONAL SLIDES



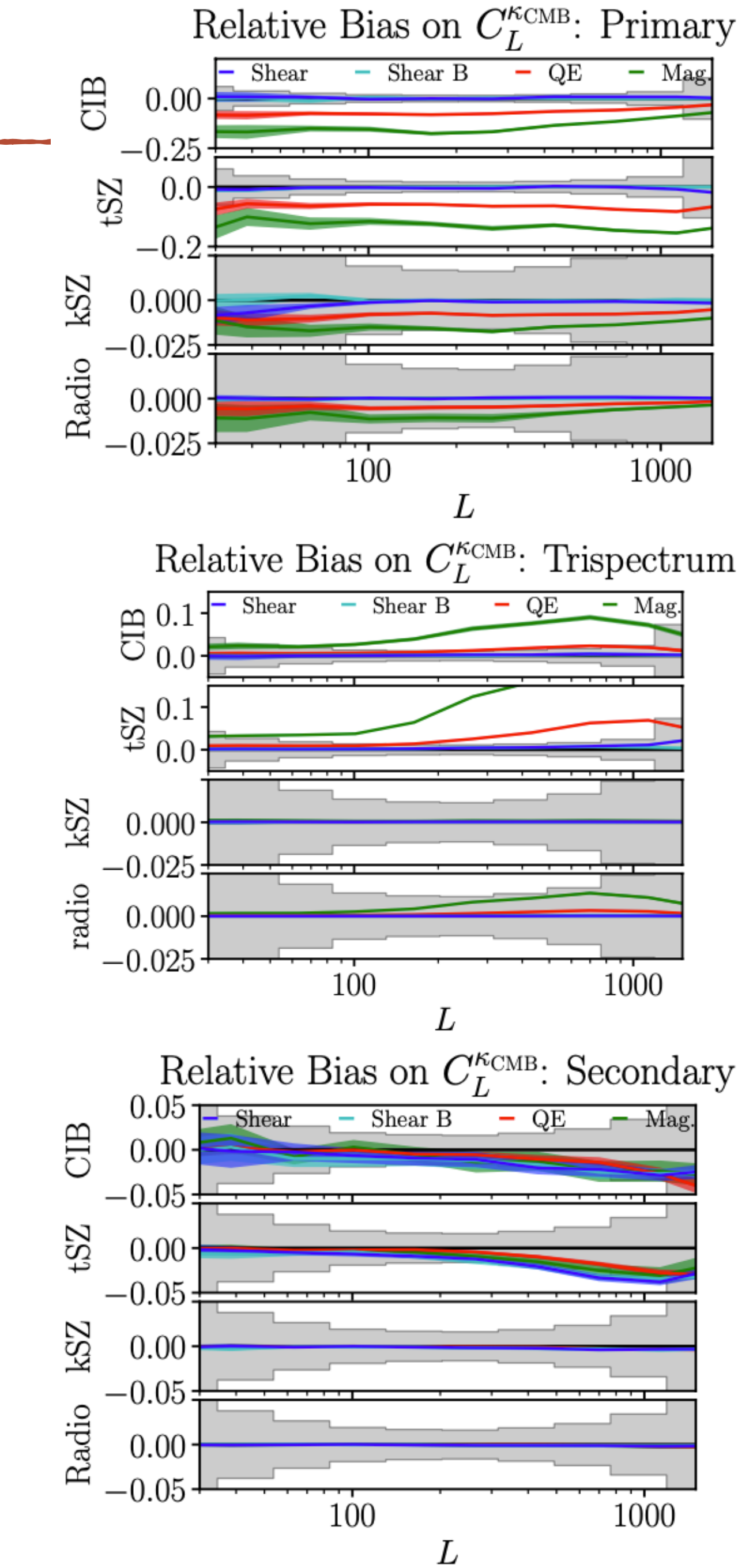
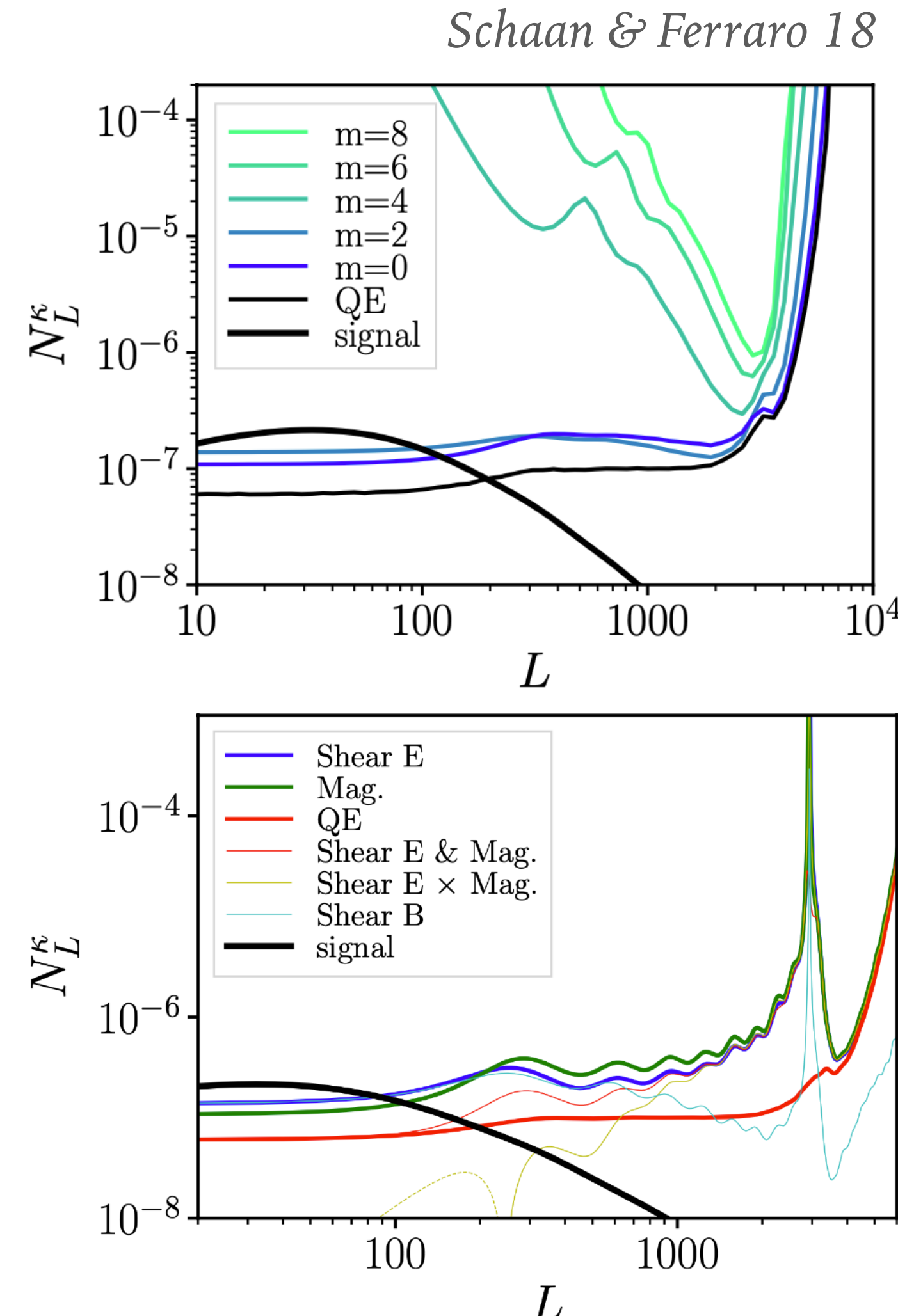
Verde, Peiris & Jimenez 06

Figure 1. The absolute value of the range traversed by the scalar field ϕ over the final 55 e-folds of inflation, $\Delta\phi$, plotted against the tensor-to-scalar ratio r : (top) all models that sustain at least 55 e-folds of inflation in a 2-million point Monte-Carlo simulation to 10th order of the inflationary flow equations; (bottom) the subset of models that satisfy current observational constraints on n_s and $dn_s/d\ln k$, as discussed in the text. Hybrid models, which have $n_s > 1$, are shown as stars, and the rest as dots (see text). This simulation has a wider prior on ${}^4\lambda_H$ and higher order slow roll parameters.

ADDITIONAL SLIDES



ADDITIONAL SLIDES - SHEAR ONLY ESTIMATORS



ADDITIONAL SLIDES - COMPARISON OF BIAS TO ESTIMATORS

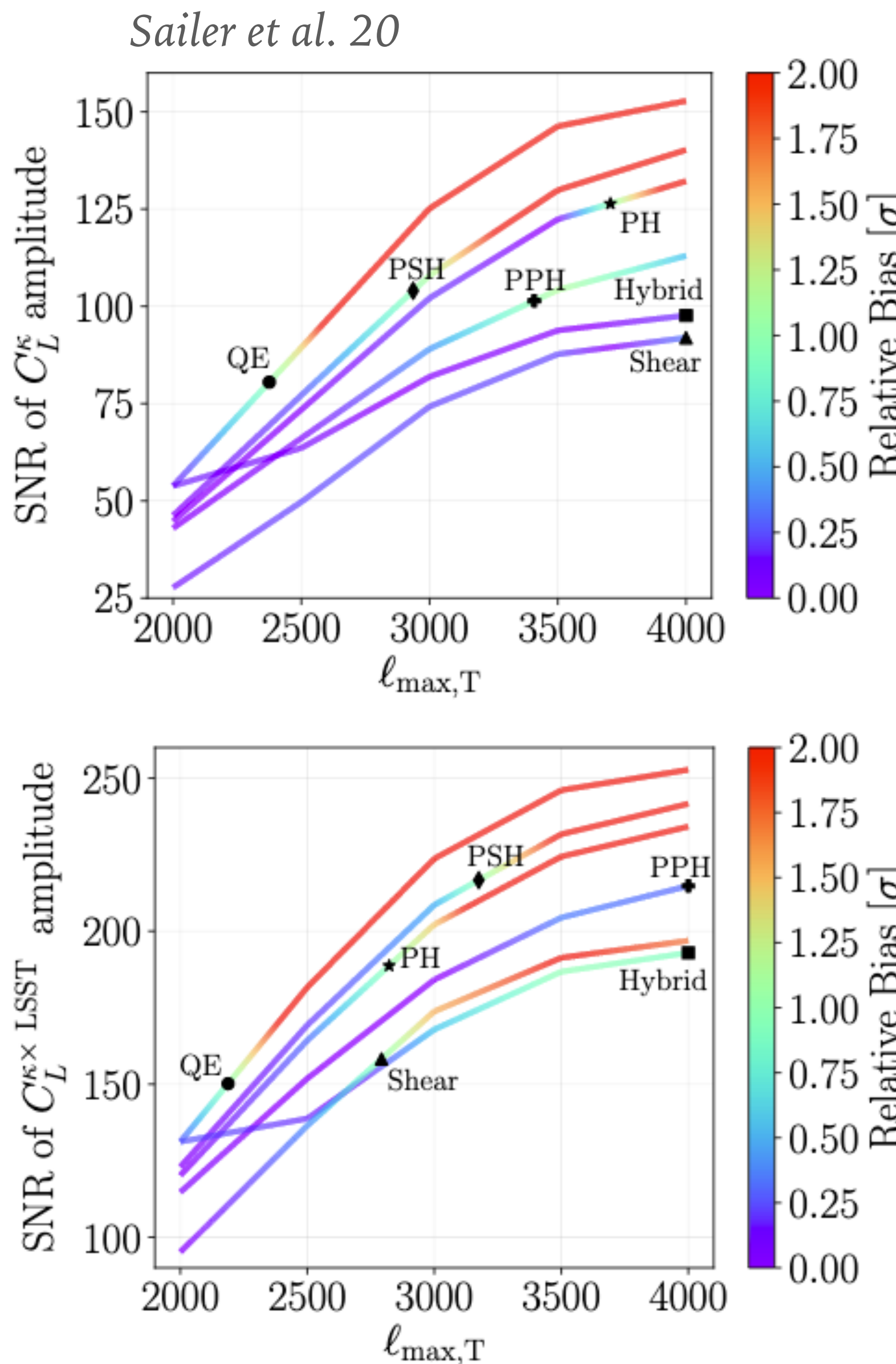


Figure 6. Total signal-to-noise of the lensing amplitude (top) and the cross correlation with LSST (bottom). The black markers denote the highest $\ell_{\max,T}$ where the bias is less than 1σ . We find that the Profile Hardened (PH) estimator reconstructs the lensing amplitude with the highest signal to noise: a $\sim 50\%$ improvement over the standard QE. We find that the Point Source Hardened (PSH) and Point source and Profile Hardened (PPH) reconstruct the cross with similar SNRs: a $\sim 50\%$ improvement over the standard QE. The Hybrid estimator is a combination of Shear and QE, and is described in greater detail in Appendix B. We note that the color-scale saturates at 2σ , and that the bias to the standard QE can be $> 10\sigma$ at $\ell_{\max,T} \gtrsim 3000$.

